

A Lagrangian fluctuation-dissipation relation for scalar turbulence

Theodore D. Drivas¹ and Gregory L. Eyink^{1,2}

¹Department of Applied Mathematics & Statistics, The Johns Hopkins University, Baltimore, MD 21218, USA

²Department of Physics & Astronomy, The Johns Hopkins University, Baltimore, MD 21218, USA

(Received ?; revised ?; accepted ?. - To be entered by editorial office)

An exact relation is derived between scalar dissipation due to molecular diffusivity and the randomness of stochastic Lagrangian particle trajectories. This result equates the dissipation of scalar fluctuations to the variance of the scalar inputs due to initial scalar values, scalar sources, and boundary fluxes as those are sampled backward in time by the stochastic trajectories. The relations are derived for a variety of boundary conditions on the scalar (periodic, imposed scalar fluxes, fixed scalar values, etc.) and for both passive and active scalars. We present here two concrete applications of this scalar fluctuation-dissipation relation. Previous work on the Kraichnan (1968) model of turbulent scalar advection has shown that anomalous scalar dissipation, non-vanishing in the limit of vanishing viscosity and diffusivity, is in that model due to Lagrangian spontaneous stochasticity, or non-determinism of the Lagrangian particle trajectories in the limit. We here extend this result to scalars advected by any divergence-free velocity field, including solutions of the incompressible Navier-Stokes equation. For active scalars we prove that anomalous scalar dissipation requires spontaneous stochasticity while for passive scalars we prove that the two phenomena are completely equivalent. These results hold for flows in domains without walls (e.g. periodic boxes) and for insulating/impermeable walls with zero scalar fluxes. On the other hand, for flows with imposed scalar values or non-vanishing scalar fluxes at the walls, spontaneous stochasticity still implies anomalous scalar dissipation but simple examples show that another distinct mechanism of non-vanishing dissipation can be thin scalar boundary layers near the walls. As a second application of the fluctuation-dissipation relation we consider an important problem of the latter type: turbulent Rayleigh-Bénard convection in a right-cylindrical cell of arbitrary cross-section. We here obtain an exact relation between the steady-state thermal dissipation and the time for diffusive tracer particles released at the top or bottom wall to mix to their final uniform value near those walls. We show that an “ultimate regime” of convection as predicted by Kraichnan (1962) will occur at high Rayleigh numbers, unless this near-wall mixing time is asymptotically much longer than the large-scale circulation time. We suggest a new criterion for the ultimate regime in terms of transition to turbulence of a thermal “mixing zone”, which is much wider than the standard thermal boundary layer. The “ultimate regime” may, however, never occur if the intensity and volume of thermal plumes decrease sufficiently rapidly with increasing Rayleigh number.

1. Introduction

A fundamental feature of turbulent flows is the enhanced dissipation of kinetic energy. It was suggested by G. I. Taylor (1917) that kinetic energy can “be dissipated in fluid

of infinitesimal viscosity”. This idea that turbulent dissipation might become independent of molecular viscosity at sufficiently high Reynolds numbers was pursued further by Kolmogorov (1941*a,c,b*) and Onsager (1945, 1949) in developing their theories of turbulence. The physical phenomenon is sometimes called the turbulent “dissipative anomaly” or even the “zeroth law of turbulence”, although it is, of course, no “law” but rather an experimentally observed phenomenon which is still only partially understood theoretically. For current empirical evidence from laboratory experiments and numerical simulations, see e.g. Kaneda *et al.* (2003); Pearson *et al.* (2002); Sreenivasan (1998), whose data are all consistent with energy dissipation in the bulk of turbulent flows being essentially independent of viscosity. Similar phenomena are expected for other turbulent systems, in particular for scalar fields advected by a turbulent fluid, such as concentrations of dyes or aerosols, temperature fluctuations, etc. It was suggested by Taylor (1922) that diffusion by turbulence should depend “little on the molecular conductivity and viscosity of the fluid” and the asymptotic independence of the dissipation rate of scalar fluctuations from the molecular transport coefficients was a fundamental assumption in the Kolmogorov-style theories of scalar turbulence developed by Obukhov (1949) and Corrsin (1951). A very comprehensive review of the empirical evidence for this hypothesis on scalar dissipation is contained in the paper of Donzis *et al.* (2005), whose compilation of data is again consistent with scalar dissipation in the bulk of turbulent flows being insensibly dependent on molecular transport coefficients at sufficiently high Reynolds and Péclet numbers. This phenomenon still requires a complete theoretical explanation.

Fundamental new ideas on the Lagrangian origin of turbulent scalar dissipation arose from mathematical work of Bernard *et al.* (1998), which was carried out in the Kraichnan (1968) model of synthetic turbulence. In this model the advecting velocity is a Gaussian random field that has Kolmogorov-type scaling of increments in space but a white-noise correlation in time. It was shown in the Kraichnan model that the dissipative anomaly for a decaying passive scalar is due to a remarkable phenomenon called *spontaneous stochasticity* (Chaves *et al.* 2003). Simply stated, Bernard *et al.* (1998) showed that Lagrangian particle trajectories become non-unique and stochastic in the infinite Reynolds-number limit for a *fixed* initial particle position and a *fixed* velocity realization, due to the spatial roughness of the advecting velocity field. More precisely, they showed that at very large Reynolds and Péclet numbers, when the velocity field is smooth but approximates a “rough” field over a long range of scales, small stochastic perturbations on Lagrangian trajectories due to molecular diffusivity lead to persistent randomness over any finite times even as the perturbations vanish. This effect is due to the explosive (super-ballistic) dispersion of particle pairs in a turbulent flow predicted by Richardson (1926), which leads to loss of memory of initial particle separations or of amplitudes of stochastic perturbations. For excellent reviews of this and related studies on the Kraichnan model, see Falkovich *et al.* (2001); Kupiainen (2003); Gawędzki (2008).

Since this pioneering work, however, there have been persistent doubts expressed concerning the validity of these results for real hydrodynamic turbulence. For example, Tsinober (2009) (section 5.4.5) has argued that in real fluids “the flow field is smooth. In such flows ‘phenomena’ like ‘spontaneous stochasticity’ and ‘breakdown of Lagrangian flow’ do not arise and one has to look at different more realistic possibilities.” This is a simple misunderstanding, because spontaneous stochasticity is a phenomenon that appears for smooth velocity fields that merely appear “rough” over a long range of scales. More serious questions have been raised concerning the approximation of a white-noise temporal correlation in the Kraichnan model. In a recent detailed comparison of passive scalars in the Kraichnan model and in fluid turbulence, Sreenivasan & Schumacher (2010) have remarked that “It is still unclear in the Kraichnan model as to which qualitative and

quantitative differences arise from the finite-time correlation of the advecting flow.” This latter paper discussed also some of the challenges in extending results for the Kraichnan model to understanding of the energy cascade in Navier-Stokes turbulence. A primary purpose of the present paper is to address the questions regarding the applicability of the dissipation mechanisms in the Kraichnan model to scalars in hydrodynamic turbulence. A main result can be stated thus: *Away from boundaries and for any advecting velocity field whatsoever, spontaneous stochasticity of Lagrangian particle trajectories is sufficient for anomalous dissipation of passive scalars, and necessary for anomalous dissipation of both passive and active scalars.* Thus, there is no possible mechanism for a scalar dissipative anomaly in such situations other than spontaneous stochasticity. In fact, it seems not to be commonly appreciated that this equivalence was already obtained by Bernard *et al.* (1998) for freely decaying turbulent scalars in domains without boundary such as periodic boxes. In section 2.2 below we shall review these arguments of Bernard *et al.* (1998) and add some additional details to emphasize their generality.

However, the principal contribution of our paper is a new approach to the theory of turbulent scalar dissipation based upon an exact *fluctuation-dissipation relation for scalars*. Our new relation expresses an exact balance between the time-averaged scalar dissipation and the input of scalar fluctuations from the initial data, boundary conditions, and interior scalar sources as these are sampled by stochastic Lagrangian trajectories. By means of this identity we can extend the results of Bernard *et al.* (1998) to scalars fed by sources and to flows in wall-bounded domains. Since most engineering and geophysical flows encounter solid boundaries, this is a physically significant extension. With no-flux (Neumann) boundary conditions for the scalar, we obtain results identical to those of Bernard *et al.* (1998) for domains without boundary: namely, spontaneous stochasticity is necessary and sufficient for anomalous dissipation of a passive scalar. However, for imposed scalar values at the wall (Dirichlet conditions) or mixed Dirichlet/Neumann conditions we obtain only a lower bound on the passive scalar dissipation rate, which can imply that spontaneous stochasticity is sufficient for anomalous dissipation. Simple examples, such as pure thermal conduction with imposed heat fluxes at the walls, show that thin scalar boundary layers can in such flows provide another distinct mechanism of non-vanishing scalar dissipation for vanishing molecular diffusivity.

The importance of our exact fluctuation-dissipation relation (FDR) is not limited, on the other hand, to analysis of anomalous scalar dissipation and it is valid even when scalar dissipation may vanish as $\nu, \kappa \rightarrow 0$. In general our relation gives a new Lagrangian viewpoint on dissipation of scalars, both active and passive. As such, it generalizes some previously derived relations, such as that of Sawford *et al.* (2005); Buaria *et al.* (2016) for scalars forced by a mean scalar gradient and the exact balance relations for stochastic scalar sources which are Gaussian white-in-time (Novikov (1965)). The wide applicability of our FDR opens up a Lagrangian perspective on scalar dissipation for a great many situations. As a particular example in this paper, we present our FDR concretely and at length for the problem of turbulent Rayleigh-Bénard convection. We show in this situation that the space- and time-averaged thermal dissipation is exactly related to the time-correlations of the successive incidences of stochastic Lagrangian trajectories on the top and bottom walls. In fact, *the time-averaged scalar dissipation rate, apart from externally controlled parameters, is directly proportional to a correlation time of wall-incidences, or, equivalently, a mixing time of near-wall particle distributions to a uniform distribution.* The connection to scalar dissipation arises because the fluctuations in scalar input are due to the variable time which each particular stochastic Lagrangian trajectory spends at the heated or cooled walls. When the particle distribution near

these walls relaxes to uniform, then each trajectory carries the same scalar input and the fluctuations vanish.

On the basis of this exact FDR, we discuss phenomenological Nusselt-Rayleigh scaling laws for Rayleigh-Bénard turbulence and their relation to near-wall mixing by coherent structures such as thermal plumes and global convective wind. (Ahlers *et al.* 2009; Chillà & Schumacher 2012). A striking consequence of our FDR is that *an “ultimate regime” of convection as predicted by Kraichnan (1962) will occur unless the near-wall mixing time is asymptotically much larger than either the free-fall time or the large-scale circulation time.* Such an “ultimate regime” can occur (in the strict sense, with no logarithmic corrections) if and only if there are dissipative anomalies for both temperature fluctuations and kinetic energy in convective turbulence. If the mixing time greatly exceeds the large-scale circulation time (as implied by Nusselt-number measurements at currently achievable Rayleigh numbers), then Lagrangian tracer particles spend this long mixing time traversing a central region of the flow outside a near-wall “mixing zone”. The latter has a width ℓ_T decreasing inversely to the square-root of the Nusselt number and which is thus much greater than the standard thermal boundary layer thickness δ_T , that is inversely proportional to Nusselt number. This “mixing zone” might be identified with the similar concept proposed by Castaing *et al.* (1989) and Procaccia *et al.* (1991). One possible explanation for the failure to observe Kraichnan’s “ultimate scaling” at moderately large Rayleigh numbers is that turbulent transport in the central region is confined to eddies well outside the “mixing zone.” We suggest that an “ultimate regime” may occur when the Reynolds-number for eddies at distance ℓ_T from the top/bottom walls reaches the critical value for transition to turbulence. On the other hand, it is possible that an “ultimate regime” never occurs for any Rayleigh number, if there is a mechanism which can lead to extremely long mixing times. Some possible mechanisms suggested by empirical observations are decreasing velocity of the global wind and decreasing volume fraction of thermal plumes with increasing Rayleigh numbers. However, it is unclear if these effects can account quantitatively for the observed deviations from Kraichnan scaling even at Rayleigh numbers achieved heretofore. We argue that further empirical studies of the mixing time and of possible mechanisms for reduced near-wall mixing can cast significant new light on the Nusselt scaling.

The detailed contents of this paper are as follows: In section 2 we first consider the case of flows in domains without walls, deriving the stochastic representation and FDR (2.1), reviewing the notion of spontaneous stochasticity (2.2), and establishing its connections with anomalous dissipation (2.3,2.4). We then turn to the case of wall-bounded flows with imposed scalar fluxes in section 3, deriving the FDR (3.1) and relating spontaneous stochasticity and anomalous dissipation (3.2). A long subsection 3.3 discusses the specific example of turbulent Rayleigh-Bénard convection with flux boundary conditions, first discussing necessary background (3.3.1), deriving the FDR concretely (3.3.2), and then drawing physical conclusions (3.3.3). The next section 4 discusses flows with imposed scalar values at the wall and mixed conditions, deriving first an FDR inequality (4.1), using it to relate spontaneous stochasticity to anomalous dissipation (4.2), then deriving an FDR equality (4.3) and discussing mixed boundary conditions (4.4), with standard Rayleigh-Bénard convection as an important concrete example. In the summary and discussion section 5 we discuss outlook and challenges, including that of relating spontaneous stochasticity to anomalous dissipation of kinetic energy. Five appendices give further details, including rigorous mathematical proofs of all of the results in the main text. These deal with the relations between spontaneous stochasticity and anomalous dissipation (Appendix A), a useful example of pure heat conduction (Appendix B), derivation of the steady-state FDR for Rayleigh-Bénard convection (Appendix C), re-

lation of the scalar FDR to some previous results in the literature (Appendix D), and discussion of numerical methods employed (Appendix E).

2. Flows in Domains Without Walls

We consider in this first section turbulent fluid flows in finite domains without walls. A relevant numerical example is DNS of turbulence in a periodic box. A set of examples from Nature is provided by large-scale flows in thin planetary atmospheres, which can be modeled as 2D flows on a sphere. Mathematically speaking, the results in this section apply to fluid flows on any compact Riemannian manifold without boundary, merely replacing the Wiener process with the Brownian motion on the manifold whose infinitesimal generator is the Laplace-Beltrami operator (Ikeda & Watanabe 1989). For simplicity of presentation, we derive the relation only for periodic domains.

Scalar fields θ (such as temperature, dye or pollutants) transported by a fluid with velocity \mathbf{u} are described by the advection-diffusion equation

$$\partial_t \theta + \mathbf{u} \cdot \nabla \theta = \kappa \Delta \theta + S \quad (2.1)$$

with $S(\mathbf{x}, t)$ a source field and with $\kappa > 0$ the molecular diffusivity of the scalar. The work of Bernard *et al.* (1998) employed a stochastic representation of the solutions of this equation which is known as the Feynman-Kac representation in the mathematics literature (Oksendal 2013) and as a stochastic Lagrangian representation in the turbulence modeling field (Sawford 2001). We discuss presently this representation only for domains Ω without boundaries, as assumed also by Bernard *et al.* (1998), and in the following section we describe the extension to wall-bounded domains. We shall further discuss in this paper only advection by an incompressible fluid satisfying

$$\nabla \cdot \mathbf{u} = 0 \quad (2.2)$$

so that the ideal advection term formally conserves all integrals of the form $I_h(t) = \int_{\Omega} d^d x h(\theta(\mathbf{x}, t))$ for any continuous function $h(\theta)$. Note that the representation applies in any space dimension d , with most immediate physical interest for $d = 2, 3$ of course.

2.1. Stochastic Representation and Exact Fluctuation-Dissipation Relation

The stochastic representation involves stochastic Lagrangian flow maps $\tilde{\xi}_{t,s}^{\nu,\kappa}(\mathbf{x})$ describing the motion of particles labelled by their positions \mathbf{x} at time t to random positions at earlier times $s < t$. The physical relevance of the backward-in-time particle trajectories can be anticipated from the fact that the advection-diffusion equation (2.1) mixes (averages) the values of the scalar field given in the past and not, of course, the future values. Mathematically, the relevant stochastic flows are governed by the backward Itô stochastic differential equations:

$$\hat{d}_s \tilde{\xi}_{t,s}^{\nu,\kappa}(\mathbf{x}) = \mathbf{u}^{\nu}(\tilde{\xi}_{t,s}^{\nu,\kappa}(\mathbf{x}), s) ds + \sqrt{2\kappa} \hat{d}\tilde{\mathbf{W}}_s, \quad \tilde{\xi}_{t,t}^{\nu,\kappa}(\mathbf{x}) = \mathbf{x}. \quad (2.3)$$

Here $\tilde{\mathbf{W}}_s$ is a standard Brownian motion and \hat{d}_s denotes the backward Itô stochastic differential in the time s . For detailed discussions of backward Itô equations and stochastic flows, see Friedman (2006); Kunita (1997). For those who are familiar with the more standard forward Itô equations, the backward equations are simply the time-reverse of the forward ones. Thus, a backward Itô equation in the time variable s is equivalent to a forward Itô equation in the time $\hat{s} = t_r - s$ reflected around a chosen reference time t_r †.

† We note that the difference between forward- and backward-Itô equations is not essentially the direction of time in which they are integrated. Rather, the difference has to do with the

The noise term involving the Brownian motion in Eq.(2.3) is proportional to the square root of the molecular diffusivity κ . The velocity field \mathbf{u}^ν is assumed to be smooth so long as the parameter $\nu > 0$. In the case of greatest physical interest when \mathbf{u}^ν is a solution of the incompressible Navier-Stokes equation, then ν represents the kinematic viscosity and we assume, for simplicity of presentation, that there is no blow-up in those solutions. (See Rezakhanlou (2014) for weak solutions.) Because equation (2.3) involves both ν and κ , its random solutions $\tilde{\xi}_{t,s}^{\nu,\kappa}$ have statistics which depend upon those parameters, represented by the superscripts. To avoid a too heavy notation, we omit those superscripts and write simply $\tilde{\xi}_{t,s}$ unless it is essential to refer to the dependence upon ν, κ . Note that when $\kappa = 0$ and \mathbf{u}^ν remains smooth, then $\xi_{t,s}^{\nu,0}(\mathbf{x})$ is no longer stochastic and gives the usual reverse Lagrangian flow from time t backward to the earlier time $s < t$.

The stochastic representation of the solutions of the advection-diffusion equation follows from the backward differential

$$\begin{aligned} \hat{d}_s \theta(\tilde{\xi}_{t,s}(\mathbf{x}), s) &= [(\partial_s + \mathbf{u}^\nu \cdot \nabla - \kappa \Delta) \theta](\tilde{\xi}_{t,s}(\mathbf{x}), s) ds + \sqrt{2\kappa} \hat{d}\tilde{\mathbf{W}}_s \cdot \nabla \theta(\tilde{\xi}_{t,s}(\mathbf{x}), s) \\ &= S(\tilde{\xi}_{t,s}(\mathbf{x}), s) ds + \sqrt{2\kappa} \hat{d}\tilde{\mathbf{W}}_s \cdot \nabla \theta(\tilde{\xi}_{t,s}(\mathbf{x}), s), \end{aligned} \quad (2.4)$$

using the backward Itô formula (Friedman 2006; Kunita 1997) in the first line and Eq.(2.1) in the second. Integrating over time s from 0 to t , gives

$$\theta(\mathbf{x}, t) = \theta_0(\tilde{\xi}_{t,0}(\mathbf{x})) + \int_0^t S(\tilde{\xi}_{t,s}(\mathbf{x}), s) ds + \sqrt{2\kappa} \int_0^t \hat{d}\tilde{\mathbf{W}}_s \cdot \nabla \theta(\tilde{\xi}_{t,s}(\mathbf{x}), s), \quad (2.5)$$

where θ_0 is the initial data for the scalar at time 0. Because the backward Itô integral term in (2.5) averages to zero, one obtains

$$\theta(\mathbf{x}, t) = \mathbb{E} \left[\theta_0(\tilde{\xi}_{t,0}(\mathbf{x})) + \int_0^t S(\tilde{\xi}_{t,s}(\mathbf{x}), s) ds \right] \quad (2.6)$$

where \mathbb{E} denotes the average over the Brownian motion. Eq.(2.6) is the desired stochastic representation of the solution. Note that the reverse statement is also true, that the field $\theta(\mathbf{x}, t)$ defined *a priori* by Eq.(2.6) is the solution of the advection-diffusion equation (2.1) for the initial data θ_0 . For a simple proof, see section 4.1 of Eyink & Drivas (2015b) which gives the analogous argument for Burgers equation.

As an aside, it is also known that the scalar values along stochastic Lagrangian trajectories $\theta(\tilde{\xi}_{t,s}(\mathbf{x}), s)$ are, for $S \equiv 0$, *martingales* backward in time. This means that

$$\mathbb{E} \left[\theta(\tilde{\xi}_{t,s}(\mathbf{x}), s) \middle| \{ \tilde{\mathbf{W}}_\tau, r < \tau < t \} \right] = \theta(\tilde{\xi}_{t,r}(\mathbf{x}), r), \quad s < r < t \quad (2.7)$$

where the expectation is conditioned upon knowledge of the Brownian motion over the time interval $[r, t]$. Thus, the conditional average value is the last known value (going backward in time). This is the property for diffusive flow which corresponds to the statement for pure smooth advection that θ is conserved along Lagrangian trajectories, or that $\theta(\xi_{t,s}(\mathbf{x}), s)$ is constant in s . The proof is obtained by integrating the differential

time-direction in which those equations are *adapted* (Friedman 2006; Kunita 1997). Thus, a forward Itô differential $b(\tilde{\mathbf{W}}_t) d\tilde{\mathbf{W}}_t$ is discretized in time as $b(\tilde{\mathbf{W}}_{t_n})(\tilde{\mathbf{W}}_{t_{n+1}} - \tilde{\mathbf{W}}_{t_n})$ for $t_{n+1} > t_n$, with the increment $\tilde{\mathbf{W}}_{t_{n+1}} - \tilde{\mathbf{W}}_{t_n}$ statistically independent of $\tilde{\mathbf{W}}_t$ for $t \leq t_n$. Instead, a backward Itô differential $b(\tilde{\mathbf{W}}_t) \hat{d}\tilde{\mathbf{W}}_t$ is discretized as $b(\tilde{\mathbf{W}}_{t_n})(\tilde{\mathbf{W}}_{t_n} - \tilde{\mathbf{W}}_{t_{n-1}})$ for $t_n > t_{n-1}$, with $\tilde{\mathbf{W}}_{t_n} - \tilde{\mathbf{W}}_{t_{n-1}}$ statistically independent of $\tilde{\mathbf{W}}_t$ for $t \geq t_n$. The distinction only matters when, as in our equation (2.4), the differential of $\tilde{\mathbf{W}}_s$ is multiplied by a stochastic function of $\tilde{\mathbf{W}}$.

(2.4) over the time-interval $[s, t]$ to obtain

$$\theta(\tilde{\xi}_{t,s}(\mathbf{x}), s) = \theta(\mathbf{x}, t) - \sqrt{2\kappa} \int_s^t \hat{d}\tilde{\mathbf{W}}_\tau \cdot \nabla \theta(\tilde{\xi}_{t,\tau}(\mathbf{x}), \tau) \, d\tau. \quad (2.8)$$

and then exploiting the corresponding martingale property of the backward Itô integral (Friedman 2006; Kunita 1997). It is important to emphasize that the martingale property like (2.7) does not hold forward in time, which would instead give a solution of the negative-diffusion equation with κ replaced by $-\kappa < 0$. Thus, the backward-in-time martingale property (2.7) expresses the arrow of time arising from the irreversibility of the diffusion process.

The main result of this paper is a new exact fluctuation-dissipation relation between scalar dissipation due to molecular diffusivity and fluctuations associated to stochastic Lagrangian trajectories. To state the result, we introduce a stochastic scalar field[†]

$$\tilde{\theta}(\mathbf{x}, t) \equiv \theta_0(\tilde{\xi}_{t,0}(\mathbf{x})) + \int_0^t S(\tilde{\xi}_{t,s}(\mathbf{x}), s) \quad (2.9)$$

which, according to Eq.(2.6), satisfies $\theta(\mathbf{x}, t) = \mathbb{E}[\tilde{\theta}(\mathbf{x}, t)]$ when averaged over Brownian motions. Thus $\tilde{\theta}(\mathbf{x}, t)$ in (2.9) represents the contribution to $\theta(\mathbf{x}, t)$ from an individual stochastic Lagrangian trajectory as it samples the initial data θ_0 and scalar source S backward in time. Using this definition and (2.6) we can rewrite (2.5) as

$$\tilde{\theta}(\mathbf{x}, t) - \mathbb{E}[\tilde{\theta}(\mathbf{x}, t)] = -\sqrt{2\kappa} \int_0^t \hat{d}\tilde{\mathbf{W}}_s \cdot \nabla \theta(\tilde{\xi}_{t,s}(\mathbf{x}), s). \quad (2.10)$$

Squaring this equation and averaging over the Brownian motion gives

$$\text{Var}[\tilde{\theta}(\mathbf{x}, t)] = 2\kappa \int_0^t ds \, \mathbb{E}[|\nabla \theta(\tilde{\xi}_{t,s}(\mathbf{x}), s)|^2], \quad (2.11)$$

where “Var” on the lefthand side denotes the stochastic scalar variance in the average over the Brownian motion and on the righthand side we have used the Itô isometry (see Oksendal (2013), section 3.1) to evaluate the mean square of the backward Itô integral. If we now average in \mathbf{x} over the flow domain Ω , use the fact that the stochastic flows $\tilde{\xi}_{t,s}$ with condition (2.2) preserve volume, and divide by 1/2 we obtain

$$\frac{1}{2} \langle \text{Var} \tilde{\theta}(t) \rangle_\Omega = \kappa \int_0^t ds \langle |\nabla \theta(s)|^2 \rangle_\Omega. \quad (2.12)$$

This is our exact *fluctuation-dissipation relation* (FDR). The quantity on the right is just the volume-averaged and cumulative (time-integrated) scalar dissipation, and the quantity on the left is (half) the stochastic scalar variance. The relation (2.12) thus represents a balance between scalar dissipation and the input of scalar fluctuations from the initial scalar field and the scalar sources, as sampled by stochastic Lagrangian trajectories backward in time.

It is important to emphasize that the origin of statistical fluctuations in our relation (2.12) is *not* that assumed in most traditional discussions of turbulence, i.e. random ensembles of initial scalar fields, of advecting velocity fields, or of stochastic scalar sources. Our FDR (2.12) is valid for fixed realizations of all of those quantities. Instead, the origin of randomness is the Brownian motions in the stochastic flow equation (2.3), which are simply a means to model mathematically the effects of molecular diffusion. We can,

[†] Note that for all $s < t$ the quantity $\tilde{\theta}(\mathbf{x}, t; s) = \theta(\tilde{\xi}_{t,s}(\mathbf{x}), s) + \int_s^t S(\tilde{\xi}_{t,r}(\mathbf{x}), r) \, dr$ is a martingale backward in time, by the same argument used previously for $S = 0$.

however, average subsequently over random ensembles of initial scalar fields, of advecting velocity fields, or of scalar sources. In this manner we recover from (2.12) as special cases some known results. For example, when the scalar source is a random field with zero mean and delta-correlated in time,

$$\langle \tilde{S}(\mathbf{x}, t) \tilde{S}(\mathbf{x}', t') \rangle = 2C_S(\mathbf{x}, \mathbf{x}') \delta(t - t'), \quad (2.13)$$

then we recover the steady-state balance equation for the scalar dissipation

$$\langle \kappa |\nabla \theta|^2 \rangle_{\Omega, \infty, S} = \frac{1}{V} \int_{\Omega} d^d x C_S(\mathbf{x}, \mathbf{x}) \quad (2.14)$$

where the average on the left is over space domain Ω , an infinite time-interval, and the random source \tilde{S} . This is the standard result usually derived for Gaussian random source fields as an application of the Furutsu-Donsker-Novikov theorem (Frisch (1995); Novikov (1965)). Similar relations hold for freely decaying scalars with no sources but random initial scalar fields. For example, when the initial scalar has a uniform random space-gradient, $\tilde{\theta}_0(\mathbf{x}) = \tilde{\mathbf{G}} \cdot \mathbf{x}$ with isotropic statistics

$$\langle \tilde{\mathbf{G}} \tilde{\mathbf{G}}^\top \rangle_G = G^2 \mathbf{I}, \quad (2.15)$$

then we recover a relation of Sawford *et al.* (2005); Buaria *et al.* (2016)

$$\kappa \int_0^t ds \langle |\nabla \theta(s)|^2 \rangle_{\Omega, \theta_0} = \frac{1}{4} G^2 \mathbb{E}^{1,2} \left\langle \left| \tilde{\boldsymbol{\xi}}_{t,0}^{(1)} - \tilde{\boldsymbol{\xi}}_{t,0}^{(2)} \right|^2 \right\rangle_{\Omega} \quad (2.16)$$

where the 1, 2 averages are taken over two independent ensembles of Brownian motion. We delay the derivation of these particular consequences to Appendix D, since the proofs require additional material which will be introduced in subsequent sections.

Note, finally, that the result (2.11) provides a spatially *local fluctuation-dissipation relation*, which we may write in the form

$$\frac{1}{2t} \text{Var} [\tilde{\theta}(\mathbf{x}, t)] = \left\langle \mathbb{E} \left[\kappa |\nabla \theta(\tilde{\boldsymbol{\xi}}_{t,s}(\mathbf{x}), s)|^2 \right] \right\rangle_t, \quad (2.17)$$

where on the right the average in s over the time interval $[0, t]$ is carried out along stochastic Lagrangian trajectories moving backward-in-time from space-time point (\mathbf{x}, t) . It follows that at short times the local scalar variance exactly recovers the local scalar dissipation:

$$\lim_{t \rightarrow 0} \frac{1}{2t} \text{Var} [\tilde{\theta}(\mathbf{x}, t)] = \kappa |\nabla \theta(\mathbf{x}, 0)|^2. \quad (2.18)$$

A substantial spatial correlation between $\frac{1}{2t} \text{Var} [\tilde{\theta}(\mathbf{x}, t)]$ and $\varepsilon_\theta(\mathbf{x}, t) = \kappa |\nabla \theta(\mathbf{x}, t)|^2$ should persist for relatively short times t . On the other hand, in the long-time limit the local scalar variance becomes *space-time-independent* and equals

$$\lim_{t \rightarrow \infty} \frac{1}{2t} \text{Var} [\tilde{\theta}(\mathbf{x}, t)] = \langle \kappa |\nabla \theta|^2 \rangle_{\Omega, \infty} \quad \text{for all } \mathbf{x} \in \Omega. \quad (2.19)$$

To see that this should be true, note that the random variables $\tilde{\boldsymbol{\xi}}_{t,s}(\mathbf{x}) \in \Omega$ for each fixed \mathbf{x} are an ergodic random process in the time-variable s for $\kappa > 0$. Because of incompressibility of the velocity field and the ergodicity of the stochastic Lagrangian flow, the variables $\tilde{\boldsymbol{\xi}}_{t,s}(\mathbf{x})$ will be nearly uniformly distributed over Ω at times $s \leq t - \tau$, where τ is a characteristic scalar mixing time. This time τ will be at most of the order L^2/κ , where L is the diameter of the domain, and thus finite for $\kappa > 0$, but usually much

shorter because of advective mixing by the velocity field. For any positive integer n

$$\lim_{t \rightarrow \infty} \frac{1}{2t} \text{Var} [\tilde{\theta}(\mathbf{x}, t)] = \lim_{t \rightarrow \infty} \frac{1}{t} \int_0^{t-n\tau} ds \mathbb{E} [\kappa |\nabla \theta(\tilde{\boldsymbol{\xi}}_{t,s}(\mathbf{x}), s)|^2], \quad (2.20)$$

since the corrections are vanishing as $O(n\tau/t)$. By choosing an n sufficiently large but fixed as $t \rightarrow \infty$, we can make the righthand side arbitrarily close to

$$\lim_{t \rightarrow \infty} \frac{1}{t - n\tau} \int_0^{t-n\tau} ds \langle \kappa |\nabla \theta(\boldsymbol{\xi}, s)|^2 \rangle_{\Omega} = \langle \kappa |\nabla \theta(\boldsymbol{\xi}, s)|^2 \rangle_{\Omega, \infty}, \quad (2.21)$$

where the space-time average $\langle \cdot \rangle_{\Omega, \infty}$ on the right is over $\boldsymbol{\xi} \in \Omega$ and $s \in [0, \infty)$. Since $\lim_{t \rightarrow \infty} \frac{1}{2t} \text{Var} [\tilde{\theta}(\mathbf{x}, t)]$ is independent of the choice of n , we obtain (2.19). Of course, here we have assumed all of the various infinite-time averages to exist, as they shall (at least along subsequences of times $t_k \rightarrow \infty$) if the space-averaged scalar dissipation remains a bounded function of time.

2.2. Spontaneous Stochasticity of Lagrangian Trajectories

We now specialize in this subsection to the source-less case $S \equiv 0$, in order to make contact with the work of Bernard *et al.* (1998) on spontaneous stochasticity and anomalous scalar dissipation. The stochastic representation (2.6) simplifies in this case to

$$\theta(\mathbf{x}, t) = \mathbb{E} [\theta_0(\tilde{\boldsymbol{\xi}}_{t,0}^{\nu, \kappa}(\mathbf{x}))] = \int d^d x_0 \theta_0(\mathbf{x}_0) p^{\nu, \kappa}(\mathbf{x}_0, 0 | \mathbf{x}, t) \quad (2.22)$$

where we have introduced the backward-in-time transition probability

$$p^{\nu, \kappa}(\mathbf{x}', t' | \mathbf{x}, t) = \mathbb{E} [\delta^d(\mathbf{x}' - \tilde{\boldsymbol{\xi}}_{t,t'}^{\nu, \kappa}(\mathbf{x}))] \quad t' < t \quad (2.23)$$

for the stochastic flow. As already noted, the stochastic flow preserves volume when the velocity field is divergence-free. In terms of the transition probability this means that

$$\int p^{\nu, \kappa}(\mathbf{x}', t' | \mathbf{x}, t) d^d x = 1, \quad (2.24)$$

where $\det(\partial \tilde{\boldsymbol{\xi}}_{t,t'}^{\nu, \kappa}(\mathbf{x}) / \partial \mathbf{x}) = 1$ is used to write $\delta^d(\mathbf{x}' - \tilde{\boldsymbol{\xi}}_{t,t'}^{\nu, \kappa}(\mathbf{x})) = \delta^d(\mathbf{x} - (\tilde{\boldsymbol{\xi}}_{t,t'}^{\nu, \kappa})^{-1}(\mathbf{x}'))$ and perform the integral over \mathbf{x} . Note that if the limit $\kappa \rightarrow 0$ is taken with ν fixed (infinite Prandtl number limit), then the stochastic flow (2.23) becomes deterministic and

$$p^{\nu, 0}(\mathbf{x}', t' | \mathbf{x}, t) = \delta^d(\mathbf{x}' - \boldsymbol{\xi}_{t,t'}^{\nu, 0}(\mathbf{x})), \quad t' < t. \quad (2.25)$$

which corresponds to a single deterministic Lagrangian trajectory passing through position \mathbf{x} at time t .

In the Kraichnan model of turbulent advection it was shown by Bernard *et al.* (1998) that the joint limit $\nu, \kappa \rightarrow 0$ with $Pr = \nu/\kappa$ fixed is non-deterministic and corresponds to more than one Lagrangian trajectory passing through space-time point (\mathbf{x}, t) . We remind the reader that the Kraichnan model of turbulent advection replaces the Navier-Stokes solution with a realization drawn from an ensemble of Gaussian random fields \mathbf{u}^{ν} with mean zero $\langle \mathbf{u}^{\nu} \rangle = \mathbf{0}$ and covariance satisfying

$$\langle [u_i^{\nu}(\mathbf{x} + \mathbf{r}, t) - u_i^{\nu}(\mathbf{x}, t)][u_j^{\nu}(\mathbf{x} + \mathbf{r}, t') - u_j^{\nu}(\mathbf{x}, t')] \rangle = D_{ij}^{\nu}(\mathbf{r}) \delta(t - t') \quad (2.26)$$

for a spatial covariance function satisfying $D_{ij}^{\nu}(\mathbf{r}) = D_{ji}^{\nu}(\mathbf{r})$, $\partial D_{ij}^{\nu}(\mathbf{r}) / \partial r_j = 0$, and

$$D_{ii}(\mathbf{r}) \sim \begin{cases} D_1 r^{\xi} & \ell_{\nu} \ll r \ll L \\ D_2 r^2 & r \ll \ell_{\nu} \end{cases} \quad (2.27)$$

for some $0 < \xi < 2$, with the effective “dissipation length”

$$\ell_\nu = (D_1/D_2)^{1/(2-\xi)}. \quad (2.28)$$

Note that $D_2 \propto \langle |\nabla \mathbf{u}^\nu|^2 \rangle$ and in real turbulence would be proportional to ε/ν , where ε is the viscous energy dissipation. Hence, $D_2 \rightarrow \infty$ or $\ell_\nu \rightarrow 0$ with D_1 fixed is the analogue for the Kraichnan model of the infinite Reynolds-number limit for Navier-Stokes turbulence. In fact, one can introduce a “viscosity” parameter ν for the Kraichnan model with units of (length)²/(time), so that $\ell_\nu = (\nu/D_1)^{1/\xi}$. For any $\nu > 0$ the velocity realizations are spatially smooth, but in the limit $\nu \rightarrow 0$ they are only Hölder continuous in space with exponent $0 < \xi/2 < 1$. It is well-known that for such “rough” limiting velocity fields the solutions of the deterministic initial-value problem

$$d\xi(s)/ds = \mathbf{u}(\xi(s), s), \quad \xi(t) = \mathbf{x} \quad (2.29)$$

need not be unique and, if not, form a continuum of solutions (e.g. see Hartman (2002)). In the Kraichnan model it has been proved in the double limit with both $\nu \rightarrow 0$ and $\kappa \rightarrow 0$ that the transition probabilities tend to a limiting form

$$p^*(\mathbf{x}', t' | \mathbf{x}, t) = \lim_{\nu, \kappa \rightarrow 0} p^{\nu, \kappa}(\mathbf{x}', t' | \mathbf{x}, t). \quad (2.30)$$

It is important to stress here that no average is taken over \mathbf{u} in defining these transition probabilities, but only an average over Brownian motions in the stochastic flow equations (2.3), while the velocity realization is held fixed[†]. Most importantly, the limiting transition probabilities for the Kraichnan model are *not* delta-distributions of the form (2.25) but nontrivial probabilities over an ensemble of non-unique solutions of the limiting ODE (2.29)! This remarkable phenomenon is called *spontaneous stochasticity*. See Bernard *et al.* (1998) and the later papers of Gawędzki & Vergassola (2000); E & Vanden-Eijnden (2000, 2001); Falkovich *et al.* (2001); Le Jan & Raimond (2002, 2004).

As shown in those works, spontaneous stochasticity occurs because of the analogue of Richardson (1926) dispersion in the Kraichnan model, which leads to a loss of influence of the molecular diffusivity κ on the separation of the perturbed Lagrangian trajectories after a short time of order $(\kappa^{2-\xi}/D_1)^{1/\xi}$. It is important to emphasize that this result does not mean that randomness in the Lagrangian trajectories suddenly “appears” only for $\nu, \kappa = 0$ but instead that the randomness *persists* even as $\nu, \kappa \rightarrow 0$. It is thus a phenomenon that can be observed with sequences of positive values, $\nu, \kappa > 0$, for which the velocity field is smooth. For the case of a divergence-free velocity that we discuss here, it is furthermore known that the result does not depend upon the order of limits $\nu \rightarrow 0$ and $\kappa \rightarrow 0$ which can be taken in either order or together[‡]. See Bernard *et al.* (1998); Gawędzki & Vergassola (2000); E & Vanden-Eijnden (2000, 2001); Falkovich *et al.* (2001); Le Jan & Raimond (2002, 2004) for discussions of this point.

There is empirical evidence for such phenomena also in Navier-Stokes turbulence ob-

[†] It would be less ambiguous to write them as $p_{\mathbf{u}^\nu}^{\nu, \kappa}(\mathbf{x}', t' | \mathbf{x}, t)$, with \mathbf{u} denoting the fixed flow realization, but this would lead to an even heavier notation.

[‡] The only delicate case is when $\kappa \rightarrow 0$ first, so that the Prandtl number goes to infinity, and then $\nu \rightarrow 0$ subsequently. Since the Brownian motion disappears from the stochastic equation (2.3) while the velocity field remains smooth, the limiting Lagrangian trajectories are deterministic. To observe spontaneous stochasticity in that limit one must additionally allow the *initial condition* to be random, e.g. with $\tilde{\xi}(t) = \mathbf{x} + \epsilon \tilde{\rho}$ for a stochastic perturbation $\tilde{\rho}$ drawn from some fixed distribution $P(\rho)$. In that case, spontaneous stochasticity appears in the double limit with $\epsilon \rightarrow 0$ and $\nu \rightarrow 0$ together and, for a divergence-free velocity \mathbf{u} , the limiting transition probabilities are identical to those obtained for the other limits involving $\kappa \rightarrow 0$. This infinite-Prandtl case is discussed carefully by Gawędzki & Vergassola (2000) and E & Vanden-Eijnden (2000).

tained from numerical studies of 2-particle dispersion. Eyink (2011) studied stochastic Lagrangian particles whose motion is governed by Eq.(2.3) in a 1024^3 DNS at $Re_\lambda = 433$ and found that the mean-square dispersion becomes independent of κ after a short time of order $(\kappa/\varepsilon)^{1/2}$. Bitane *et al.* (2013) studied dispersion of deterministic Lagrangian trajectories ($\kappa = 0$) in a 2048^3 DNS at $Re_\lambda = 460$ and a 4096^3 DNS at $Re_\lambda = 730$, and found that the mean-square dispersion becomes independent of the initial separation r_0 of particle pairs in a short time of order $r_0^{2/3}/\varepsilon^{1/3}$. The results of these studies provide evidence of Lagrangian spontaneous stochasticity for Navier-Stokes solutions. The primary limitation of those works is that the joint limit $\nu, \kappa \rightarrow 0$ could not be studied (although Bitane *et al.* (2013) did find consistent Richardson-dispersion statistics for the two Reynolds numbers studied there). One should consider together with the limit $\kappa \rightarrow 0$ also a limit $\nu \rightarrow 0$ so that the Navier-Stokes solution \mathbf{u}^ν converges to a fixed velocity \mathbf{u} that is some sort of weak solution of Euler (as always occurs along a suitable subsequence $\nu_k \rightarrow 0$; see Lions (1996), section 4.4)¶. In addition, both of these previous studies averaged over the release points \mathbf{x} of the particles. A particle dispersion averaged over release points which remains non-vanishing in the joint limit $\nu, \kappa \rightarrow 0$ is enough to infer spontaneous stochasticity for a set of points \mathbf{x} of non-zero volume measure (Bernard *et al.* 1998). However, averaging over \mathbf{x} removes information about the effects of spatial intermittency and the local fluid environment on the limiting behavior of the particle distributions $p^{\nu, \kappa}(\mathbf{x}', t' | \mathbf{x}, t)$ for specific release locations \mathbf{x} .

We present here new data obtained from numerical experiments on a high Reynolds-number turbulence simulation in a 2π -periodic box, for a couple of representative release points. We use simulation data from the homogeneous, isotropic dataset in the Johns Hopkins Turbulence Database (Li *et al.* (2008); Yu *et al.* (2012)), publicly available online at <http://turbulence.pha.jhu.edu>. It is ideal for our purposes, since the entire time-history of the velocity is stored for a full large-scale eddy-turnover time, allowing us to integrate backward in time the flow equations (2.3). We consider two release points \mathbf{x} at time $t_f = 2.048$, the final database time, one chosen in a typical turbulent “background” region and the other in the vicinity of a strong, large-scale vorticity. We study stochastic trajectories with diffusivities κ corresponding to three values of the Prandtl number, $Pr = 0.1, 1, \text{ and } 10$. We solved Eq.(2.3) with the Euler-Maruyama scheme, which for additive noise is 1st-order in both weak and strong sense (Kloeden & Platen 1992). The turbulent velocity field in Eq.(2.3) was retrieved with the `getVelocity` database function, which returns velocities at requested points interpolated in space by 6th-order Lagrange polynomials and in time by piecewise-cubic Hermite polynomials. We used time-step $\Delta s = 6.6 \times 10^{-4}$, or 1/3 of the time between database frames. We calculated statistics with averages over independent solutions of Eq.(2.3) and, to test for weak convergence in the time-integration, we doubled Δs , with relative change $< 0.1\%$.

In Figure 1 the top panels show 30 representative particle trajectories for the two release points and for each of the three Prandtl numbers. To illustrate the local fluid environment, we also plot isosurfaces of the vorticity filtered with a box-filter of width $L/4$ (L the integral scale) at the time $s = (2/3)T_L$ (T_L the large-scale turnover time). The isosurfaces are for magnitudes of filtered vorticity equal to $15/T_L$. The left panel shows the particles released in a typical “background” region with spottier, weaker vortices and the right shows particles released near a strong vortex. The three colors of the trajectories (red/blue/green) represent the three values of the Prandtl numbers $Pr = 0.1, 1, 10$, resp. As one can see by eye, the ensembles of trajectories are quite similar for the three Pr -

¶ Amusingly, the direct experimental observation of spontaneous stochasticity in such a joint limit may be easier in quantum mechanics than in fluid mechanics. See Eyink & Drivas (2015a).

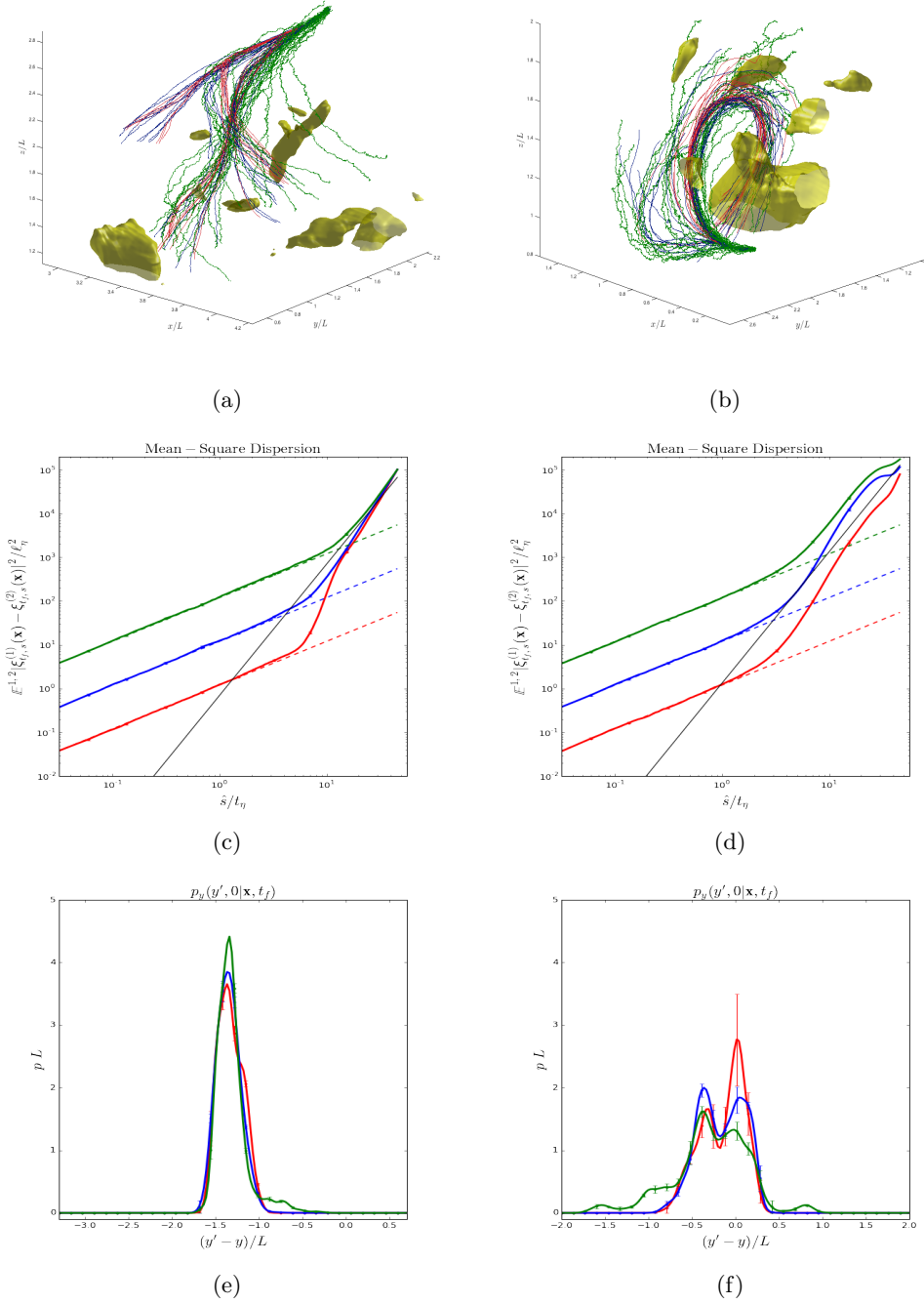


Figure 1: *Left panels* are for release at $\mathbf{x} = (4.9637, 3.1416, 3.8488)$ in background region, *Right panels* for release at $\mathbf{x} = (0.2610, 3.1416, 1.4617)$ near a strong vortex. Top panels (a),(b) plot 30 representative stochastic trajectories for $Pr = 0.1$ (green), 1.0 (blue) and 10 (red) together with isosurfaces of coarse-grained vorticity $|\bar{\omega}|T_L = 15$ (yellow) at time $s = (2/3)T_L$. Middle panels (c),(d) plot particle dispersions and short-time results $12\kappa\hat{s}$ for each Pr with the same colors as (a),(b), and a plot in **black** of $g\varepsilon\hat{s}^3$ with $g = 0.7$ (left), $g = 4/3$ (right). The bottom panels (e),(f) plot $p_y(y', 0 | \mathbf{x}, t_f)$ for the three Pr -values.

values. To make this observation more quantitative, we plot in the middle panels of Fig. 1 the mean-square dispersion of the stochastic particles for the two release points and the three Prandtl numbers. The error bars (almost too small to be observed) represent the standard error of the mean (s.e.m.) for averages over $N=1024$ sample trajectories. For both release points there is an initial period (going backward in time) where the dispersion grows diffusively as $12\kappa\hat{s}$ with $\hat{s} = t_f - s$, but which then crosses over to a regime of super-ballistic separation that is close to the \hat{s}^3 -growth predicted by Richardson (1926) and is approximately independent of Pr . The two release points shown here illustrate behavior that we have observed also in many other points of the turbulent fluid, where we find that the Richardson \hat{s}^3 -law is quite robust, without the necessity of averaging over release points \mathbf{x} . This is especially so for points \mathbf{x} in “background” regions, and is at least approximately observed for \mathbf{x} located in more intermittent regions. Finally, we plot in the bottom panels of Fig. 1 particle transition probabilities, which provide even further information about the limiting behavior. We plot at time 0, in the approximate Richardson range, the 1-dimensional PDF’s of the y -coordinate or

$$p_y^{\nu,\kappa}(y', 0|\mathbf{x}, t_f) = \int dx' dz' p^{\nu,\kappa}(\mathbf{x}', 0|\mathbf{x}, t_f) \quad (2.31)$$

for each of the two release points \mathbf{x} and three Prandtl numbers. We observe very similar behavior also for the x - and z -coordinates. In order to minimize the number of samples required to construct the PDF’s numerically, we employed kernel density estimator techniques that gave us good results with only $N = 6144$ samples. See Silverman (1986) and Appendix E, where our numerical procedures are completely described. Error bars represent both s.e.m. for the N -sample averages and the effects of variation in the kernel density bandwidth. Consistent with the dispersion plots, we see that the transition PDF’s are approximately independent of κ for times in the super-ballistic dispersion range. This is especially true for the release point \mathbf{x} in the “background” region, and for the strong vorticity region such independence holds better for the two smallest values of κ (largest Pr). Recall that in the Kraichnan model with incompressible velocity fields, the limiting densities $p^*(\mathbf{x}', 0|\mathbf{x}, t_f)$ are independent of the Prandtl number for $\nu, \kappa \rightarrow 0$ with Pr fixed (Gawędzki & Vergassola 2000; E & Vanden-Eijnden 2000, 2001) and this is approximately observed to be true in our numerical results for incompressible fluid turbulence. These numerical studies illustrate the present quality of direct evidence for Lagrangian spontaneous stochasticity in high-Reynolds-number Navier-Stokes turbulence. As we shall now demonstrate, observations of anomalous scalar dissipation provide further evidence, as the two phenomena are essentially related.

2.3. Spontaneous Stochasticity and Anomalous Dissipation

The phenomenon of spontaneous stochasticity leads to a simple explanation of anomalous dissipation for decaying scalars (no sources) in a turbulent flow, as was first pointed out by Bernard *et al.* (1998) for the Kraichnan model. Note that the stochastic representation (2.22) of the advected scalar in the limit $\nu, \kappa \rightarrow 0$ becomes, using (2.30),

$$\theta^*(\mathbf{x}, t) = \int d^d x_0 \theta_0(\mathbf{x}_0) p^*(\mathbf{x}_0, 0|\mathbf{x}, t). \quad (2.32)$$

where $\theta^*(\mathbf{x}, t)$ is a weak solution of the ideal advection equation, $\partial_t \theta^* + \mathbf{u} \cdot \nabla \theta^* = 0$. It follows from (2.32) that for any strictly convex function $h(\theta)$, e.g. $h(\theta) = \frac{1}{2}\theta^2$,

$$h(\theta^*(\mathbf{x}, t)) \leq \int d^d x_0 h(\theta_0(\mathbf{x}_0)) p^*(\mathbf{x}_0, 0|\mathbf{x}, t), \quad (2.33)$$

and equality holds if and only the transition probability is a delta-distribution of type (2.25). This is the so-called Jensen inequality (e.g. see Itô (1984)). Since the limiting transition probabilities are not delta-distributions in the Kraichnan model, the inequality in (2.33) is strict. Furthermore, the limiting transition probabilities for $\nu, \kappa \rightarrow 0$ inherit the volume-preservation property (2.24), so that

$$\int p^*(\mathbf{x}', t' | \mathbf{x}, t) d^d x = 1. \quad (2.34)$$

In that case, integrating (2.33) over \mathbf{x} gives

$$\int h(\theta^*(\mathbf{x}, t)) d^d x < \int h(\theta_0(\mathbf{x}_0)) d^d x_0, \quad (2.35)$$

so that the h -integral is decaying (dissipated) even in the limit $\nu, \kappa \rightarrow 0$. The anomalous scalar dissipation in the Kraichnan model thus has an elegant Lagrangian mechanism. Essentially, the molecular diffusivity is replaced by a “turbulent diffusivity” associated to the persistent stochasticity of the Lagrangian trajectories, which continues to homogenize the scalar field even as the molecular diffusivity vanishes.

As a matter of fact, this same argument works for a passive scalar (and, in part, for an active scalar) advected by any velocity field \mathbf{u}^ν whatsoever, as long as there are no scalar sources and the flow domain is a compact (closed, bounded) region without boundaries. In particular, the argument works when \mathbf{u}^ν is a Navier-Stokes solution in a periodic domain. More precisely, it is not known *a priori* whether spontaneous stochasticity occurs or not for a general velocity field \mathbf{u}^ν in the limit $\nu, \kappa \rightarrow 0$, but the inference which can be drawn is that *anomalous dissipation of a passive scalar occurs in the limit $\nu, \kappa \rightarrow 0$ if and only if spontaneous stochasticity of Lagrangian trajectories occurs in the same limit*. The two phenomena can only occur together. It is clear that this fact was already understood by Bernard *et al.* (1998), but it is still not widely appreciated. The same argument applies in one direction also to active scalars, showing then that anomalous scalar dissipation requires spontaneous stochasticity. Hence, for general scalars, active and passive, away from boundaries, there is no possible mechanism for anomalous scalar dissipation other than spontaneous stochasticity. It is therefore worthwhile to give the argument carefully.

We first note that the limit (2.30) of the transition probabilities as $\nu, \kappa \rightarrow 0$ holds quite generally under the stated assumptions, at least along suitably chosen subsequences $\nu_n, \kappa_n \rightarrow 0$. This can be shown using Young measure methods similar to those which have been employed previously to study statistical equilibria for 2D Euler solutions (Robert 1991; Robert & Sommeria 1991; Sommeria *et al.* 1991). Because the proof of this result is a bit technical, we give it in Appendix A. Assuming this result, we demonstrate here the equivalence of anomalous scalar dissipation and spontaneous stochasticity of Lagrangian trajectories. We first demonstrate that spontaneous stochasticity implies anomalous dissipation of passive scalars, using the same ideas as for the Kraichnan model. We give an indirect proof, supposing that there is no anomalous dissipation and showing that there can then be no spontaneous stochasticity, in contradiction to the starting assumption. Thus, we assume for some strictly convex function h that

$$\int h(\theta^*(\mathbf{x}, t)) d^d x = \int h(\theta_0(\mathbf{x}_0)) d^d x_0, \quad (2.36)$$

for all smooth initial data θ_0 . Using the volume-conserving property (2.34), we can write this equality as

$$\int d^d x \left[\int d^d x_0 h(\theta_0(\mathbf{x}_0)) p^*(\mathbf{x}_0, 0 | \mathbf{x}, t) - h(\theta^*(\mathbf{x}, t)) \right] = 0. \quad (2.37)$$

Because of Jensen's inequality (2.33) the integrand in the square bracket is non-negative and thus

$$h(\theta^*(\mathbf{x}, t)) = \int d^d x_0 h(\theta_0(\mathbf{x}_0)) p^*(\mathbf{x}_0, 0 | \mathbf{x}, t) \quad (2.38)$$

holds pointwise in space for Lebesgue almost every \mathbf{x} . We can rewrite this equality in terms of the PDF of the random variable $\tilde{\theta}(\mathbf{x}, t) = \theta_0(\tilde{\xi}_{t,0}^*(\mathbf{x}))$ to assume the value ψ or

$$p_\theta^*(\psi | \mathbf{x}, t) = \int d^d x_0 \delta(\psi - \theta_0(\mathbf{x}_0)) p^*(\mathbf{x}_0, 0 | \mathbf{x}, t), \quad (2.39)$$

so that (2.38) becomes

$$h(\theta^*(\mathbf{x}, t)) = \int d\psi h(\psi) p_\theta^*(\psi | \mathbf{x}, t) \quad (2.40)$$

with $\theta^*(\mathbf{x}, t) = \int d\psi \psi p_\theta^*(\psi | \mathbf{x}, t)$. Because of strict convexity of h , Jensen's inequality together with (2.40) immediately implies that $p_\theta^*(\psi | \mathbf{x}, t)$ is a delta-distribution, or

$$p_\theta^*(\psi | \mathbf{x}, t) = \delta(\psi - \theta^*(\mathbf{x}, t)), \quad (2.41)$$

and thus $\tilde{\theta}(\mathbf{x}, t)$ is deterministic. Notice that this conclusion holds for active as well as passive scalars. However, (2.41) by itself does not necessarily contradict spontaneous stochasticity, because particle positions $\tilde{\xi}_{t,0}^*(\mathbf{x})$ may remain random but sample only one isosurface of θ_0 for a fixed value θ^* ! This latter possibility seems very unlikely to be true, even for an active scalar, for every choice of θ_0 . However, we cannot presently rule out a possible “conspiracy” for an active scalar in which changing θ_0 would always alter the velocity field \mathbf{u} so that the limiting particle positions $\tilde{\xi}_{t,0}^*(\mathbf{x})$ would remain in an isosurface of θ_0 †. For a passive scalar, fortunately, we are free to choose $\theta_0(\mathbf{x})$ in a completely arbitrary manner without altering the velocity field \mathbf{u} and we can then conclude that the particle positions themselves must be deterministic. For example, one argument is to take $\theta_0(\mathbf{x}) = x_i$, the i th-coordinate of \mathbf{x} in the periodic domain, which implies that each i th coordinate of $\tilde{\xi}_{t,0}^*(\mathbf{x})$ must be deterministic‡. Since this clearly contradicts the assumed spontaneous stochasticity of the limiting particle positions, we conclude that for each strictly convex function h , there indeed must be anomalous scalar dissipation for some initial data θ_0 .

Now assume instead that there is anomalous scalar dissipation, which means that the “deficit” in the ideally-conserved integral

$$\Delta^{\nu, \kappa}(t) \equiv \int h(\theta_0(\mathbf{x}_0)) d^d x_0 - \int h(\theta^{\nu, \kappa}(\mathbf{x}, t)) d^d x, \quad t > 0 \quad (2.42)$$

converges to some limiting value $\Delta(t) > 0$ as $\nu, \kappa \rightarrow 0$. Here we have explicitly indicated

† Although our proof does not work for active scalars, we conjecture that if there is some θ_0 for which spontaneous stochasticity occurs for an active scalar, then there shall be anomalous scalar dissipation for “generic” perturbations of θ_0 . More formally, in a neighborhood of θ_0 there shall be a dense G_δ set of scalar initial data which produce anomalous dissipation. Note that for passive scalars also we expect anomalous dissipation for generic θ_0 , although our proofs only guarantee the existence of one initial datum leading to anomalous dissipation.

‡ If the periodic domain has diameter L_i in the i th direction, we can take $-L_i/2 \leq x_i < L_i/2$. Then $\theta_0(\mathbf{x}) = x_i$ is clearly not continuous at $x_i = \pm L_i/2$! This technical difficulty can be overcome, if $p^*(\mathbf{x}_0, 0 | \mathbf{x}, t)$ is a measurable function of \mathbf{x}_0 , by choosing sequences of continuous functions $\theta_0(\mathbf{x})$ which converge to x_i pointwise. A completely different and fully general approach is to integrate (2.41) over ψ^2 , or, equivalently, to take $h(\theta) = \theta^2$, which gives $\int d^d x_0 \theta_0^2(\mathbf{x}_0) p^*(\mathbf{x}_0, 0 | \mathbf{x}, t) = \int d^d x_0 \int d^d x'_0 \theta(\mathbf{x}_0) \theta(\mathbf{x}'_0) p^*(\mathbf{x}_0, 0 | \mathbf{x}, t) p^*(\mathbf{x}'_0, 0 | \mathbf{x}, t)$, and to use the argument of the following section 2.4 and Appendix A.2.

the dependence of the solution $\theta^{\nu,\kappa}(\mathbf{x}, t)$ of the scalar advection-diffusion equation upon ν, κ and note further that

$$\theta^{\nu,\kappa}(\mathbf{x}, t) = \int d^d x_0 \theta_0(\mathbf{x}_0) p^{\nu,\kappa}(\mathbf{x}_0, 0 | \mathbf{x}, t). \quad (2.43)$$

In particular, if $\Delta^{\nu,\kappa}(t) \rightarrow \Delta(t)$ as $\nu, \kappa \rightarrow 0$, then for all sufficiently small ν, κ , one has $\Delta^{\nu,\kappa}(t) > \Delta(t)/2$, say, or, in other words,

$$\int h(\theta^{\nu,\kappa}(\mathbf{x}, t)) d^d x < \int h(\theta_0(\mathbf{x}_0)) d^d x_0 - \frac{1}{2} \Delta(t) \quad (2.44)$$

for $\nu < \nu_0, \kappa < \kappa_0$. Taking the limit $\nu, \kappa \rightarrow 0$ along a suitable subsequence ν_n, κ_n so that the limit of the transition probability exists and with $\nu_n < \nu_0, \kappa_n < \kappa_0$, one obtains

$$\int h(\theta^*(\mathbf{x}, t)) d^d x \leq \int h(\theta_0(\mathbf{x}_0)) d^d x_0 - \frac{1}{2} \Delta(t) < \int h(\theta_0(\mathbf{x}_0)) d^d x_0. \quad (2.45)$$

There must therefore be at least a positive measure set (non-zero volume) of points \mathbf{x} for which

$$h(\theta^*(\mathbf{x}, t)) < \int h(\theta_0(\mathbf{x}_0)) p^*(\mathbf{x}_0, 0 | \mathbf{x}, t) d^d x_0, \quad (2.46)$$

since otherwise the inequality (2.45) would be violated. Because the analogue of (2.32) holds for the limiting transition probability, i.e.

$$\theta^*(\mathbf{x}, t) = \int d^d x_0 \theta_0(\mathbf{x}_0) p^*(\mathbf{x}_0, 0 | \mathbf{x}, t), \quad (2.47)$$

and when h is strictly convex, one can conclude that the limiting transition probabilities $p^*(\mathbf{x}_0, 0 | \mathbf{x}, t)$ obtained along the particular subsequence $\nu_n, \kappa_n \rightarrow 0$ are *not* delta-distributions of type (2.25). Thus, spontaneous stochasticity must hold for at least this positive measure set of space points \mathbf{x} . Note that this direction of the proof did not assume a passive scalar. *QED*. Some of the finer technical details of this argument are treated carefully in the Appendix A.1.

2.4. More General Derivation Using the FDR

The same conclusion can be obtained more directly and more generally (with non-vanishing sources) using our fluctuation-dissipation relation. It is intuitively clear from the FDR (2.12) that there can be scalar dissipation non-vanishing in the limit $\kappa \rightarrow 0$ if and only if the Lagrangian trajectories remain stochastic in that same limit. Let us make this argument more precise.

We first discuss the technically simpler case with $S \equiv 0$ and then show that the same argument extends easily to the case with a non-zero scalar source. When $S \equiv 0$ we can rewrite the lefthand side of the FDR (2.12) using

$$\begin{aligned} \text{Var} \left[\theta_0(\tilde{\xi}_{t,0}(\mathbf{x})) \right] &= \int d^d x_0 \int d^d x'_0 \theta_0(\mathbf{x}_0) \theta_0(\mathbf{x}'_0) \\ &\times \left[p_2^{\nu,\kappa}(\mathbf{x}_0, 0; \mathbf{x}'_0, 0 | \mathbf{x}, t) - p^{\nu,\kappa}(\mathbf{x}_0, 0 | \mathbf{x}, t) p^{\nu,\kappa}(\mathbf{x}'_0, 0 | \mathbf{x}, t) \right]. \end{aligned} \quad (2.48)$$

where we have introduced the 2-time (backward-in-time) transition probability density

$$p_2^{\nu,\kappa}(\mathbf{y}, s; \mathbf{y}', s' | \mathbf{x}, t) = \mathbb{E} \left[\delta^d(\mathbf{y} - \tilde{\xi}_{t,s}^{\nu,\kappa}(\mathbf{x})) \delta^d(\mathbf{y}' - \tilde{\xi}_{t,s'}^{\nu,\kappa}(\mathbf{x})) \right], \quad s < t \quad (2.49)$$

which gives the joint probability for the particle to end up at \mathbf{y} at time $s < t$ and at \mathbf{y}' at time $s' < t$, given that it started at \mathbf{x}' at the final time t (moving backward from final

to earlier times). At equal times $s = s'$

$$p_2^{\nu,\kappa}(\mathbf{y}, s; \mathbf{y}', s | \mathbf{x}, t) = \delta^d(\mathbf{y} - \mathbf{y}') p^{\nu,\kappa}(\mathbf{y}, s | \mathbf{x}, t). \quad (2.50)$$

For the situation furthermore where the Lagrangian particles move according to a deterministic flow $\xi_{t,s}$, one easily sees that the 2-time transition probability factorizes as

$$p_2(\mathbf{y}, s; \mathbf{y}', s' | \mathbf{x}, t) = \delta^d(\mathbf{y} - \xi_{t,s}(\mathbf{x})) \delta^d(\mathbf{y}' - \xi_{t,s'}(\mathbf{x})) = p(\mathbf{y}, s | \mathbf{x}, t) p(\mathbf{y}', s' | \mathbf{x}, t). \quad (2.51)$$

Hence, non-factorization in the limit $\nu, \kappa \rightarrow 0$ is an unequivocal sign of spontaneous stochasticity. The variance on the lefthand of the FDR (2.12) can only be non-vanishing in the limit if factorization fails, so that anomalous dissipation clearly requires spontaneous stochasticity. In the other direction, if there is spontaneous stochasticity and thus factorization fails for some positive-measure set of $\mathbf{x} \in \Omega$, then the contribution to the volume-integrated variance from that subset must be positive for some suitable smooth choice of θ_0 , which implies a positive lower bound to the cumulative, volume-integrated scalar dissipation. In short, anomalous scalar dissipation and Lagrangian spontaneous stochasticity are again seen to be equivalent. This argument is given as a formal mathematical proof in the Appendix A.2.

Just as for the argument of Bernard *et al.* (1998), this argument using the FDR succeeds only for a passive scalar to show that spontaneous stochasticity implies anomalous dissipation. For active scalars, the initial data θ_0 partially determines the velocity field \mathbf{u} and so is not free to vary. In order to conclude sufficiency in that case one needs to assume that the resulting velocity field does not “conspire” with the initial scalar to cause the variance to vanish, i.e. for the random trajectories to sample only points on a single level set of θ_0 . If this remarkable behavior did happen to occur for some choice of θ_0 , then one would not expect it to persist for a small perturbation of θ_0 . Thus, it is highly likely also for active scalars that spontaneous stochasticity implies anomalous dissipation, but we have not proved that with the FDR. We can however conclude rigorously both for passive and for active scalars that anomalous dissipation implies spontaneous stochasticity. The above proposition shows that any evidence for anomalous scalar dissipation in the free decay of an active or passive scalar (no sources) obtained from DNS in a periodic box is also evidence for spontaneous stochasticity. The argument in this section is a strong motivation to perform DNS studies to verify anomalous dissipation in the free decay of a scalar, since this would provide additional confirmation of spontaneous stochasticity. All of the DNS cited by Yeung *et al.* (2005), section 2.1, employed sources (e.g. a mean scalar gradient coupled to the velocity field) that maintained a statistical steady-state for the scalar fluctuations.

Including a non-zero scalar source involves only minor changes to the previous argument. First note that

$$\begin{aligned} \text{Var} \left[\theta_0(\tilde{\xi}_{t,0}(\mathbf{x})) + \int_0^t S(\tilde{\xi}_{t,s}(\mathbf{x}), s) ds \right] &= \text{Var} \left[\theta_0(\tilde{\xi}_{t,0}(\mathbf{x})) \right] \\ + 2 \text{Cov} \left[\theta_0(\tilde{\xi}_{t,0}(\mathbf{x})), \int_0^t S(\tilde{\xi}_{t,s}(\mathbf{x}), s) ds \right] &+ \text{Var} \left[\int_0^t S(\tilde{\xi}_{t,s}(\mathbf{x}), s) ds \right]. \end{aligned} \quad (2.52)$$

Furthermore, one has for the variance of the time-integrated source sampled along the stochastic particle trajectory that

$$\begin{aligned} \text{Var} \left[\int_0^t S(\tilde{\xi}_{t,s}(\mathbf{x}), s) ds \right] &= \int_0^t ds \int_0^t ds' \int d^d y \int d^d y' S(\mathbf{y}, s) S(\mathbf{y}', s') \\ &\times \left[p_2^{\nu,\kappa}(\mathbf{y}, s; \mathbf{y}', s' | \mathbf{x}, t) - p^{\nu,\kappa}(\mathbf{y}, s | \mathbf{x}, t) p^{\nu,\kappa}(\mathbf{y}', s' | \mathbf{x}, t) \right]. \end{aligned} \quad (2.53)$$

and for the covariance between the sampled initial data and integrated source that

$$\begin{aligned} \text{Cov} \left[\theta_0(\tilde{\boldsymbol{\xi}}_{t,0}(\mathbf{x})), \int_0^t S(\tilde{\boldsymbol{\xi}}_{t,s}(\mathbf{x}), s) ds \right] &= \int_0^t ds \int d^d x_0 \int d^d y \theta_0(\mathbf{x}_0) S(\mathbf{y}, s) \\ &\times \left[p_2^{\nu,\kappa}(\mathbf{x}_0, 0; \mathbf{y}, s | \mathbf{x}, t) - p^{\nu,\kappa}(\mathbf{x}_0, 0 | \mathbf{x}, t) p^{\nu,\kappa}(\mathbf{y}, s | \mathbf{x}, t) \right]. \end{aligned} \quad (2.54)$$

Clearly, anomalous scalar dissipation requires spontaneous stochasticity. For a passive scalar we can also argue in the other direction. Indeed, we can repeat the previous argument to conclude that, if there is spontaneous stochasticity for a positive measure set of \mathbf{x} , then not only is there a smooth choice of θ_0 so that the variance associated to the initial condition in (2.48) is positive when integrated over this set of \mathbf{x} , but also there is a smooth choice of source field S so that the contribution of the variance (2.53) is positive. This is already enough to conclude that there must be anomalous dissipation for the scalar with initial condition 0 and with the chosen source S . We can also conclude that there is anomalous dissipation for the initial condition θ_0 and the source S . Indeed, if the total variance contribution in (2.52) is not positive then it must vanish, which implies that the covariance term in (2.54) provides a negative contribution. In that case, simply take $S \rightarrow -S$ to make the contributions of all three terms (2.48),(2.53),(2.54) positive. We thus conclude that, also for the passive scalar rejuvenated by a source, there is equivalence between anomalous scalar dissipation and Lagrangian spontaneous stochasticity. The argument is given more carefully in Appendix A.2. It does not seem to be possible to use the original argument of Bernard *et al.* (1998) to reach this conclusion. Furthermore, the advantages of the FDR (2.12) become even more apparent in the case of wall-bounded flows, which we consider next.

3. Wall-Bounded Flows with Imposed Scalar Fluxes at the Wall

Wall-bounded flows are ubiquitous both in engineering applications and in nature. Scalar fields in such flows are governed by Eq. (2.1) in the interior of the flow domain Ω with appropriate conditions specified on the boundary $\partial\Omega$. Typical situations are those in which scalar field is held fixed on the boundary (Dirichlet conditions), those in which the scalar flux through the wall is fixed (Neumann conditions), or a mixture of these along different parts of the boundary decomposed as $\partial\Omega = \partial\Omega_D \cup \partial\Omega_N$. More formally, for a function $\psi(\mathbf{x}, t)$ specifying scalar boundary values and a function $g(\mathbf{x}, t)$ specifying the fluxes through the wall, one solves Eq. (2.1) subject to the conditions

$$\text{Dirichlet:} \quad \theta(\mathbf{x}, t) = \psi(\mathbf{x}, t), \quad \mathbf{x} \in \partial\Omega_D \quad (3.1)$$

$$\text{Neumann:} \quad -\boldsymbol{\mu}(\mathbf{x}, t) \cdot \nabla\theta(\mathbf{x}, t) = g(\mathbf{x}, t) \quad \mathbf{x} \in \partial\Omega_N \quad (3.2)$$

where $\boldsymbol{\mu} = \kappa \mathbf{n}^\dagger$ with $\mathbf{n}(\mathbf{x})$ being the unit inward normal to the boundary $\partial\Omega$. Additionally, appropriate boundary conditions must be specified for the velocity field at the wall. Throughout this paper, we consider the most common stick (or no-slip) boundary conditions:

$$\mathbf{u}(\mathbf{x}, t) = \mathbf{0}, \quad \mathbf{x} \in \partial\Omega. \quad (3.3)$$

As we shall discuss, stochastic representations like Eq.(2.6) for solutions of the scalar advection equation hold also, in modified form, for flows in wall-bounded domains with

† All of our considerations in this paper apply with straightforward modifications to the more general situation where the scalar flux is given by an anisotropic Fick's law as $\mathbf{j}(\mathbf{x}, t) = -\mathbf{K}(\mathbf{x}, t)\nabla\theta(\mathbf{x}, t)$ for a positive-definite, symmetric diffusivity tensor \mathbf{K} . In that case, the component of the flux normal to the boundary is $j_n = \mathbf{n} \cdot \mathbf{j} = -\boldsymbol{\mu} \cdot \nabla\theta$ with the so-called co-normal vector $\boldsymbol{\mu} = \mathbf{K}\mathbf{n}$ satisfying $\boldsymbol{\mu} \cdot \mathbf{n} = \mathbf{n}^\top \mathbf{K}\mathbf{n} > 0$.

boundary conditions either of Dirichlet, Neumann, or mixed form (e.g. see Soner (2007)). Using these representations, we shall prove below analogues of the fluctuation-dissipation relation of the previous section 2 and use them to establish relationships between spontaneous stochasticity and anomalous scalar dissipation also for wall-bounded flows.

We consider in this section a scalar $\theta(\mathbf{x}, t)$ with pure Neumann boundary conditions ($\partial\Omega_N = \partial\Omega$), satisfying:

$$\begin{aligned} \partial_t \theta + \mathbf{u} \cdot \nabla \theta &= \kappa \Delta \theta + S & \mathbf{x} \in \Omega, \\ -\boldsymbol{\mu}(\mathbf{x}, t) \cdot \nabla \theta(\mathbf{x}, t) &= g(\mathbf{x}, t) & \mathbf{x} \in \partial\Omega. \end{aligned} \quad (3.4)$$

for given initial data θ_0 , a given flux function g , and co-normal vector field $\boldsymbol{\mu}$. After reviewing the stochastic representation of this problem, we shall derive an FDR and use it to discuss the connection between spontaneous stochasticity and anomalous scalar dissipation in this general context. We present some numerical results for stochastic Lagrangian trajectories in a typical example of a wall-bounded flow, a turbulent channel flow. As a physically important example, we shall work out detailed theoretical consequences of our FDR for Rayleigh-Bénard convection in closed cells with imposed heat flux at the top and bottom walls and with insulating side-walls. In the following section 4 we shall similarly consider pure Dirichlet and mixed conditions, and, as an example of the latter, Rayleigh-Bénard convection with fixed temperatures maintained at the top and bottom walls and with insulating sidewalls.

3.1. Stochastic Representation and Fluctuation-Dissipation Relation

The stochastic representation of solutions of pure Neumann problems has been discussed in many earlier publications, such as Freidlin (1985); Burdzy *et al.* (2004); Soner (2007) on fundamental mathematical theory and Mil'shtein (1996); Keanini (2007); Słomiński (2013) for numerical methods. In order to impose Neumann conditions, essentially, one averages over stochastic trajectories which reflect off the boundary of the domain, contributing to the solution a correction related to their sojourn time on the walls. We briefly review the subject here.

The fundamental notion is the *boundary local time density* $\tilde{\ell}_{t,s}(\mathbf{x})$ (Stroock & Varadhan 1971; Lions & Sznitman 1984; Burdzy *et al.* 2004), which, for a stochastic Lagrangian particle located at $\mathbf{x} \in \Omega$ at time t , is the time within the interval $[s, t]$ which is spent near the boundary $\partial\Omega$ per unit distance. Its physical units are thus (time)/(length) or $1/(\text{velocity})$. Note that we consider here the backward-in-time process, as also in Burdzy *et al.* (2004), in contrast to the more usual forward-time case. We thus take the boundary local time density to be a non-positive, non-increasing random process which decreases (backward in time) only when the stochastic particle is on the boundary. It is defined via the ‘‘Skorohod problem’’, in conjunction with the (backward) stochastic flow $\tilde{\boldsymbol{\xi}}_{t,s}^{\nu,\kappa}(\mathbf{x})$ with reflecting b.c. which satisfies

$$\hat{d}\tilde{\boldsymbol{\xi}}_{t,s}(\mathbf{x}) = \mathbf{u}^\nu(\tilde{\boldsymbol{\xi}}_{t,s}(\mathbf{x}), s) ds + \sqrt{2\kappa} \hat{d}\tilde{\mathbf{W}}_s - \boldsymbol{\mu}(\tilde{\boldsymbol{\xi}}_{t,s}(\mathbf{x}), s) \hat{d}\tilde{\ell}_{t,s}(\mathbf{x}) \quad (3.5)$$

with $\tilde{\boldsymbol{\xi}}_{t,t}(\mathbf{x}) = \mathbf{x}$ as usual. The boundary local time is then given by the formula

$$\tilde{\ell}_{t,s}(\mathbf{x}) = \int_t^s dr \delta(\text{dist}(\tilde{\boldsymbol{\xi}}_{t,r}(\mathbf{x}), \partial\Omega)) \equiv \lim_{\varepsilon \rightarrow 0} \frac{1}{\varepsilon} \int_t^s dr \chi_{\partial\Omega_\varepsilon}(\tilde{\boldsymbol{\xi}}_{t,r}(\mathbf{x})), \quad s < t, \quad (3.6)$$

in terms of an ‘‘ ε -thickened boundary’’

$$\partial\Omega_\varepsilon = \{\mathbf{x} \in \Omega : \text{dist}(\mathbf{x}, \partial\Omega) < \varepsilon\}. \quad (3.7)$$

See Burdzy *et al.* (2004), Theorem 2.6[†]. Here we denote by χ_A the characteristic function of a set defined as

$$\chi_A(\mathbf{x}) = \begin{cases} 1 & \mathbf{x} \in A \\ 0 & \mathbf{x} \notin A \end{cases} \quad (3.8)$$

Lions & Sznitman (1984) have proved existence and uniqueness of strong solutions to this ‘‘Skorohod problem’’ with Lipschitz velocity fields \mathbf{u} and sufficient regular normal vectors \mathbf{n} at a smooth boundary. Of some interest for the consideration of non-smooth velocity fields that might appear in the limit $\nu \rightarrow 0$, Stroock & Varadhan (1971) obtain solutions when \mathbf{u} is merely bounded, measurable and establish uniqueness in law. The spatial regularity in \mathbf{x} of the processes $(\tilde{\xi}_{t,s}(\mathbf{x}), \tilde{\ell}_{t,s}(\mathbf{x}))$ defined jointly as above is the subject of recent works on stochastic flows with reflecting b.c (Pilipenko 2005, 2014; Burdzy 2009). Note that the stochastic particles described by $\tilde{\xi}_{t,s}(\mathbf{x})$ are reflected in the direction of $\boldsymbol{\mu}$ when they hit the wall, thus staying forever within Ω , and the flow preserves the volume within the domain when $\nabla \cdot \mathbf{u}^\nu = 0$, as assumed here.

By means of the above notions one can obtain a stochastic representation for solutions to the initial-value problem of the system (3.4). The backward Itô formula applied to $\theta(\tilde{\xi}_{t,s}(\mathbf{x}), s)$ gives

$$\begin{aligned} \hat{d}\theta(\tilde{\xi}_{t,s}(\mathbf{x}), s) &= \left[(\partial_s \theta + \mathbf{u} \cdot \nabla \theta - \kappa \Delta \theta) ds - (\nabla \theta \cdot \boldsymbol{\mu}) \hat{d}\tilde{\ell}_{t,s} + \sqrt{2\kappa} \hat{d}\tilde{\mathbf{W}}_s \cdot \nabla \theta \right]_{(\tilde{\xi}_{t,s}(\mathbf{x}), s)} \\ &= S(\tilde{\xi}_{t,s}(\mathbf{x}), s) ds + g(\tilde{\xi}_{t,s}(\mathbf{x}), s) \hat{d}\tilde{\ell}_{t,s} + \sqrt{2\kappa} \hat{d}\tilde{\mathbf{W}}_s \cdot \nabla \theta(\tilde{\xi}_{t,s}(\mathbf{x}), s) \end{aligned} \quad (3.9)$$

where in the second line we have used the fact that $\theta(\mathbf{x}, s)$ solves the system (3.4). We find upon integration from 0 to t ,

$$\begin{aligned} \theta(\mathbf{x}, t) &= \theta_0(\tilde{\xi}_{t,0}(\mathbf{x})) + \int_0^t ds S(\tilde{\xi}_{t,s}(\mathbf{x}), s) + \int_0^t g(\tilde{\xi}_{t,s}(\mathbf{x}), s) \hat{d}\tilde{\ell}_{t,s} \\ &\quad + \sqrt{2\kappa} \int_0^t \hat{d}\tilde{\mathbf{W}}_s \cdot \nabla \theta(\tilde{\xi}_{t,s}^{\nu, \kappa}(\mathbf{x}), s) \end{aligned} \quad (3.10)$$

and thus expectation over the Brownian motion yields the representation

$$\begin{aligned} \theta(\mathbf{x}, t) &= \mathbb{E} \left[\theta_0(\tilde{\xi}_{t,0}(\mathbf{x})) + \int_0^t ds S(\tilde{\xi}_{t,s}(\mathbf{x}), s) + \int_0^t g(\tilde{\xi}_{t,s}(\mathbf{x}), s) \hat{d}\tilde{\ell}_{t,s} \right] \\ &= \int_{\Omega} d^d \mathbf{x}_0 \theta_0(\mathbf{x}_0) p(\mathbf{x}_0, 0 | \mathbf{x}, t) + \int_0^t ds \int_{\Omega} d^d \mathbf{y} S(\mathbf{y}, s) p(\mathbf{y}, s | \mathbf{x}, t) \\ &\quad + \int_0^t ds \int_{\partial\Omega} dH^{d-1}(\mathbf{z}) g(\mathbf{z}, s) p(\mathbf{z}, s | \mathbf{x}, t), \end{aligned} \quad (3.11)$$

where H^{d-1} is the $(d-1)$ -dimensional Hausdorff measure (surface area) over the smooth boundary $\partial\Omega$ ‡. Clearly, the scalar value $\theta(\mathbf{x}, t)$ is an average of the randomly sampled initial data and the scalar inputs from the internal source and the scalar flux through the boundary along a random history.

Just as for domains without walls, we introduce a stochastic scalar field which repre-

[†] Note that the eq.(2.7) of Burdzy *et al.* (2004) contains an additional factor of 1/2, because their local time density is our $\kappa \tilde{\ell}_{t,s}(\mathbf{x})$ and they consider only the case $\kappa = 1/2$.

[‡] It follows formally from (3.6) that $\tilde{\ell}_{t,s}(\mathbf{x}) = \int_t^s dr \int_{\partial\Omega} dH^{d-1}(\mathbf{z}) \delta^d(\mathbf{z} - \tilde{\xi}_{t,r}(\mathbf{x}))$. We have not found this intuitive formula in the probability theory literature, but it should be possible to prove rigorously with suitable smoothness assumptions on the boundary $\partial\Omega$ of the domain.

sents the contribution for a specific stochastic Lagrangian trajectory

$$\tilde{\theta}(\mathbf{x}, t) \equiv \theta_0(\tilde{\boldsymbol{\xi}}_{t,0}(\mathbf{x})) + \int_0^t ds S(\tilde{\boldsymbol{\xi}}_{t,s}(\mathbf{x}), s) + \int_0^t g(\tilde{\boldsymbol{\xi}}_{t,s}(\mathbf{x}), s) \hat{d}\tilde{\ell}_{t,s}, \quad (3.12)$$

that now includes the boundary-flux term, so that $\theta(\mathbf{x}, t) = \mathbb{E}[\tilde{\theta}(\mathbf{x}, t)]$. The by-now-standard Itô-isometry argument yields

$$\frac{1}{2} \text{Var}[\tilde{\theta}(\mathbf{x}, t)] = \kappa \mathbb{E} \int_0^t ds |\nabla\theta(\tilde{\boldsymbol{\xi}}_{t,s}(\mathbf{x}), s)|^2, \quad (3.13)$$

which is a local FDR. Integrating over the bounded domain and invoking volume preservation, we obtain:

$$\frac{1}{2} \langle \text{Var} \tilde{\theta}(t) \rangle_{\Omega} = \kappa \int_0^t ds \langle |\nabla\theta(s)|^2 \rangle_{\Omega} \quad (3.14)$$

This, together with (3.12), is our exact FDR for scalars (either passive or active) with general Neumann boundary conditions. Just as for (2.19) in the case of domains without walls, we obtain for the infinite-time limit of the local scalar variance

$$\lim_{t \rightarrow \infty} \frac{1}{2t} \text{Var}[\tilde{\theta}(\mathbf{x}, t)] = \langle \kappa |\nabla\theta|^2 \rangle_{\Omega, \infty}, \quad \text{for all } \mathbf{x} \in \Omega \quad (3.15)$$

which is thus independent of the space point \mathbf{x} .

To provide some additional insight into these concepts, we present in Appendix B an elementary analytical example: pure heat conduction on a finite interval with a constant heat flux imposed at the two ends. In addition, we present now some numerical results on stochastic Lagrangian trajectories and boundary local time densities for a prototypical wall-bounded flow, turbulent channel flow. These numerical results are directly relevant to turbulent thermal transport in a channel with imposed heat fluxes at the walls. They also have relevance to the problem of Rayleigh-Bénard convection which will be discussed in section 3.3, since channel flow provides the simplest example of a turbulent shear flow with a logarithmic law-of-the-wall of the type conjectured to exist at very high Rayleigh numbers in turbulent convection (Kraichnan 1962). For the purpose of our study, we use the $Re_{\tau} = 1000$ channel-flow dataset in the Johns Hopkins Turbulence Database (see Graham *et al.* (2016) and <http://turbulence.pha.jhu.edu>). We follow the notations in these references and, in particular, the x direction is streamwise, y is wall-normal, and z is spanwise. As in our previous numerical study of isotropic turbulence, we solve the stochastic equations (3.5), (3.6) with interpolated velocities retrieved using the `getVelocity` database function. To implement the reflecting boundary conditions we have found it convenient to use the very simple Euler algorithm of Lépingle (1995), which is ideally suited to the parallel plane boundaries of the channel flow. This method reduces to the standard Euler-Maruyama scheme at some specified small distance ϵ away from the walls. Furthermore, the algorithm yields strong approximations to the joint process $(\tilde{\boldsymbol{\xi}}_{t,s}(\mathbf{x}), \tilde{\ell}_{t,s}(\mathbf{x}))$ for any \mathbf{x} . For details, see Lépingle (1995) and Appendix E.2. To illustrate the output, we plot in Figure 2 for three choices of Prandtl number ($Pr = 0.1, 1, 10$) a single realization of $(\tilde{\boldsymbol{\xi}}_{t,s}(\mathbf{x}), \tilde{\ell}_{t,s}(\mathbf{x}))$ for a stochastic particle released at a point \mathbf{x} on the lower wall $y = -h$ at the final time t_f in the database, then evolved backward in time. Using Cartesian coordinates $\tilde{\boldsymbol{\xi}}_{t,s} = (\tilde{\xi}_{t,s}, \tilde{\eta}_{t,s}, \tilde{\zeta}_{t,s})$, the left panel of Fig. 2 plots the wall-normal particle position $\tilde{\eta}_{t,s}(\mathbf{x})$ as height above the wall $\Delta y = y + h$ and the right panel plots the local time density $\tilde{\ell}_{t,s}(\mathbf{x})$, both as functions of shifted time $s - t_f$. All quantities are expressed in wall units, in terms of the friction velocity u_{τ} , the viscous length $\delta_{\tau} = \nu/u_{\tau}$, and the viscous time $\tau_{\nu} = \nu/u_{\tau}^2$. Note that to achieve strong convergence for a

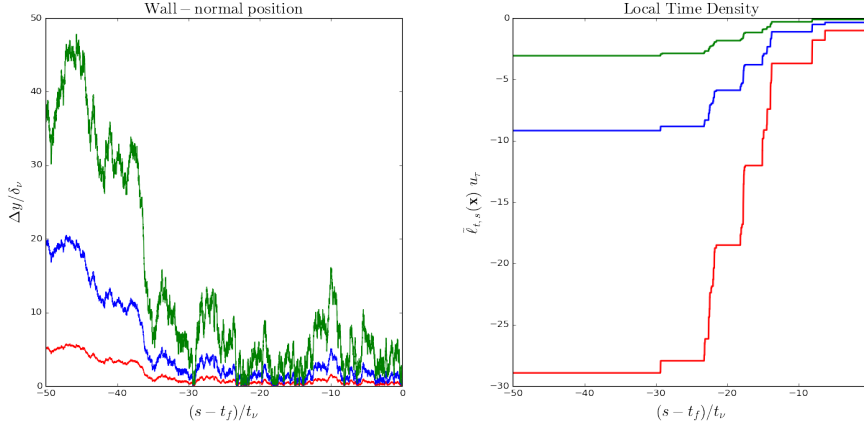


Figure 2: Realizations of wall-normal position (left panel) and local time density process (right panel) for a single particle released on the lower wall at $(x, z) = (3543.84\delta_\nu, 1891.56\delta_\nu)$ for Prandtl numbers $Pr = 0.1$ (green), 1.0 (blue), and 10 (red).

single realization of the driving Brownian process $\widetilde{\mathbf{W}}_s$ required a very small time-step $\Delta s \approx 6.5 \times 10^{-6}$, or 1/1000th of the time between the stored database frames (for more discussion, see Appendix E.2). Important features to observe in Fig. 2 are the jumps in the local time density at the instants when the particles are incident upon the wall and reflected. These incidences occur predominantly near the release time and eventually cease (backward in time) as the particles are transported away from the wall. This escape from the wall occurs slower for smaller κ or larger Pr , and the local times at the wall are correspondingly larger magnitude for larger Pr .

We next discuss statistics of the entire ensemble of stochastic particles for two specific release points at the wall, one point selected inside a low-speed streak and the other a high-speed streak. The selection is illustrated in Figure 3, which plots the streamwise velocity in the buffer layer at distance $\Delta y = 10\delta_\tau$ above the bottom channel wall. The low-speed streaks associated with “ejections” from the wall and high-speed streaks associated with “sweeps” toward the wall seen there are characteristic of turbulent boundary layers (Kline *et al.* 1967). The x - z coordinates of the two release points are indicated by the diamonds (\diamond) in Fig. 3 (and note that the point selected in the low-speed streak is that featured in the previous Fig. 2). For each of these two release points and for the three choices of Prandtl number $Pr = 0.1, 1, 10$, we used $N = 1024$ independent solutions of Eqs.(3.5),(3.6) to calculate the dispersion of the stochastic trajectories and the PDF’s of the local-time densities backward in time. The requirements are much less stringent for weak convergence as time-step $\Delta s \rightarrow 0$ of such statistical averages over Brownian motions than for the strong convergence at fixed $\widetilde{\mathbf{W}}_s$ studied in Fig. 2. The averages presented below are well-converged for $\Delta s \approx 2 \times 10^{-3}$, or 1/3 of the time between database frames. Error analysis is discussed more carefully in Appendix E.2. Error bars in the plots represent s.e.m. for the N -sample averages and in addition, for the PDF’s, the effects of variation in kernel density bandwidth.

In Figure 4, the top panels show 30 representative particle trajectories for the two release points (left within a high-speed streak, right in a low-speed) and for each of the three Prandtl numbers. By eye, the ensembles of trajectories for the three different Prandtl numbers appear quite similar. In the middle panels of Fig. 4, we plot the mean-

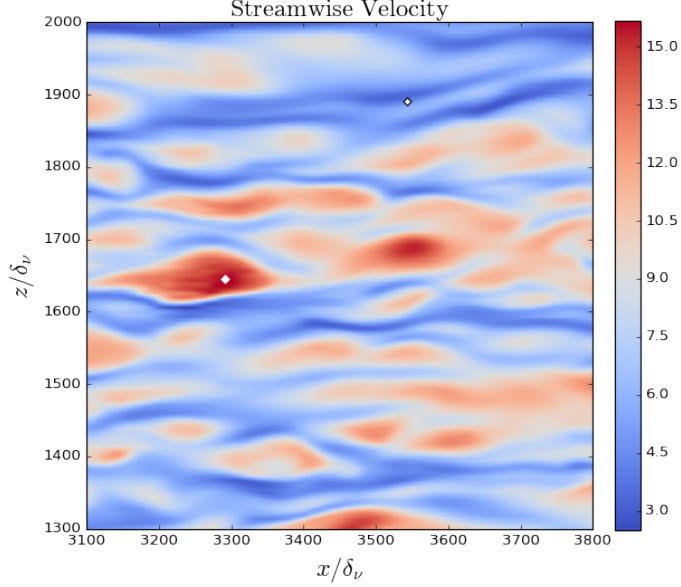


Figure 3: Streamwise velocity at normal distance $\Delta y = 10\delta_\nu$ from the lower wall, non-dimensionalized by the friction velocity u_τ . The open diamonds (\diamond) mark the (x, z) coordinates, $(3291.73\delta_\nu, 1644.98\delta_\nu)$ and $(3543.84\delta_\nu, 1891.56\delta_\nu)$, of the selected release points at wall-parallel positions of high-speed (red) and low-speed (blue) streaks, respectively.

squared dispersion of the stochastic particles for the two release points and the three Prandtl numbers. There is an initial period (backward in time) where the dispersion grows with $\hat{s} = t_f - s$ as $4\kappa(3 - 2/\pi)\hat{s}$, which is the analytical result for a 3D Brownian motion reflected from a plane[†]. There is then a crossover to a limited regime of super-ballistic separation that is close to \hat{s}^3 -growth. At still larger \hat{s} , the growth clearly slows but remains super-ballistic. It would be quite surprising to observe Richardson dispersion in this channel-flow dataset, since the energy spectra published in Graham *et al.* (2016) and <http://turbulence.pha.jhu.edu> show that the Reynolds number is still too low to support a Kolmogorov-type inertial-range. We believe that the cubic power-law growth observed arises instead from a simple combination of stochastic diffusion and mean shear, a molecular version of the turbulent shear dispersion discussed by Corrsin (1953). A toy model which illustrates this mechanism is a 2D shear flow with $\mathbf{u}(\mathbf{x}) = (Sy, 0)$, where

$$d\tilde{\xi}_t = S\tilde{\eta}_t + \sqrt{2\kappa} d\tilde{W}_x(t), \quad d\tilde{\eta}_t = \sqrt{2\kappa} d\tilde{W}_y(t). \quad (3.16)$$

Integration gives $\tilde{\xi}_t = \sqrt{2\kappa}(S \int_0^t \tilde{W}_y(s) ds + \tilde{W}_x(t))$ and $\tilde{\eta}_t = \sqrt{2\kappa} \tilde{W}_y(t)$ when $(\tilde{\xi}_0, \tilde{\eta}_0) = (0, 0)$, and the shear contributes a t^3 -term to the x -component of the dispersion:

$$\mathbb{E}^{1,2} |\tilde{\xi}_t^{(1)} - \tilde{\xi}_t^{(2)}|^2 = 4\kappa(t + \frac{1}{3}S^2t^3). \quad (3.17)$$

[†] If $\tilde{W}(t)$ is standard 1D Brownian motion with diffusivity κ , then $|\tilde{W}(t)|$ is the Brownian motion reflected at 0 and it is elementary to show that $\mathbb{E}^{1,2} [\{|\tilde{W}^{(1)}(t)| - |\tilde{W}^{(2)}(t)|\}^2] = 4\kappa(1 - 2/\pi)t$.

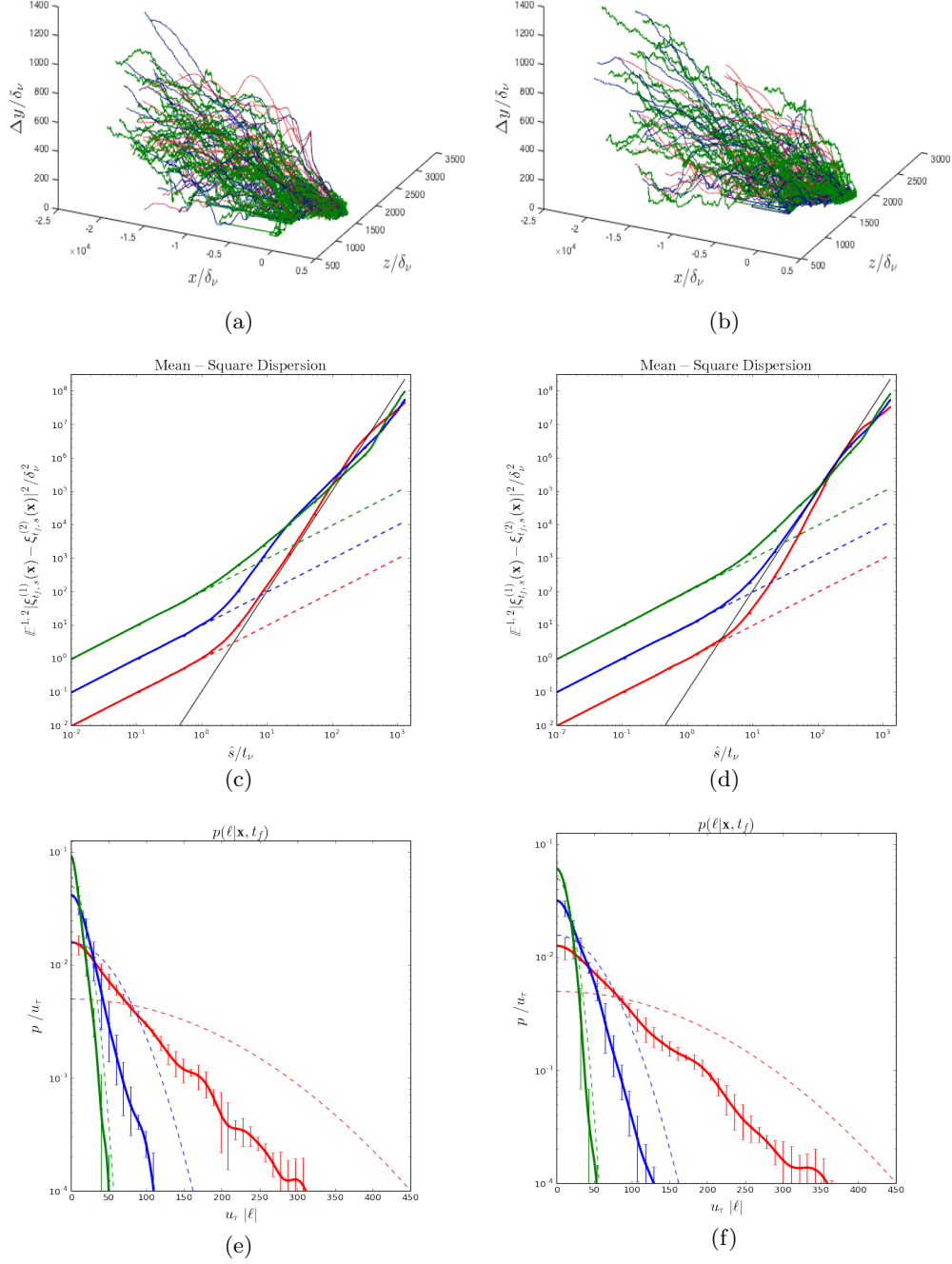


Figure 4: *Left panels* are for release at bottom wall near a high-speed streak, *right panels* for release near a low-speed streak. See markers on Figure 3. Top panels (a),(b) show 30 representative reflected stochastic trajectories for $Pr = 0.1$ (green), 1.0 (blue) and 10 (red). Middle panels (c),(d) plot particle dispersion and short-time results $4\kappa(3 - \frac{2}{\pi})\hat{s}$ for each Pr with the same colors as (a),(b), and a plot in **black** of $g(\nu/t_\nu^2)\hat{s}^3$ with $g = 0.1$. The bottom panels (e),(f) plot PDF's of (absolute values of) boundary local times for channel flow (solid lines) and pure diffusion (dashed lines) for the three Pr -values.

In this toy model, the y -component of dispersion grows only diffusively. In qualitative agreement with this simple model, we have found that the cubic power-law growth in the channel-flow particle dispersion indeed arises solely from the streamwise component of the particle separation vector. We do not show this here, but the effect can be observed in the particle trajectories plotted in the top panels of Fig. 4, where the particles are dispersed farthest along the streamwise direction. The t^3 dispersion in (3.17) differs notably from Richardson dispersion in that it is proportional to κ and it produces no spontaneous stochasticity, since it vanishes as $\kappa \rightarrow 0$. In the channel-flow \hat{s}^3 -regime in Fig. 4c,d ($10^1 \lesssim \hat{s}/t_\eta \lesssim 10^2$) there is likewise an observable dependence on the diffusivity.

In the bottom panels of Figure 4, we plot PDF's of the local time density $\tilde{\ell}_{t_f,0}(\mathbf{x})$ accumulated backward over the entire time interval of the channel-flow database (one flow-through time), for the two release points and the three values of Prandtl number. As could be expected, smaller κ (or larger Pr) correspond to more time at the wall and a PDF supported on larger local time densities. Comparing the results for the two release points, it can be seen that particles starting on the wall inside the high-speed streak tend to spend somewhat less time near the wall than those starting near the low-speed streak. This is easy to understand, if one recalls that low-speed streaks correspond to “ejections” from the wall and high-speed streaks to “sweeps” toward the wall. Backward in time, however, the fluid motions are exactly reversed. Thus, particles starting at the wall inside high-speed streaks are being swept away from the wall by the fluid motion backward in time, and those starting inside low-speed streaks are brought toward the wall. However, the location of the release point has a quite small effect on the PDF of the local-time density accumulated over one flow-through time, and it is plausible that this effect would be reduced by taking t_f even larger. Finally, we have also plotted in the bottom panels of Fig. 4 the analytical results for the local time PDF's of a pure Brownian motion with diffusivity κ that is reflected from a planar wall (see Appendix B.3 and (3.23) below). Compared with these results for Brownian motion, the corresponding channel-flow local-time PDF's exhibit in all cases a substantial reduction of time spent at the wall. These results show that turbulent fluctuations enhance transport away from the wall, even when the local flow initially carries the particles toward the wall. Although we show these results only for two release points here, we have observed similar behavior at all other locations on the wall that we have examined. This observation has importance for the problem of turbulent convection, where it was argued by Kraichnan (1962) that “. . . the effect of the small-scale turbulence that arises locally in the shear boundary layer should be to increase heat transport.” We shall return to this issue in section 3.3, but first we discuss the relation of anomalous dissipation and spontaneous stochasticity for turbulent advection of a general scalar with flux boundary conditions.

3.2. Spontaneous Stochasticity and Anomalous Dissipation

As a first application of our FDR (3.14),(3.12) for flows with imposed scalar fluxes at the walls, we discuss the equivalence between spontaneous stochasticity and anomalous scalar dissipation in this context. As we shall see, the effects of the walls can be profound.

The simplest situation is the case of vanishing wall-fluxes, $g \equiv 0$, which corresponds to *insulating/adiabatic walls* when the scalar is the temperature and to *impermeable walls* when the scalar is the concentration of an advected substance (e.g. a dye, aerosol, etc.) In this case, the flux contribution proportional to the local time density in (3.12) vanishes, and our FDR then becomes simply

$$\frac{1}{2} \left\langle \text{Var} \left[\theta_0(\tilde{\xi}_{t,0}) + \int_0^t ds S(\tilde{\xi}_{t,s}, s) \right] \right\rangle_\Omega = \kappa \int_0^t ds \langle |\nabla\theta(s)|^2 \rangle_\Omega. \quad (3.18)$$

This is formally identical to the relation (2.12),(2.52) for flows in domains without boundaries, with the simple stochastic flow replaced by a reflected stochastic flow. We can therefore repeat *verbatim* the arguments from section 2 to conclude that, for walls that do not support fluxes, spontaneous stochasticity is equivalent to anomalous dissipation for passive scalars and for active scalars spontaneous stochasticity is (at least) necessary for anomalous scalar dissipation. This result is relevant for many physical situations, such as a dye injected into a turbulent Taylor-Couette flow. The commonplace example of cream stirred into coffee is also essentially of this type, since the cup walls and surface of the stirrer are impermeable boundaries and there is also no transport of cream across the free fluid surface. The extension of our FDR (3.18) to problems with moving walls and free-fluid surfaces should be relatively straightforward (and, indeed, the main result of the paper of Burdzy *et al.* (2004) was the construction of reflected Brownian processes for domains enclosed by moving boundaries). In all of these situations, any evidence for anomalous scalar dissipation is also evidence for (requires) spontaneous stochasticity.

The situations with non-vanishing fluxes through the walls are, however, essentially different. From a mathematical point of view, the problem is “loss of compactness.” While the trajectories of the reflected diffusion process satisfy uniformly in ν, κ the condition that $\tilde{\xi}_{t,s}^{\nu,\kappa}(\mathbf{x}) \in \bar{\Omega}$, a closed, bounded domain, the local time densities $\tilde{\ell}_{t,s}^{\nu,\kappa}(\mathbf{x})$ may become unboundedly large as $\nu, \kappa \rightarrow 0$. This creates a fundamental difficulty for arguments of the type employed previously, where limits as $\nu, \kappa \rightarrow 0$ were guaranteed to exist (along subsequences). To understand better the problem, consider how we might try to adapt those arguments to the present context. We can rewrite our FDR (3.14),(3.12) as

$$\begin{aligned} \kappa \int_0^t ds \langle |\nabla \theta(s)|^2 \rangle_{\Omega} &= \frac{1}{2} \left\langle \text{Var} \left[\tilde{\theta}^{\nu,\kappa}(t) \right] \right\rangle_{\Omega} \\ &= \frac{1}{2} \left\langle \int d\psi \int d\psi' \psi \psi' \left[p_2^{\nu,\kappa}(\psi, \psi' | \cdot, t) - p^{\nu,\kappa}(\psi | \cdot, t) p^{\nu,\kappa}(\psi' | \cdot, t) \right] \right\rangle_{\Omega}, \end{aligned} \quad (3.19)$$

where

$$p^{\nu,\kappa}(\psi | \mathbf{x}, t) = \mathbb{E} \left[\delta(\psi - \tilde{\theta}^{\nu,\kappa}(\mathbf{x}, t)) \right] \quad (3.20)$$

and

$$p_2^{\nu,\kappa}(\psi, \psi' | \mathbf{x}, t) = \mathbb{E} \left[\delta(\psi - \tilde{\theta}^{\nu,\kappa}(\mathbf{x}, t)) \delta(\psi' - \tilde{\theta}^{\nu,\kappa}(\mathbf{x}, t)) \right] = \delta(\psi - \psi') p^{\nu,\kappa}(\psi | \mathbf{x}, t), \quad (3.21)$$

with $\tilde{\theta}^{\nu,\kappa}(\mathbf{x}, t)$ given by (3.12). If weak limits $p^*(\psi | \mathbf{x}, t) = w\text{-}\lim_{\nu,\kappa \rightarrow 0} p^{\nu,\kappa}(\psi | \mathbf{x}, t)$ existed, then arguments of exactly the type given before would show that anomalous dissipation requires non-factorization of p_2^* into $p^* \cdot p^*$ and, hence, spontaneous stochasticity. The reverse argument that spontaneous stochasticity implies anomalous dissipation for passive scalars would also be essentially the same.

Simple examples show, however, that weak limits $p^*(\psi | \mathbf{x}, t) = w\text{-}\lim_{\nu,\kappa \rightarrow 0} p^{\nu,\kappa}(\psi | \mathbf{x}, t)$ may not exist when wall-fluxes are not vanishing. Consider the case where $\theta_0 = S \equiv 0$ and the flux into the domain is a space-time constant $g(\mathbf{x}, s) = J > 0$. In that case

$$\tilde{\theta}(\mathbf{x}, t) = \int_0^t g(\tilde{\xi}_{t,s}(\mathbf{x}), s) \hat{d}\tilde{\ell}_{t,s}(\mathbf{x}) = -J\tilde{\ell}_{t,0}(\mathbf{x}) \geq 0, \quad (3.22)$$

and the stochastic scalar field for one realization of the Brownian process is proportional by a constant to the local time density itself. Consider furthermore the simple case of pure heat-conduction, where the advecting velocity field also vanishes, $\mathbf{u}^{\nu} \equiv \mathbf{0}$. In this case, the distribution of $\tilde{\ell}_{t,0}(\mathbf{x})$ is known analytically in many cases. A very simple example which serves to make our point takes the domain to be the semi-infinite one-dimensional

interval $\Omega = [0, \infty)$ with boundary at 0. In that case, for $x \geq 0$

$$p^\kappa(\psi|x, t) = \frac{1}{J} \sqrt{\frac{\kappa}{\pi t}} \exp\left[-\frac{(x + \kappa\psi/J)^2}{4\kappa t}\right] \eta(\psi) + [2\Phi_{\kappa, t}(x) - 1] \delta(\psi) \quad (3.23)$$

where $\eta(\psi)$ is the Heaviside step function and

$$\Phi_{\kappa, t}(x) = \frac{1}{\sqrt{4\kappa\pi t}} \int_{-\infty}^x dy \exp(-y^2/4\kappa t). \quad (3.24)$$

For details see Appendix B.3. It is easy to see mathematically from the above expression that weak limits exist for fixed $x > 0$ and, indeed,

$$w\text{-}\lim_{\kappa \rightarrow 0} p^\kappa(\psi|x, t) = \delta(\psi), \quad x > 0. \quad (3.25)$$

This is also intuitively obvious, because a stochastic particle released at $x > 0$ never makes it to the boundary at 0 when $\kappa \rightarrow 0$. However, *the distribution $p^\kappa(\psi|0, t)$ does not converge weakly as $\kappa \rightarrow 0$* , but instead tends to become uniformly spread on the semi-infinite interval. This also makes sense, because a particle released at 0 should tend to stay there as $\kappa \rightarrow 0$ and the local time density at 0 will diverge[†].

The physical origin of the problem in this simple example is a *scalar boundary layer* near $x = 0$. A direct solution of the Neumann problem for the scalar field or integration over the above distribution shows that

$$\theta(x, t) = -J\mathbb{E}[\tilde{\ell}_{t,0}(x)] \sim J\sqrt{\frac{t}{\kappa}} f\left(\frac{x}{\sqrt{\kappa t}}\right) \quad (3.26)$$

for a suitable scaling function f . See Appendix B.1. There is thus a scalar boundary layer of thickness $\sim \sqrt{\kappa t}$ near 0 where the scalar field diverges as $\theta \sim J\sqrt{t/\kappa}$ as $\kappa \rightarrow 0$. Because there is a constant flux J into the domain and diffusive transport into the interior vanishes as $\kappa \rightarrow 0$, there is a “pile-up” of the scalar near $x = 0$. The scalar dissipation field due to this boundary layer is

$$\varepsilon_\theta(x, t) = \kappa |\partial_x \theta(x, t)|^2 \sim \frac{J^2}{\kappa} \left| f'\left(\frac{x}{\sqrt{\kappa t}}\right) \right|^2, \quad (3.27)$$

from which one can infer a total scalar dissipation $\propto J^2 \sqrt{t/\kappa} \rightarrow \infty$ as $\kappa \rightarrow 0$. This “dissipative anomaly” occurs even though there is clearly no spontaneous stochasticity in this simple example with $\mathbf{u}^\nu \equiv 0$!

The above example shows that the “loss of compactness” is not a mere technical mathematical difficulty, but instead that there may no longer be equivalence of spontaneous stochasticity and non-vanishing dissipation. Scalar boundary layers in wall-bounded flow domains with flux through the walls are a new possible source of scalar dissipation that can be non-zero (or even diverging) as $\nu, \kappa \rightarrow 0$, quite distinct from the spontaneous stochasticity mechanism. Of course, our FDR (3.14),(3.12) is valid even when there is either no spontaneous stochasticity or no anomalous dissipation. As we shall now discuss, the FDR can give physical information on the mechanisms and asymptotic behaviour of scalar dissipation also in such cases.

[†] In fact, if we consider the 1-point compactification $[0, \infty]$ of the range $[0, \infty)$ of possible scalar values, then $\lim_{\kappa \rightarrow 0} p^\kappa(\psi|0, t) = \delta_\infty(\psi)$, the delta-function at infinity. However, this compactification of the problem does not yield any result on spontaneous stochasticity.

3.3. Rayleigh-Bénard Convection with Flux Boundary Conditions

As a concrete example, we discuss Rayleigh-Bénard convection with imposed heat flux at the boundary, which has been previously studied as a model for poorly conducting top and bottom walls (Otero *et al.* 2002; Johnston & Doering 2009; Goluskin 2015). We begin by briefly reviewing the Rayleigh-Bénard problem in general. The most well-studied situation is a Boussinesq fluid in a right cylindrical cell with height H and cross-section S of arbitrary but fixed shape, with temperature imposed at the top and bottom and insulating side-walls (Bergé & Dubois 1984; Grossmann & Lohse 2000; Ahlers *et al.* 2009; Chillà & Schumacher 2012):

$$\partial_t \mathbf{u} + \mathbf{u} \cdot \nabla \mathbf{u} = -\nabla p + \nu \Delta \mathbf{u} + \alpha g T \hat{\mathbf{z}}, \quad (3.28)$$

$$\partial_t T + \mathbf{u} \cdot \nabla T = \kappa \Delta T, \quad (3.29)$$

$$\nabla \cdot \mathbf{u} = 0. \quad (3.30)$$

with boundary conditions:

$$\mathbf{u} = 0 \quad \text{no-slip at top, bottom, and side walls} \quad (3.31)$$

$$T|_{z=\pm H/2} = T_{top/bot} \quad \text{isothermal top/bottom walls} \quad (3.32)$$

$$\hat{\mathbf{n}} \cdot \nabla T = 0 \quad \text{insulating/adiabatic side walls} \quad (3.33)$$

where $T_{top} < T_{bot}$ are imposed space-time constant values which lead to convective instability. In the above equations, ν is the kinematic viscosity of the fluid, κ the thermal diffusivity, g the acceleration due to gravity and the constant α is the isobaric thermal expansion coefficient. Three dimensionless combinations of parameters characterize the system: the Rayleigh number, Prandtl number, and aspect ratio, defined respectively by

$$Ra = \frac{\alpha g H^3 \Delta T}{\kappa \nu}, \quad Pr = \frac{\nu}{\kappa}, \quad \Gamma = \frac{D}{H} \quad (3.34)$$

where $\Delta T = T_{bot} - T_{top}$ and $D = \text{diam}(S)$ is the diameter of the cell cross-section. A major question of interest is the heat transport across the cell, quantified by the vertical heat flux averaged over volume V and finite time-interval $[0, t]$:

$$J \equiv \langle u_z T - \kappa \partial_z T \rangle_{V,t}. \quad (3.35)$$

This is usually expressed as the dimensionless Nusselt number, which is the ratio between the total heat flux and the flux due to thermal conduction:

$$Nu = \frac{J}{\kappa \Delta T / H}. \quad (3.36)$$

The object of many studies has been to determine the functional dependence of Nu upon the dimensionless parameters Ra , Pr , and Γ of the problem.

This standard Rayleigh-Bénard problem corresponds, mathematically, to a system with mixed Neumann and Dirichlet boundary conditions for the temperature, which is an active scalar. Because of the mixed conditions, our results as so far discussed do not apply (but see section 4.4). However, there is a natural modification of the problem where the Dirichlet b.c. (3.32) for the temperature is replaced by a Neumann condition:

$$-\kappa \frac{\partial T}{\partial z} \Big|_{z=\pm H/2} = J_{in} \quad \text{imposed flux at top/bottom walls} \quad (3.37)$$

with J_{in} a space-time constant value. As we see below, J_{in} is the same as J given by (3.35) when a statistical steady-state exists at $t \rightarrow \infty$ with bounded temperature. The Nusselt number is still defined by (3.36) but the roles of J and ΔT as response and

control variables are reversed, with now $\Delta T = \langle T \rangle_{bot} - \langle T \rangle_{top}$ for T space-averaged over top and bottom walls and time-averaged over $[0, t]$. The natural dimensionless control variable in this problem is not the Rayleigh number but instead

$$Ra_* = \frac{\alpha g J H^4}{\kappa^2 \nu} = Ra \ Nu, \quad (3.38)$$

as noted by Otero *et al.* (2002). Numerical studies of Johnston & Doering (2009) suggest that Rayleigh-Bénard convection with temperature-b.c. and with flux-b.c. exhibit essentially identical behaviour in the turbulent regime, including both Nu - Ra scaling and morphology of the flow, such as thermal plumes.

There is an important formal difference between temperature-b.c and flux-b.c., however, with regard to thermal dissipative anomalies. This can be seen already for the problem of pure conduction with vanishing velocity field. The exact steady-state solution has $\partial T / \partial z = -J / \kappa = -\Delta T / H$ throughout the domain, and thus the mean thermal dissipation is $\langle \kappa |\nabla T|^2 \rangle_V = J^2 / \kappa = \kappa (\Delta T)^2 / H$ (for more discussion of this example, see Appendix B.2). For fixed ΔT as $\kappa \rightarrow 0$ of course $\langle \kappa |\nabla T|^2 \rangle_V \rightarrow 0$, but for fixed J instead $\langle \kappa |\nabla T|^2 \rangle_V \rightarrow \infty$! This is a trivial divergence for pure conduction, which can be eliminated by instead holding the vertical temperature-gradient $\partial T / \partial z = \beta$ fixed at $z = \pm H / 2$ as $\kappa \rightarrow 0$. However, in the case of turbulent Rayleigh-Bénard convection it is *a priori* unclear how to choose the κ, ν dependence of J so that ΔT remains fixed in the limit $\kappa, \nu \rightarrow 0$. Furthermore, even if ΔT is held fixed, the asymptotic behavior of the thermal dissipation is unknown. This question has great importance, since it is known that the dissipation of kinetic energy and temperature fluctuations determine the scaling of Nu at high Ra for the fixed- ΔT problem (Shraiman & Siggia 1990; Ahlers *et al.* 2009). To understand the implications of our fluctuation-dissipation relation for Rayleigh-Bénard convection with flux-b.c., we must therefore first discuss the role of dissipation, both of kinetic energy and temperature fluctuations, for Nu - Ra scaling in the fixed- J problem.

3.3.1. Anomalous Dissipation and “Ultimate” Scaling Theories

Global balances of conserved quantities impose simple but crucial constraints on turbulent Rayleigh-Bénard convection (Shraiman & Siggia 1990; Ahlers *et al.* 2009). Averaging the equation for conservation of kinetic energy over the cell volume and finite time-interval $[0, t]$ gives

$$\alpha g \left(J - \frac{\kappa}{H} \Delta T \right) = \nu \langle |\nabla \mathbf{u}|^2 \rangle_{V,t} + \langle \partial_t \left(\frac{1}{2} u^2 \right) \rangle_{V,t}, \quad (3.39)$$

where the lefthand side is input of kinetic energy by buoyancy force and the righthand side is the sum of viscous dissipation and kinetic energy growth. Likewise, the mean temperature fluctuation balance is

$$\frac{\Delta(TJ)}{H} = \kappa \langle |\nabla T|^2 \rangle_{V,t} + \langle \partial_t \left(\frac{1}{2} T^2 \right) \rangle_{V,t} \quad (3.40)$$

with $\Delta(TJ) = \langle TJ \rangle_{bot} - \langle TJ \rangle_{top}$, where the lefthand side is the input of temperature fluctuations from the boundary and the righthand side is the sum of thermal dissipation and growth of mean temperature fluctuation. These equations hold for both temperature- and flux-b.c. However, for temperature-b.c. $\Delta(TJ) = T_{bot} \langle J \rangle_{bot} - T_{top} \langle J \rangle_{top}$ whereas for flux-b.c. $\Delta(TJ) = (\langle T \rangle_{bot} - \langle T \rangle_{top}) J_{in} = \Delta T J_{in}$ and J_{in} imposed at the top and bottom is *a priori* distinct from J defined as the volume-average (3.35).

Further simplification occurs for the long-time $t \rightarrow \infty$ limit. In that case, the time-derivative terms in (3.39)-(3.40) converge to zero, as long as volume-average kinetic energy and temperature fluctuation remain bounded uniformly in time at constant $\nu, \kappa > 0$.

The balance equation for the mean of the temperature then gives the additional information that $\partial J(z)/\partial z = 0$ where

$$J(z) = \langle u_z T - \kappa \partial_z T \rangle_{A, \infty} = J \quad (3.41)$$

is the vertical heat flux area-averaged over the cross-section S of the cell at height z . The constancy of the vertical heat flux with height implies that $J_{in} = J$ for flux-b.c. and $\langle J \rangle_{top} = \langle J \rangle_{bot} = J$ for temperature-b.c. The long-time global balance equations then become identical for temperature-b.c. and flux-b.c.:

$$\alpha g \left(J - \frac{\kappa}{H} \Delta T \right) = \nu \langle |\nabla \mathbf{u}|^2 \rangle_{V, \infty} = \varepsilon_u \quad (3.42)$$

$$\frac{J \Delta T}{H} = \kappa \langle |\nabla T|^2 \rangle_{V, \infty} = \varepsilon_T, \quad (3.43)$$

but the role of J and ΔT as control and response variable is reversed for the two cases.

Now consider the limit $\nu, \kappa \rightarrow 0$ with Pr fixed. First note that $J - \kappa \frac{\Delta T}{H} = J(1 - \frac{1}{Nu}) \simeq J$ for $Nu \gg 1$. Defining as usual the free-fall velocity

$$U = (\alpha g \Delta T H)^{1/2} \quad (3.44)$$

and neglecting the small $\frac{1}{Nu}$ correction term in the energy balance,

$$\frac{\varepsilon_u}{U^3/H} = \frac{\varepsilon_T}{(\Delta T)^2 U/H} = \frac{J}{U \Delta T} = \frac{Nu}{\sqrt{Ra} Pr}. \quad (3.45)$$

The scaling law $Nu \sim C \cdot Ra^{1/2} Pr^{1/2}$ of Kraichnan (1962) and Spiegel (1971) holds if and only if at fixed Pr

$$\lim_{\nu, \kappa \rightarrow 0} \frac{\varepsilon_u}{U^3/H} = \lim_{\nu, \kappa \rightarrow 0} \frac{\varepsilon_T}{(\Delta T)^2 U/H} = C > 0. \quad (3.46)$$

This equivalence holds for both temperature-b.c. and flux-b.c. Our argument formalizes the dimensional reasoning of Spiegel (1971), whereas Kraichnan (1962) based his conclusions on a conjectured turbulent shear-layer at very high Rayleigh numbers and obtained a Nusselt number smaller by a factor $\propto [\ln Ra]^{-3/2}$. For standard temperature-b.c. Rayleigh-Bénard convection, the relation (3.46) corresponds to both kinetic and thermal dissipation anomalies, if ΔT (and thus also U) is taken to be independent of ν, κ in the limit $\nu, \kappa \rightarrow 0$. This is only true, strictly speaking, for the Spiegel (1971) dimensional predictions, whereas the Kraichnan (1962) results correspond instead to dissipation both of thermal fluctuations and of kinetic energy vanishing very slowly (logarithmically) as $\nu, \kappa \rightarrow 0$ with all other parameters fixed.

A similar interpretation of Kraichnan-Spiegel scaling in terms of dissipative anomalies is also true for Rayleigh-Bénard convection with flux-b.c., but it requires a bit more explanation. For the latter problem one can define velocity and temperature scales

$$U_* = (\alpha g J H)^{1/3}, \quad \Delta T_* = J/U_*. \quad (3.47)$$

Note that $Ra_* = Re_*^3 Pr^2$ with $Re_* = U_* H/\nu$. Neglecting again the $1/Nu$ correction in the energy balance,

$$\frac{\varepsilon_u}{U_*^3/H} = 1, \quad \frac{\varepsilon_T}{(\Delta T_*)^2 U_*/H} = \frac{\Delta T}{\Delta T_*}. \quad (3.48)$$

If one chooses J to be fixed as $\nu, \kappa \rightarrow 0$, then the first equation has the interesting implication that there is necessarily a dissipative anomaly for kinetic energy in flux-b.c. Rayleigh-Bénard convection, whenever a finite-energy long-time limit exists[†]. It is also

[†] This is not an argument for existence of such a dissipative anomaly, but just a statement

easy to check that

$$\frac{\varepsilon_u}{U^3/H} = \frac{\varepsilon_T}{(\Delta T)^2 U/H} = \left(\frac{U_*}{U}\right)^3 = \left(\frac{\Delta T_*}{\Delta T}\right)^{3/2}. \quad (3.49)$$

Hence, validity of Kraichnan-Spiegel dimensional scaling is equivalent to

$$\lim_{\nu, \kappa \rightarrow \infty} \frac{\Delta T_*}{\Delta T} = C^{2/3}, \quad (3.50)$$

that is, dissipative anomalies for both kinetic and scalar energies in the limit $\nu, \kappa \rightarrow 0$ for flux-b.c. with J chosen to be independent of ν, κ . In the presence of anomalous dissipation, holding J fixed as $\nu, \kappa \rightarrow 0$ is equivalent to holding ΔT fixed.

It is important to stress that the relations (3.49) hold no matter whether flux-b.c. or temperature-b.c. are employed. It is thus physically more natural to associate dissipative anomalies with the non-vanishing of the dimensionless ratios in (3.49) as $\nu, \kappa \rightarrow 0$ rather than with the non-vanishing of $\varepsilon_u, \varepsilon_T$ as $\nu, \kappa \rightarrow 0$. With this interpretation, the absence of dissipative anomalies requires that $\Delta T/\Delta T_* \rightarrow \infty$ as $\nu, \kappa \rightarrow 0$. Comparing with (3.48) this means that when J is held fixed as $\nu, \kappa \rightarrow 0$, then $\varepsilon_T \rightarrow \infty$. It may appear odd to associate this behavior with “absence of dissipative anomaly”, but it should be kept in mind that for fixed J as $\nu, \kappa \rightarrow 0$, then $\varepsilon_T \rightarrow \infty$ even for the problem of pure heat conduction. Instead, dissipative anomalies in the physical sense are associated with ε_T remaining finite for $\nu, \kappa \rightarrow 0$ with J held fixed. It is easy to check by using the definitions of the various quantities that there is equivalence of the general scaling relations

$$Nu \sim Ra^x Pr^y \iff \frac{\Delta T}{\Delta T_*} \sim Ra_*^z Pr^w \quad (3.51)$$

with

$$x = \frac{1-3z}{2+3z}, \quad y = \frac{1-3w}{2+3z}. \quad (3.52)$$

These can be interpreted as a relation between J and ΔT

$$J \sim \frac{\kappa^{1-2x}(\alpha g)^x}{H^{1-3x}} Pr^{y-x} (\Delta T)^{1+x} \quad (3.53)$$

which must be maintained with flux-b.c. in order to hold ΔT fixed as $\nu, \kappa \rightarrow 0$. It follows from the rigorous bound of Otero *et al.* (2002) that $x \leq 1/2$. If $x < 1/2$, the Kraichnan-Spiegel value, then $J \rightarrow 0$ as $\nu, \kappa \rightarrow 0$ at fixed ΔT . In that case, $\Delta T/\Delta T_* \rightarrow \infty$ as $\nu, \kappa \rightarrow 0$ because the denominator $\Delta T_* \rightarrow 0$.

3.3.2. Fluctuation-Dissipation Relation for Rayleigh-Bénard Convection with Flux B. C.

With this clear understanding of the relevance of dissipative anomalies for turbulent Nu - Ra scaling for Rayleigh-Bénard convection with flux-b.c., we can now discuss the stochastic Lagrangian representation for the temperature field and our fluctuation-dissipation relation for the thermal dissipation. Using the notation $\tilde{\xi}_{t,s} = (\tilde{\xi}_{t,s}, \tilde{\eta}_{t,s}, \tilde{\zeta}_{t,s})$ and $\mathbf{x} = (x, y, z)$ for the Cartesian components, we can write separate expressions for the local times densities at the top and bottom wall:

$$\tilde{l}_{t,s}^{top}(\mathbf{x}) = \int_t^s dr \delta\left(\tilde{\zeta}_{t,r}(\mathbf{x}) - \frac{H}{2}\right), \quad \tilde{l}_{t,s}^{bot}(\mathbf{x}) = \int_t^s dr \delta\left(\tilde{\zeta}_{t,r}(\mathbf{x}) + \frac{H}{2}\right). \quad (3.54)$$

that no finite-energy steady-state can exist in the limit $\nu, \kappa \rightarrow 0$ without a dissipative anomaly for the kinetic energy. For example, this can be seen from eq.(3.39) for mean energy balance over a finite time t , which shows that, if there is no anomaly at finite time as $\kappa \rightarrow 0$, then $\alpha g J = \langle \partial_t(\frac{1}{2}u^2) \rangle_V$ and the space-average kinetic energy must grow linearly in time for fixed J .

The stochastic representation of the temperature field for this problem then becomes:

$$\begin{aligned} T(\mathbf{x}, t) &= \mathbb{E} \left[T_0(\tilde{\boldsymbol{\xi}}_{t,0}(\mathbf{x})) + J \left(\tilde{\ell}_{t,0}^{top}(\mathbf{x}) - \tilde{\ell}_{t,0}^{bot}(\mathbf{x}) \right) \right] \\ &= \int d^3x_0 T_0(\mathbf{x}_0) p(\mathbf{x}_0, 0|\mathbf{x}, t) \\ &\quad - J \int_0^t ds p_z(H/2, s|\mathbf{x}, t) + J \int_0^t ds p_z(-H/2, s|\mathbf{x}, t), \end{aligned} \quad (3.55)$$

with the conditional probability density for the z -component of the particle position:

$$p_z(z', s|\mathbf{x}, t) = \iint_S dx' dy' p(x', y', z', s|\mathbf{x}, t) = \mathbb{E} \left[\delta \left(z' - \tilde{\zeta}_{t,r}(\mathbf{x}) \right) \right]. \quad (3.56)$$

It is illuminating to discuss the properties of this stochastic representation in the long-time $t \rightarrow \infty$ limit. Because of incompressibility of the velocity field and ergodicity of the stochastic Lagrangian flow for $\kappa > 0$, the particle distributions must asymptotically become uniform over the domain:

$$\lim_{t \rightarrow \infty} p(\mathbf{y}, s|\mathbf{x}, t) = \frac{1}{V}, \quad \lim_{t \rightarrow \infty} p_z(z', s|\mathbf{x}, t) = \frac{1}{H}, \quad (3.57)$$

with \mathbf{y} , z' , s , and \mathbf{x} fixed as $t \rightarrow \infty$, where $V = HA$ is the volume of the cylindrical cell with cross-sectional area A . Thus,

$$\lim_{t \rightarrow \infty} \int d^3x_0 T_0(\mathbf{x}_0) p(\mathbf{x}_0, 0|\mathbf{x}, t) = \frac{1}{V} \int d^3x_0 T_0(\mathbf{x}_0) = \langle T_0 \rangle_V. \quad (3.58)$$

For flux-b.c. the volume average of $T(\mathbf{x}, t)$ is conserved in time so that memory of the initial average must be preserved. We assume for simplicity that $\langle T_0 \rangle_V = 0$, so that

$$T(\mathbf{x}, t) \simeq -J \int_0^t ds \left(p_z(H/2, s|\mathbf{x}, t) - \frac{1}{H} \right) + J \int_0^t ds \left(p_z(-H/2, s|\mathbf{x}, t) - \frac{1}{H} \right), \quad (3.59)$$

where the term Jt/H has been added and subtracted to make each of the integrands tend to zero for large time separations. From this expression one can see that the dependence upon the distant past for $s \ll t$ is negligible in comparison to the contribution from the recent past for $s \lesssim t$. One can also understand why generally $T(\mathbf{x}, t) > 0$ for $z \gtrsim -H/2$, since then usually

$$p_z(H/2, s|\mathbf{x}, t) < \frac{1}{H}, \quad p_z(-H/2, s|\mathbf{x}, t) > \frac{1}{H}, \quad s \lesssim t. \quad (3.60)$$

Exactly the opposite inequalities generally hold for $z \lesssim H/2$. Of course, $T(\mathbf{x}, t)$ evolves chaotically in time through the dependence of the transition probabilities upon \mathbf{u} , and there can be rare fluctuations of temperature with the “wrong” sign near both the top and bottom of the cell. Note that the long-time average is given by

$$\begin{aligned} \langle T(\mathbf{x}) \rangle_\infty &= \lim_{t \rightarrow \infty} \frac{1}{t} \int_0^t ds T(\mathbf{x}, s) \\ &= -J \int_{-\infty}^0 ds \left(p_z(H/2, s|\mathbf{x}, 0) - \frac{1}{H} \right) + J \int_{-\infty}^0 ds \left(p_z(-H/2, s|\mathbf{x}, 0) - \frac{1}{H} \right), \end{aligned} \quad (3.61)$$

whenever the latter integrals are convergent. These long-time averages will no longer depend upon the initial conditions \mathbf{u}_0 and T_0 at $s = -\infty$ if there is ergodicity of Eulerian dynamics for the Boussinesq fluid system at high Ra_* .

We can now write out concretely our fluctuation-dissipation relation for Rayleigh-

Bénard convection with flux-b.c.:

$$\kappa \int_0^t ds \langle |\nabla T(s)|^2 \rangle_V = \frac{1}{2} \left\langle \text{Var} \left[T_0(\tilde{\xi}_{t,0}) + J \left(\tilde{\ell}_{t,0}^{\text{top}} - \tilde{\ell}_{t,0}^{\text{bot}} \right) \right] \right\rangle_V \quad (3.62)$$

with $\text{Var} \left[T_0(\tilde{\xi}_{t,0}(\mathbf{x})) \right]$ given by the expression (2.48), and furthermore with

$$\begin{aligned} & \frac{1}{2} \text{Var} \left[J \left(\tilde{\ell}_{t,0}^{\text{top}}(\mathbf{x}) - \tilde{\ell}_{t,0}^{\text{bot}}(\mathbf{x}) \right) \right] \\ &= \frac{J^2}{2} \int_0^t ds \int_0^t ds' \left[p_{2z}(+H/2, s; +H/2, s' | \mathbf{x}, t) - p_z(+H/2, s | \mathbf{x}, t) p_z(+H/2, s' | \mathbf{x}, t) \right] \\ &+ \frac{J^2}{2} \int_0^t ds \int_0^t ds' \left[p_{2z}(-H/2, s; -H/2, s' | \mathbf{x}, t) - p_z(-H/2, s | \mathbf{x}, t) p_z(-H/2, s' | \mathbf{x}, t) \right] \\ &- \frac{J^2}{2} \int_0^t ds \int_0^t ds' \left[p_{2z}(+H/2, s; -H/2, s' | \mathbf{x}, t) - p_z(+H/2, s | \mathbf{x}, t) p_z(-H/2, s' | \mathbf{x}, t) \right] \\ &- \frac{J^2}{2} \int_0^t ds \int_0^t ds' \left[p_{2z}(-H/2, s; +H/2, s' | \mathbf{x}, t) - p_z(-H/2, s | \mathbf{x}, t) p_z(+H/2, s' | \mathbf{x}, t) \right] \end{aligned} \quad (3.63)$$

where

$$p_{2z}(z', s; z'', s' | \mathbf{x}, t) = \iint_S dx' dy' \iint_S dx'' dy'' p_2(x', y', z', s; x'', y'', z'', s' | \mathbf{x}, t). \quad (3.64)$$

and

$$\begin{aligned} & \text{Cov} \left[T_0(\tilde{\xi}_{t,0}(\mathbf{x})), J \left(\tilde{\ell}_{t,0}^{\text{top}}(\mathbf{x}) - \tilde{\ell}_{t,0}^{\text{bot}}(\mathbf{x}) \right) \right] \\ &= -J \int d^3 x_0 T_0(\mathbf{x}_0) \int_0^t ds \iint_S dx' dy' \\ &\quad \times \left[p_2(\mathbf{x}_0, 0; x', y', H/2, s | \mathbf{x}, t) - p(\mathbf{x}_0, 0 | \mathbf{x}, t) p(x', y', H/2, s | \mathbf{x}, t) \right] \\ &+ J \int d^3 x_0 T_0(\mathbf{x}_0) \int_0^t ds \iint_S dx' dy' \\ &\quad \times \left[p_2(\mathbf{x}_0, 0; x', y', -H/2, s | \mathbf{x}, t) - p(\mathbf{x}_0, 0 | \mathbf{x}, t) p(x', y', -H/2, s | \mathbf{x}, t) \right] \end{aligned} \quad (3.65)$$

These formulas provide a purely Lagrangian representation of the thermal dissipation. It is notable that the entire expression vanishes if the particle trajectories are statistically independent at distinct times (or, in particular, if particle positions are deterministic).

The finite-time fluctuation-dissipation relation is a bit complicated because of the several terms. However, all of the T_0 -dependence disappears in the long-time limit where the following simpler relation holds:

$$\begin{aligned} \langle \kappa |\nabla T|^2 \rangle_{V, \infty} &= \lim_{t \rightarrow \infty} \frac{1}{2t} \left\langle \text{Var} \left[J \left(\tilde{\ell}_{t,0}^{\text{top}} - \tilde{\ell}_{t,0}^{\text{bot}} \right) \right] \right\rangle_V \\ &= \sum_{\lambda, \lambda'} \lambda \lambda' \lim_{t \rightarrow \infty} \frac{J^2}{2t} \left\langle \text{Cov} \left[J \left(\tilde{\ell}_{t,0}^\lambda, \tilde{\ell}_{t,0}^{\lambda'} \right) \right] \right\rangle_V \end{aligned} \quad (3.66)$$

with $\lambda, \lambda' = \pm$, where we denote top/bottom walls by $+/-$. Indeed, it is rigorously true that $\lim_{t \rightarrow \infty} \frac{1}{t} \text{Var} \left[T_0(\tilde{\xi}_{t,0}(\mathbf{x})) \right] = 0$ for bounded initial data T_0 , since the variance is then at most $2(\max |T_0|)^2$. One can also argue that the contribution to the long-time average from the covariance (3.65) divided by t gives a vanishing contribution, since particle positions at time 0 and time s will become independent for $s \gg 0$ and thus

the s -integrals in (3.65) are expected to converge for $t \rightarrow \infty^\dagger$. For the same reason, the surviving contribution (3.66) is expected to be finite as $t \rightarrow \infty$ since in the double time-integration over s, s' in (C1) the integrand is non-negligible only for $s \simeq s'$.

According to the general result (3.15), the limit in (3.66) should furthermore be \mathbf{x} -independent without averaging over space. This may in fact be shown by a direct argument, which yields the much simpler formula

$$\lim_{t \rightarrow \infty} \frac{\lambda\lambda'}{2t} \text{Cov} \left[\tilde{\ell}_{t,0}^\lambda(\mathbf{x}), \tilde{\ell}_{t,0}^{\lambda'}(\mathbf{x}) \right] = \frac{\lambda\lambda'}{H} \int_{-\infty}^0 ds \left(p_z(\lambda H/2, s|\lambda' H/2, 0) - \frac{1}{H} \right). \quad (3.67)$$

We have defined

$$p_z(z, s|z', s') = \frac{1}{A} \iint_S dx' dy' p_z(z, s|x', y', z', s') \quad (3.68)$$

which gives the transition probability for vertical heights of the particles, if at time s' a uniform distribution of particles is taken over the volume \ddagger . The formulas (3.66),(3.67) are our *steady-state fluctuation-dissipation relation for Rayleigh-Bénard convection* with flux-b.c. The remarkable result is that the long-time average of the thermal dissipation is, in the Lagrangian sense, entirely due to statistical correlations of incidences of single fluid particles on the top and bottom walls at two distinct times. Because the derivation of the formula (3.67) is a bit technical, we present it in Appendix C.

The result of combining (3.66) and (3.67) can, in fact, be obtained by a simpler argument directly from the Eulerian balance relation (3.43) for thermal fluctuations in the long-time steady-state. To see this, use the Lagrangian formula (3.61) for the time-averaged temperature field and the definition (3.68) to write the area-averaged steady-state temperatures at the top/bottom walls as

$$\bar{T}^\lambda = -J \sum_{\lambda'=\pm} \lambda' \int_{-\infty}^0 ds \left(p_z(\lambda H/2, s|\lambda' H/2, 0) - \frac{1}{H} \right) \quad (3.69)$$

for $\lambda, \lambda' = \pm$. Thus, the steady-state temperature difference $\Delta T = \bar{T}^- - \bar{T}^+$ between the bottom and top plates is

$$\Delta T = J \sum_{\lambda, \lambda'=\pm} \lambda\lambda' \int_{-\infty}^0 ds \left(p_z(\lambda H/2, s|\lambda' H/2, 0) - \frac{1}{H} \right). \quad (3.70)$$

The result of substituting this Lagrangian expression for ΔT into the steady-state temperature balance $\varepsilon_T = J\Delta T/H$ in (3.43) is completely equivalent to the combination of our equations (3.66) and (3.67). The additional information provided by our FDR is contained in the separate expression (3.67), which relates the four different ΔT -contributions in (3.70) to statistical correlations of boundary local-time densities. We now discuss some of the implications of this fact.

Let us denote the pointwise scalar variance as

$$\langle \varepsilon_T^{fluc}(\mathbf{x}) \rangle_t \equiv \frac{1}{2t} \text{Var} \left[J \left(\tilde{\ell}_{t,0}^{top}(\mathbf{x}) - \tilde{\ell}_{t,0}^{bot}(\mathbf{x}) \right) \right], \quad (3.71)$$

which is a spatially-local measure in terms of statistical Lagrangian trajectories of the

\dagger Vanishing of the contribution from (3.65) follows also from the Cauchy-Schwartz inequality $\left| \frac{1}{2t} \text{Cov} \left[T_0(\tilde{\xi}_{t,0}(\mathbf{x})), J \left(\tilde{\ell}_{t,0}^{top}(\mathbf{x}) - \tilde{\ell}_{t,0}^{bot}(\mathbf{x}) \right) \right] \right|^2 \leq \frac{1}{2t} \text{Var} \left[T_0(\tilde{\xi}_{t,0}(\mathbf{x})) \right] \cdot \frac{1}{2t} \text{Var} \left[J \left(\tilde{\ell}_{t,0}^{top}(\mathbf{x}) - \tilde{\ell}_{t,0}^{bot}(\mathbf{x}) \right) \right]$.

\ddagger A uniform distribution over the volume implies a uniform distribution in area over the cross-section S at each height z . By incompressibility of the flow, the uniform distribution of particles over the volume is preserved in time. Thus, $\int dz' p_z(z, s|z', s') = 1$ for all z, s, s'

thermal dissipation averaged over the time-interval $[0, t]$. It is related by our FDR to the space-time average thermal dissipation as

$$\langle \varepsilon_T^{fluc} \rangle_\infty \equiv \lim_{t \rightarrow \infty} \langle \varepsilon_T^{fluc}(\mathbf{x}) \rangle_t = \langle \kappa |\nabla T|^2 \rangle_{V, \infty} = \varepsilon_T, \quad (3.72)$$

so that knowledge of $\langle \varepsilon_T^{fluc}(\mathbf{x}) \rangle_t$ suffices to determine the global mean thermal dissipation. It may be expected for relatively short times that $\langle \varepsilon_T^{fluc}(\mathbf{x}) \rangle_t$ and $\langle \kappa |\nabla T(\mathbf{x}, s)|^2 \rangle_t$ are well correlated in space, especially when the Boussinesq system (3.28)-(3.33) is solved with initial condition $T_0 = (\text{const.})$, so that both $\text{Var}[T_0(\xi_{t,0}(\mathbf{x}))]$ and the covariance term in (3.65) vanish identically. Of course, by its definition $\langle \varepsilon_T^{fluc}(\mathbf{x}) \rangle_t \geq 0$.

In the long-time limit, each of the four separate terms in (3.67) should be positive separately. This can be seen from (3.67) since wall-incidences of stochastic Lagrangian particles for near times $s \simeq s'$ are correlated for same-wall (*homohedral*) incidences but anti-correlated for opposite-wall (*heterohedral*) incidences. Indeed, for $s = s'$

$$p_z(z, s|x, y', z', s) = \iint_S dx dy \delta^3(\mathbf{x} - \mathbf{x}') = \delta(z - z'), \quad (3.73)$$

so that one must have

$$\lim_{s' \rightarrow s} p_z(\pm H/2, s | \pm H/2, s') = \infty, \quad (3.74)$$

whereas

$$\lim_{s' \rightarrow s} p_z(\mp H/2, s | \pm H/2, s') = 0. \quad (3.75)$$

For $s \ll s'$ the integrands of all four terms converge to zero as the incidences at widely separated times become independent and the (anti-)correlations decay. Because of the positive sign before the homohedral (variance) terms and the negative sign before the heterohedral (covariance) terms, all four contributions are presumably positive separately. Of the four terms in (3.67), positivity necessarily holds for the two variance terms

$$\langle \varepsilon_T^{fluc} \rangle_\infty^{++} = \lim_{t \rightarrow \infty} \frac{J^2}{2t} \text{Var} \left[\tilde{\ell}_{t,0}^{top}(\mathbf{x}) \right] \geq 0, \quad (3.76)$$

$$\langle \varepsilon_T^{fluc} \rangle_\infty^{--} = \lim_{t \rightarrow \infty} \frac{J^2}{2t} \text{Var} \left[\tilde{\ell}_{t,0}^{bot}(\mathbf{x}) \right] \geq 0, \quad (3.77)$$

and is plausibly true by the previous argument for the two covariance terms

$$\langle \varepsilon_T^{fluc} \rangle_\infty^{+-} = - \lim_{t \rightarrow \infty} \frac{J^2}{2t} \text{Cov} \left[\tilde{\ell}_{t,0}^{top}(\mathbf{x}), \tilde{\ell}_{t,0}^{bot}(\mathbf{x}) \right] = \langle \varepsilon_T^{fluc} \rangle_\infty^{-+}. \quad (3.78)$$

Note that

$$\langle \varepsilon_T^{fluc} \rangle_\infty^{+-} = \langle \varepsilon_T^{fluc} \rangle_\infty^{-+} \leq \frac{\langle \varepsilon_T^{fluc} \rangle_\infty^{++} + \langle \varepsilon_T^{fluc} \rangle_\infty^{--}}{2} \quad (3.79)$$

as a direct consequence of the Young inequality $uv \leq (u^2 + v^2)/2$ and that

$$\langle \varepsilon_T^{fluc} \rangle_\infty^{--} = \langle \varepsilon_T^{fluc} \rangle_\infty^{++} \quad (3.80)$$

because of the exact symmetry $z \rightarrow -z$, $u_z \rightarrow -u_z$, $T \rightarrow -T$ of the Boussinesq system with flux-b.c (3.28)-(3.33), which transforms one solution into another solution.

Since the natural scale of each of the probability density functions p_z in (3.67) is $1/H$, one can write these fluctuational dissipation contributions exactly for $\lambda, \lambda' = \pm$ as

$$\langle \varepsilon_T^{fluc} \rangle_\infty^{\lambda, \lambda'} = \frac{J^2}{H^2} \tau_{corr}^{\lambda \lambda'}, \quad \tau_{corr}^{\lambda \lambda'} = \lambda \lambda' \int_{-\infty}^0 ds [H \cdot p_z(\lambda H/2, s | \lambda' H/2, 0) - 1]. \quad (3.81)$$

Here $\tau_{corr}^{\lambda\lambda'}$ is an integral correlation time which measures the length of time required for the (anti-)correlations in (3.67) to decay for $|s - s'| \rightarrow \infty$, that is, the time required for the particle distributions near the walls to relax to uniform $1/H$ distributions. Long relaxation times correspond to large thermal dissipation. Summing over $\lambda, \lambda' = \pm$, we reach the important exact conclusion

$$\varepsilon_T = \frac{J^2}{H^2} \tau_{corr} \quad (3.82)$$

where $\tau_{corr} = \tau_{corr}^{hom} + \tau_{corr}^{het}$ is the sum of all correlation/mixing times with

$$\tau_{corr}^{hom} = \tau_{corr}^{++} + \tau_{corr}^{--}, \quad \tau_{corr}^{het} = \tau_{corr}^{+-} + \tau_{corr}^{-+}, \quad (3.83)$$

and

$$\tau_{corr}^{het} \leq \tau_{corr}^{hom}. \quad (3.84)$$

The scaling of ε_T with physical parameters is therefore completely determined by the scaling of τ_{corr} . This is an area-averaged mixing time for stochastic fluid particles starting at all locations on the heated walls to achieve a uniform density $1/H$, at least near the top and bottom walls. Note that non-uniform particle distributions in these vicinities are required to feed temperature fluctuations into the flow.

3.3.3. Thermal Dissipation, Near-Wall Mixing, and Lagrangian Mechanisms

We now discuss some of the physical implications of our fluctuation-dissipation relation for turbulent Rayleigh-Bénard convection. In the case of pure thermal conduction where $\mathbf{u} \equiv 0$ identically, it may be shown from formula (3.67) that

$$\tau_{corr}^{hom} = \frac{2}{3} \frac{H^2}{\kappa}, \quad \tau_{corr}^{het} = \frac{1}{3} \frac{H^2}{\kappa}. \quad (3.85)$$

See Appendix B.2 for this derivation. For pure conduction the incidence correlation times scale as the time to diffuse across the cell height H , reproducing the exact result for that problem that $\varepsilon_T = J^2/\kappa$. For turbulent convection, the Lagrangian relation (3.70) immediately gives $\tau_{corr} = H\Delta T/J$, which may be written as

$$\tau_{corr} = H/U_{flux} \equiv \tau_{flux}. \quad (3.86)$$

Here we have defined a *scalar flux velocity*

$$U_{flux} = J/\Delta T, \quad (3.87)$$

which is the equivalent fluid velocity required to maintain a flux J by convection of a temperature difference ΔT . The definition of Nusselt number $Nu = J/(\kappa\Delta T/H)$ implies

$$Nu = \frac{\tau_{diff}}{\tau_{flux}}, \quad \tau_{diff} = H^2/\kappa. \quad (3.88)$$

Thus, for large Nu one has $\tau_{corr} = \tau_{flux} \ll \tau_{diff} = H^2/\kappa$. Likewise, from the definitions of U, U_* , and U_{flux} and eq.(3.49) it follows immediately that

$$U_*^3 = U_{flux} U^2 \implies \frac{U_{flux}}{U} = \left(\frac{U_*}{U}\right)^3 = \frac{\varepsilon_T}{U(\Delta T)^2/H}. \quad (3.89)$$

Hence, in the Spiegel (1971) scenario $U_{flux} \simeq U_* \simeq U$ (equality up to order-unity constants) at high- Ra and all of the times $\tau_{corr} = \tau_{flux}$, H/U_* , and H/U are of the same order. Kraichnan (1962) assumed instead that $Pe_T = u_\tau \delta_T/\kappa$, where Pe_T is a critical Péclet number (estimated to be about 3) and u_τ is the friction velocity at the

top/bottom walls. This can be restated precisely in our framework as the conjecture that $U_{flux} = u_\tau/2Pe_T$. Appeal to the standard logarithmic law-of-the-wall led Kraichnan (1962) to conclude that $u_{rms} \propto U/\ln(Ra)$ and $u_\tau \propto U/\ln^{3/2}(Ra)$. For any other possible scaling behavior, $U_{flux} \ll U_* \ll U$ and one has $\tau_{corr} = \tau_{flux} \gg H/U_* \gg H/U$. This is our key conclusion for Rayleigh-Bénard turbulence.

Recall that the free-fall velocity U is observed empirically to be of the same order as the velocity U_{lsc} of the large-scale circulation or global wind (Ahlers *et al.* 2009), so that the free-fall time L/U is roughly of the same order as the large-scale circulation time. For example, it follows directly from the definition of the free-fall velocity that the U -based Reynolds number is $UH/\nu = Ra^{1/2}Pr^{-1/2}$, whereas experiments show that $U_{lsc}H/\nu$ scales very similarly in Ra , with an exponent only slightly smaller than $1/2$ (Niemela & Sreenivasan (2003), Appendix D; Ahlers *et al.* (2009), section IV) and numerical simulations give similar results (e.g. Scheel & Schumacher (2014), section 2). Our key conclusion may thus be nearly equivalently stated that existence of dissipative anomalies and validity of Kraichnan-Spiegel scaling requires τ_{corr} of order the large-scale turnover time, whereas for any other scaling $\tau_{corr} \gg H/U$ (and, in fact, even $\tau_{corr} \gg H/U_*$) and the distributions of particles released at the wall remain unmixed for many, many large-scale circulation times. From $\tau_{corr} = H\Delta T/J$ it is easy to see that

$$\tau_{corr} = \frac{H}{U} \frac{\sqrt{RaPr}}{Nu}. \quad (3.90)$$

Thus, τ_{corr} differs from H/U by precisely the same degree that the Kraichnan-Spiegel dimensional prediction differs from the true Nusselt number. This relation is consistent with $\tau_{corr} \gg H/U$ at $Ra \gg 1$ for any power-law $Nu \sim Ra^x Pr^y$ with $x < 1/2$. Nevertheless, it is *a priori* quite surprising that wall-incidences could remain correlated over so many large-scale circulation times. This requires some discussion of the underlying Lagrangian mechanisms.

Thermal plumes play a well-known role in the Lagrangian dynamics of the temperature field (Ahlers *et al.* 2009; Chillà & Schumacher 2012). In particular, plumes should transport thermal fluctuations from the boundary into the interior and create large values of $\langle \varepsilon_T^{fluc}(\mathbf{x}) \rangle_t$ at points \mathbf{x} within the bulk of the flow well way from the walls. If a plume reaches the interior point \mathbf{x} within the time t , then going backward in time the particle is transported to very near the wall of origin of the plume, at which point the stochastic noise $\propto \sqrt{\kappa}$ can then allow the particle to hit the wall. Note that, since the fluid velocity \mathbf{u} vanishes smoothly at the wall for $\nu, \kappa > 0$, advection on its own can never produce a wall incidence. The non-vanishing of the boundary local time densities $\tilde{\ell}_{t,0}^{top/bot}(\mathbf{x})$ for points \mathbf{x} in the bulk of the flow is thus presumably due largely to the mediation of the plumes when $Ra \gg 1$. In particular, one expects enhanced values of $\langle \varepsilon_T^{fluc}(\mathbf{x}) \rangle_t$ at times t for which \mathbf{x} is within a plume. Observe that enhanced values of the thermal dissipation $\varepsilon_T(\mathbf{x}, t)$ itself are observed within plumes (e.g. see Emran & Schumacher (2012)).

However, to understand possible mechanisms that could give $\tau_{corr} \gg H/U$ it is more important to understand the Lagrangian dynamics that could lead stochastic particles to hit the top/bottom walls forward in time or, equivalently, to escape from the top/bottom wall backward in time. In order for a stochastic particle starting at the top or bottom wall to achieve a uniform density $1/H$ of vertical-distances near these walls, the particle must have travelled at least several times between the top and bottom wall across distance H . Note that $\tau_{corr}^{hom} \gg H/U$ means that a particle currently at the top/bottom wall had a high probability to be at the same wall over a very long period of earlier times (many turnover times). Similarly, $\tau_{corr}^{het} \gg H/U$ means that a particle currently at the top/bottom wall

had a very low probability to be at the opposite wall over a very long period of earlier times (many turnover times) Thus, turbulent convection must not be very efficient at bringing particles close to the wall if $\tau_{corr} \gg H/U$, else the particles would readily escape backward in time. The obvious fluid motions which carry stochastic Lagrangian particles from interior points to points close to the wall consist of the large-scale circulation and “old” plumes which have completed a transit between top and bottom. These motions will carry particles between points near the top and bottom in a time H/U_{lsc} which is only slightly larger than H/U .

Hence, $\tau_{corr} \gg H/U$ means that these motions must not typically bring the particles close enough to actually hit the wall, and instead the interior particles will circulate many, many turnover times before finally hitting the top or bottom wall. In order to be guaranteed to hit the wall in time τ_{corr} , the particles must be advected to a distance $\ell_T = \sqrt{\kappa\tau_{corr}}$ from the top/bottom wall, since thermal diffusion then suffices to carry the particle the remaining distance. Using Eq.(3.88) gives

$$\ell_T = \sqrt{\kappa\tau_{corr}} = H/\sqrt{Nu}. \quad (3.91)$$

Consider any distance δ asymptotically much smaller than ℓ_T for $Ra \gg 1$, in particular, the traditional outer thermal boundary layer thickness $\delta_T = H/2Nu$. Our results imply that bulk fluid particles cannot reach a distance δ_T from the top/bottom walls in any time less than τ_{corr} , with $\tau_{corr} \gg H/U$ if Kraichnan-Spiegel scaling fails. The time for particles at the top/bottom wall to diffuse across the thermal boundary layer is $\delta_T^2/\kappa = \tau_{corr}/4Nu$, which is much shorter than the time τ_{corr} to transit effectively the bulk. The region within distance ℓ_T of the top/bottom walls but further away from those walls than δ_T might possibly be identified with the “plume mixing zone” proposed by Castaing *et al.* (1989); see also Procaccia *et al.* (1991). The inner boundary of this “mixing zone” was considered to be δ_T , while the outer boundary distance (denoted ℓ_m or d_m) was predicted to scale as $\ell_m \sim H/Ra^{1/7}$. Since Castaing *et al.* (1989) and Procaccia *et al.* (1991) also predicted $Nu \sim Ra^{2/7}$, this is consistent with our result (3.91) for the scaling of ℓ_T †. If we adopt the terminology of Castaing *et al.* (1989), then it is in the “central region”, at distances further than ℓ_T from the top/bottom walls, where particles must be “trapped” for many large-scale circulation times, if Kraichnan-Spiegel scaling fails.

If an “ultimate regime” with Kraichnan-Spiegel scaling does exist at very high Rayleigh numbers, then our Lagrangian analysis suggests that a Reynolds number $Re_\ell \equiv u(\ell_T)\ell_T/\nu$ is most appropriate to signal the possible transition. Here $u(\ell_T)$ is a typical (e.g. rms) velocity at distance ℓ_T from the top/bottom walls. When the Reynolds number Re_ℓ becomes critical, then turbulent mixing reaches to eddies within distance ℓ_T of the top/bottom

† However, this may be a coincidence. The plausible equations $u_{rms} \sim (\alpha g H T_{rms})^{1/2}$ [(3.2)] and $J \sim u_{rms} T_{rms}$ [(3.3)] of Castaing *et al.* (1989) together with their proposed relation $\delta_T/\ell_m \sim T_{rms}/\Delta T \sim Re^\gamma$ [(3.18)] imply for a general scaling law $Nu \sim Ra^\beta$ that $\gamma = (2\beta - 1)/3$ [(3.4)]. The condition $\gamma = -\beta/2$ that follows from identifying $\ell_m \sim \ell_T$ is only satisfied for the choice $\beta = 2/7$ and thus one does not obtain $\ell_m \sim H/\sqrt{Nu}$ in general. A possible way out of this conclusion was indicated by Castaing *et al.* (1989), p.20: “To introduce a different scaling, one would need to assume that the thermals fill only a vanishing fraction of the space, at large Ra .” Accordingly, one can modify their (3.3) to $J \sim u_{rms} T_{rms} f$ where the volume fraction $f \sim Ra^{-\delta}$. If one leaves (3.2) and (3.18) of Castaing *et al.* (1989) unchanged, their (3.4) is replaced by $\varepsilon = (1 + \gamma)/2$, $\gamma = (2\beta + 2\delta - 1)/3$, where ε is the Reynolds exponent in $Re_{rms} \sim Ra^\varepsilon$. If one imposes our condition $\gamma = -\beta/2$, one obtains $\delta = (2 - 7\beta)/4$. In that case, $\delta < 0$ for any $\beta > 2/7$ and, in particular, for the observed values $\beta \doteq 0.3 - 0.43$ at current highest Rayleigh numbers. One is led to an unreasonable conclusion that f should increase as a positive power of Ra ! Thus, either one of the assumptions (3.2), (3.3), or (3.18) of Castaing *et al.* (1989) is wrong (we find the last the most dubious) or else the identification $\ell_T \sim \ell_m$ is generally invalid.

walls, and one may plausibly expect that $\tau_{corr} \sim H/U$. This is similar to the arguments of Niemela & Sreenivasan (2003), Niemela & Sreenivasan (2006), and He *et al.* (2012), but replacing the kinetic boundary layer thickness $\delta_v = aH/\sqrt{Re}$ with $\ell_T = bH/\sqrt{Nu}$ ‡. If Kraichnan-Spiegel scaling holds, then both δ_v and ℓ_T scale with Rayleigh number as $Ra^{-1/4}$, so that at fixed Prandtl number one may essentially identify $\delta_v \sim \ell_T$. However, alternate theories predict $Nu \sim Ra^x$ with $x < 1/2$, and the rigorous upper bound of Otero *et al.* (2002) for flux-b.c. requires $x \leq 1/2$. In that case, $\ell_T/\delta_v \sim (b/a)Ra^{(1-2x)/4}$ (where we assume the approximate scaling $Re \sim Ra^{1/2}$), and $\ell_T > \delta_v$ at sufficiently high Rayleigh numbers. At lower Rayleigh numbers, one may have instead $\ell_T < \delta_v$ if $b < a$. For example, assuming the predicted scaling exponent $x = 1/3$ of Malkus (1954), Priestley (1959), and Kraichnan (1962) at intermediate Rayleigh numbers, a ratio $b/a = 1/10$ at $Pr = 1$ would lead to $\ell_T < \delta_v$ up to $Ra = 10^{12}$. It is thus unclear whether our suggested criterion for an “ultimate regime” is more stringent or weaker than those based on standard shear Reynolds numbers (Niemela & Sreenivasan 2003, 2006; He *et al.* 2012).

Our considerations do not allow us to make a definite theoretical prediction for Nu as a function of Ra and Pr , so that we must consider briefly the observations. There seem to have been relatively few empirical studies of turbulent Rayleigh-Bénard convection with flux-b.c. The 2D numerical study of Johnston & Doering (2009) exhibited a scaling law $Nu \sim Ra^x$ with non-Kraichnan-Spiegel exponent $x \doteq 0.285$ up to $Ra = 10^{10}$. This study also found identical scaling with temperature-b.c. in the turbulent regime and suggested that the two types of boundary conditions would exhibit generally equivalent physical behavior in the turbulent regime also in 3D. A subsequent 3D simulation of Stevens *et al.* (2011) with temperature b.c. at the top wall and flux-b.c. at the bottom wall provides some corroboration of this hypothesis. With this assumption, we may also compare with the much larger body of work for temperature-b.c. In contrast to the empirical results for turbulent dissipation of passive scalars summarized by Donzis *et al.* (2005), experimental and numerical studies up to Rayleigh numbers of order 10^{10} show that thermal dissipation in turbulent Rayleigh-Bénard convection scales as

$$\frac{\varepsilon_T}{(\Delta T)^2 U/H} \sim Ra^z \quad (3.92)$$

with a *negative* exponent $z \doteq -0.20$ (Emran & Schumacher 2008, 2012; He *et al.* 2007; He & Tong 2009). Thus, empirical evidence does not support existence of a thermal dissipative anomaly in this range of Rayleigh numbers. Consistently, these experiments and simulations observe $Nu \sim Ra^x$ with exponent $x = 0.5 + z \doteq 0.3 < 1/2$, which represents a 40% difference from the Kraichnan-Spiegel scaling exponent. Experiments at even higher Rayleigh numbers see somewhat larger exponents $x \doteq 0.32-0.43$ but apparently still at least 10-20% smaller than the Kraichnan-Spiegel exponent $x = 0.5$ (Ahlers *et al.* 2009; Chillà & Schumacher 2012). Two experimental groups that observed the largest exponents have interpreted their results, not implausibly †, as transitions to an “ultimate regime” with logarithmic corrections of the sort predicted by Kraichnan (Roche *et al.* 2010; He *et al.* 2012).

Another possible explanation of the deviations from Kraichnan-Spiegel scaling is pro-

‡ Here we have introduced a dimensionless prefactor b of order unity, whose precise value could be important at moderately large Rayleigh numbers. It must hold that $b \lesssim 1$, since the time to diffuse across the distance ℓ_T should be a fraction of τ_{corr} . A reasonable choice would be perhaps to set $b = 1$ by convention, so that $\ell_T^2/2\kappa = \frac{1}{2}\tau_{corr}$.

† Based on the data published in Roche *et al.* (2010) and He *et al.* (2012), one can estimate the Reynolds number $Re_\ell = u(\ell_T)\ell_T/\nu$ at the apparent onset of a new Nusselt-scaling to be of the order of several hundreds, in the range where transition to turbulence is expected.

vided by the numerical results of Emran & Schumacher (2012), who found that the thermal plumes occupy a smaller volume of the flow (and are associated with decreased thermal dissipation) for increasing Ra . Thus, convective transport across the cell height is less efficient and larger τ_{corr} values are required to achieve near-wall vertical mixing. However, the decrease of the volume fraction of plumes f_{pl} observed in Fig. 6 of Emran & Schumacher (2012) is rather weak, declining only from 75% to 65% in 3.5 decades, roughly $f_{pl} \sim Ra^{-0.02}$. If we assume that the “effective transport velocity” is $U_{eff} = U f_{pl}$, then we see from (3.90) and the empirical results cited above that

$$\tau_{corr} \sim \frac{H}{U_{eff}} Ra^{0.18}, \quad (3.93)$$

and still $\tau_{corr} \gg H/U_{eff}$ or, equivalently, $U_{flux} \ll U_{eff}$ for $Ra \gg 1$. Likewise, the measurements of Re_{lsc} in the experiment of Qiu & Tong (2002) reviewed by Ahlers *et al.* (2009) imply that $U_{lsc}/U \sim Ra^{-0.04}$, and the numerical results of Scheel & Schumacher (2014) on the Reynolds number Re_{rms} imply an rms flow velocity $u_{rms}/U \sim Ra^{-0.01}$. The theoretical suggestion $U_{flux} \simeq u_\tau$ of Kraichnan (1962) with $u_\tau/U \sim A/\ln^{3/2}(Ra)$ shows even a weaker decrease with Ra . None of these effects, alone or in combination, seem clearly sufficient to explain the large value $\tau_{corr} \sim (H/U)Ra^{0.1-0.2}$ that is inferred from existing Nusselt-number measurements[†].

There is thus not only an issue to account for the observed deviations from Kraichnan-Spiegel scaling, but even to explain how current empirical results can be consistent with our exact fluctuation-dissipation relation (3.67)! One fact which may be relevant is that our long-time FDR as derived in (2.19) or (3.67) is only valid for times $t \gg \tau_{corr}$. If $\tau_{corr} \gg H/U$ as evidence suggests, then no experiments or simulations are averaging over the very long time-intervals required to see the infinite-time limit. Thus, a more exotic speculation is that all current experiments and simulations may be observing very long-lived but transient regimes with no dissipative anomalies and different scaling from the true infinite-time limit. This might be the case if there is no finite-time singularity for the ideal Boussinesq equations, but if singularities do appear in the opposite limit $t \rightarrow \infty$ first and then $\nu, \kappa \rightarrow 0$ (similar to what is expected for 2D turbulence). All of these issues would be greatly illuminated by direct experimental and numerical measurements of τ_{corr} at currently achievable Rayleigh numbers using passive tracers. While we can offer no final resolution of these puzzles, we believe that our approach will have great value for further theoretical and empirical investigations of turbulent convection, because it provides an exact connection between the thermal dissipation rate and the underlying Lagrangian fluid mechanisms.

4. Imposed Scalar Values at the Wall and Mixed Conditions

In this section we extend our previous results as far as possible to advection-diffusion of scalars in wall-bounded domains with the general mixed Dirichlet-Neumann conditions (3.1),(3.2). We first consider the special case of a scalar $\theta(\mathbf{x}, t)$ with pure Dirichlet boundary conditions ($\partial\Omega_D = \partial\Omega$):

$$\begin{aligned} \partial_t \theta + \mathbf{u} \cdot \nabla \theta &= \kappa \Delta \theta + S & \text{for } \mathbf{x} \in \Omega, \\ \theta(\mathbf{x}, t) &= \psi(\mathbf{x}, t) & \text{for } \mathbf{x} \in \partial\Omega. \end{aligned} \quad (4.1)$$

[†] However, with different thresholds in defining “plumes”, Emran & Schumacher (2012) find an f_{pl} which is smaller and declines faster. For example, with the parameter $\delta = 1$ of that paper their Fig. 7 shows a decline of f_{pl} from 50% to 20% over 3.5 decades or $f_{pl} \sim Ra^{-0.11}$.

for given initial data θ_0 and boundary data ψ . Of course, pure Dirichlet conditions are often encountered in practice, e.g. turbulent channel flow with opposite walls held at two fixed temperatures. This special case already presents the essential new difficulties and, after analyzing it in detail, we shall briefly comment on modifications required for the general mixed case. As a particular example of the latter, we shall discuss briefly the problem of turbulent convection in a standard Rayleigh-Bénard experiment with insulated side-walls and imposed temperatures at the top and bottom walls.

4.1. Stochastic Representation and Fluctuation-Dissipation Relation

The standard stochastic representation of solutions of the problem (4.1) involves stochastic particles which are stopped at the boundary, contributing a term due to the value maintained at the wall (Keanini 2007; Soner 2007; Oksendal 2013). A brief review of this theory is in order. The stochastic flow may again be defined with reflection at the boundary, governed by the equation (3.5) involving the boundary local time. The new notion is the (*backward*) *stopping time*, which is defined for $\mathbf{x} \in \Omega$ by the larger of $\{\sup\{s : \tilde{\xi}_{t,s}(\mathbf{x}) \in \partial\Omega\}, 0\}$, the first time to hit the spatial boundary, and initial time 0, or

$$\tilde{\tau}(\mathbf{x}, t) = \max \left\{ \sup\{s : \tilde{\xi}_{t,s}(\mathbf{x}) \in \partial\Omega\}, 0 \right\}, \quad (4.2)$$

This time is the first (going backward) at which the stochastic Lagrangian particle hits the closed set \mathcal{S} which is the union of the “side surface” $\mathcal{S}_s = \partial\Omega \times [0, t)$ and the “base” $\mathcal{S}_b = \Omega \times \{0\}$ of the right cylindrical domain $\mathcal{D} = \Omega \times [0, t)$ in $(d+1)$ -dimensional space-time, when starting at a point (\mathbf{x}, t) in the “top” $\mathcal{S}_t = \Omega \times \{t\}$. To state conveniently the stochastic representation, we define the function which gives the data on \mathcal{S} :

$$\Theta(\mathbf{x}, s) = \begin{cases} \psi(\mathbf{x}, s), & s > 0 \text{ and } \mathbf{x} \in \partial\Omega \\ \theta_0(\mathbf{x}), & s = 0 \text{ and } \mathbf{x} \in \Omega \end{cases}. \quad (4.3)$$

Using the backward Itô formula (3.9) and integrating from time t down to the stopping time $\tilde{\tau}(\mathbf{x}, t)$ gives

$$\begin{aligned} \theta(\mathbf{x}, t) &= \Theta(\tilde{\xi}_{t, \tilde{\tau}(\mathbf{x}, t)}(\mathbf{x}), \tilde{\tau}(\mathbf{x}, t)) + \int_{\tilde{\tau}(\mathbf{x}, t)}^t dt' S(\tilde{\xi}_{t, t'}(\mathbf{x}), t') \\ &\quad + \sqrt{2\kappa} \int_{\tilde{\tau}(\mathbf{x}, t)}^t \hat{d}\tilde{\mathbf{W}}_{t'} \cdot \nabla \theta(\tilde{\xi}_{t, t'}(\mathbf{x}), t'), \end{aligned} \quad (4.4)$$

where we used the fact that $\tilde{l}_{t,s}(\mathbf{x}) \equiv 0$ for all $\tilde{\tau}(\mathbf{x}, t) < s < t$ and also used the equations (4.1). Taking the expectation over the Brownian motion then yields for solutions of the initial-boundary value problem the following stochastic representation:

$$\theta(\mathbf{x}, t) = \mathbb{E} \left[\Theta(\tilde{\xi}_{t, \tilde{\tau}(\mathbf{x}, t)}(\mathbf{x}), \tilde{\tau}(\mathbf{x}, t)) + \int_{\tilde{\tau}(\mathbf{x}, t)}^t ds S(\tilde{\xi}_{t,s}(\mathbf{x}), s) \right] \quad (4.5)$$

See Keanini (2007); Soner (2007); Oksendal (2013) for more details. In particular, the Itô integral in (4.4) is a (backward) martingale by the optional stopping theorem (Oksendal 2013). This formula represents the solution $\theta(\mathbf{x}, t)$ to the scalar advection-diffusion equation as an average over randomly sampled sources and initial-boundary data.

It is now straightforward to obtain a fluctuation-dissipation relation. Applying the Itô isometry valid with the random stopping time as the lower range of the integral (e.g. see

Oksendal (2013), Theorem 7.4.1)

$$\mathbb{E} \left| \int_{\tilde{\tau}(\mathbf{x},t)}^t \hat{d}\widetilde{\mathbf{W}}_s \cdot \nabla \theta(\tilde{\boldsymbol{\xi}}_{t,s}(\mathbf{x}), s) \right|^2 = 2 \mathbb{E} \left[\int_{\tilde{\tau}(\mathbf{x},t)}^t ds |\nabla \theta(\tilde{\boldsymbol{\xi}}_{t,s}(\mathbf{x}), s)|^2 \right] \quad (4.6)$$

Thus we obtain from (4.4),(4.5) that

$$\begin{aligned} \text{Var} \left[\Theta(\tilde{\boldsymbol{\xi}}_{t,\tilde{\tau}(\mathbf{x},t)}(\mathbf{x}), \tilde{\tau}(\mathbf{x},t)) + \int_{\tilde{\tau}(\mathbf{x},t)}^t ds S(\tilde{\boldsymbol{\xi}}_{t,s}(\mathbf{x}), s) \right] \\ = 2\kappa \mathbb{E} \left[\int_{\tilde{\tau}(\mathbf{x},t)}^t ds |\nabla \theta(\tilde{\boldsymbol{\xi}}_{t,s}(\mathbf{x}), s)|^2 \right]. \end{aligned} \quad (4.7)$$

Finally, averaging over the space domain yields

$$\begin{aligned} \frac{1}{2} \left\langle \text{Var} \left[\Theta(\tilde{\boldsymbol{\xi}}_{t,\tilde{\tau}(t)}(\tilde{\tau}(t)), \tilde{\tau}(t)) + \int_{\tilde{\tau}(t)}^t ds S(\tilde{\boldsymbol{\xi}}_{t,s}, s) \right] \right\rangle_{\Omega} \\ = \kappa \left\langle \mathbb{E} \left[\int_{\tilde{\tau}(t)}^t ds |\nabla \theta(\tilde{\boldsymbol{\xi}}_{t,s}, s)|^2 \right] \right\rangle_{\Omega}. \end{aligned} \quad (4.8)$$

This exact result is one possible version of a fluctuation-dissipation relation for scalar turbulence with general Dirichlet boundary conditions.

Unlike our previous relations, however, the righthand side of the above is not the total time-integrated scalar dissipation over the entire domain of the flow. The relation easily yields a lower bound on the total scalar dissipation by simply extending the time integration down to $s = 0$,

$$\begin{aligned} \frac{1}{2} \left\langle \text{Var} \left[\Theta(\tilde{\boldsymbol{\xi}}_{t,\tilde{\tau}(t)}(\tilde{\tau}(t)) + \int_{\tilde{\tau}(t)}^t ds S(\tilde{\boldsymbol{\xi}}_{t,s}, s) \right] \right\rangle_{\Omega} \\ \leq \kappa \left\langle \mathbb{E} \left[\int_0^t ds |\nabla \theta(s)|^2 \right] \right\rangle_{\Omega}. \end{aligned} \quad (4.9)$$

because the s -integrand is non-negative and the reflected stochastic flow is volume-preserving. The difference between the righthand and lefthand sides is

$$\begin{aligned} \Delta^{\nu,\kappa}(t) &\equiv \kappa \int_0^t ds \frac{1}{|\Omega|} \int_{\Omega} d^d x |\nabla \theta(\mathbf{x}, s)|^2 - \kappa \mathbb{E} \left[\frac{1}{|\Omega|} \int_{\Omega} d^d x \int_{\tilde{\tau}(\mathbf{x},t)}^t ds |\nabla \theta(\tilde{\boldsymbol{\xi}}_{t,s}(\mathbf{x}), s)|^2 \right] \\ &= \kappa \int_0^t ds \mathbb{E} \left[\frac{1}{|\Omega|} \int_{\tilde{\Omega}_{t,s}} d^d x |\nabla \theta(\tilde{\boldsymbol{\xi}}_{t,s}(\mathbf{x}), s)|^2 \right] \end{aligned} \quad (4.10)$$

where

$$\tilde{\Omega}_{t,s} = \{\mathbf{x} \in \Omega : \tilde{\tau}(\mathbf{x}, t) > s\} \quad (4.11)$$

is the set of positions \mathbf{x} for which the stochastic particle has already hit the boundary by time s (going backward). The inequality (4.9) thus fails to be an equality because of the missing contributions to total dissipation at positions of reflected particles. We shall discuss further below the sharpness of the inequality (4.9) and whether it should, in a suitable limit, become equality.

To gain further insight, we present now some numerical results on PDF's of hitting-times for the channel-flow database. We considered two release points in the buffer layer at height $\Delta y = 10\delta_\tau$ above the bottom wall and at the final time t_f of the database. The

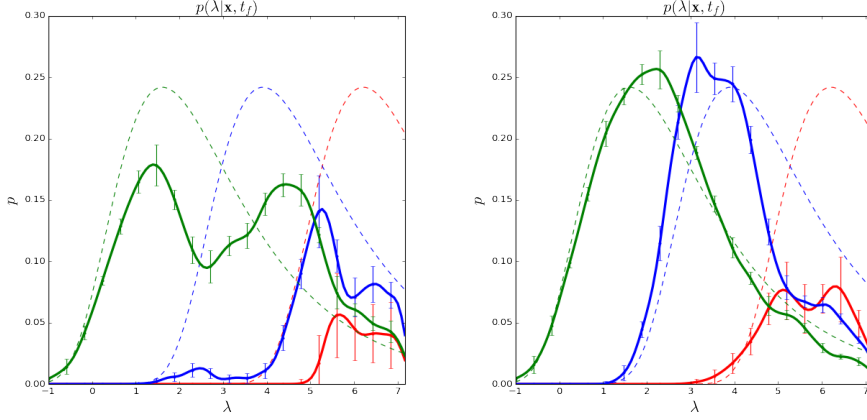


Figure 5: PDF's of the logarithmic hitting-time variable $\lambda = \ln((t_f - \tau)/t_\nu)$. *Left panel*: Particles released in a high-speed streak, *Right panel*: particles released in a low-speed streak, for channel flow (solid lines) and pure diffusion (dashed lines) and for the three Prandtl numbers $Pr = 0.1$ (green), 1.0 (blue) and 10 (red).

wall-parallel positions of the release points are those shown in Figure 3, and thus one is in a high-speed streak and the other in a low-speed streak. In order to calculate hitting-time PDF's, we evolved $N = 14,336$ samples of stochastic particles solving Eq. (3.5) for three Prandtl numbers $Pr = 0.1, 1, 10$ at both release points. Note that hitting-times τ satisfying $t_f - \tau \ll t_\nu$ and $t_f - \tau \gg t_\nu$ are both very rare events which could not be observed even with so many samples. We thus consider here the logarithmic variable $\lambda \equiv \ln((t_f - \tau)/t_\nu)$ which is appropriate to typical values and calculate PDF's $p(\lambda|\mathbf{x}, t_f)$. The numerical procedures are discussed at length in Appendix E.3. Here we just note that the PDF's are obtained up to the largest available $\lambda = \ln(t_f/t_\nu) \doteq 7.17$ and down to $\lambda = -1$, but the PDF's at the two extremes contain further errors that are not indicated by the error bars (representing both s.e.m. for N -samples averages and variation with kernel bandwidth). The PDF's for $\lambda < 1.6$ are shifted to the right by about 5%, because our time-step $\Delta s \doteq 2 \times 10^{-3}$ cannot fully resolve the smaller hitting times. For $\lambda > 6.5$ the PDF's from kernel-density estimates are too small, because of the endpoint effect due to unavailability of samples for $\lambda > 7.17$. Our numerical procedures show the same deficiencies when applied to pure Brownian motion, but successfully recover the known analytical results for that case in the range $1.6 < \lambda < 6.5$.

We plot in Fig. 5 the PDF's $p(\lambda|\mathbf{x}, t_f)$ for the two choices of \mathbf{x} , the left panel corresponding to particles released in a high-speed streak and the right to particles released in a low-speed streak. We also plot for comparison the analytical results for hitting-time PDF's with pure diffusion (see eqn. (E 8) of Appendix E.3). One can see in Fig. 5 a very strong effect of the release point on the hitting-time statistics, unlike the situation for the boundary local-times accumulated over one flow-through time. At $Pr = 0.1$ and 1 , hitting-times are clearly larger than those of pure diffusion for release in a high-speed streak and smaller for release in a low-speed streak. This effect is easy to understand, because particles released in a low-speed streak are advected toward the wall backward in time, and those released in a high-speed streak swept away from the wall. This effect is not observed for $Pr = 10$, with hitting times for pure diffusion very obviously shorter than those for advected particles started in both high-speed and low-speed streaks. This

occurs presumably because advection alone can never bring a particle to the wall (because of the vanishing velocity there) and as diffusivity κ decreases one sees more strongly the effect of fluid advection, which transports the particles away from the wall. One can see in general a strong effect of diffusivity on the hitting times, with smaller values of κ (or larger Pr) leading to larger hitting times backward in time. We shall refer to this property in our discussion below of the sharpness of the inequality Eq. (4.9). However, we first exploit this inequality to prove also for Dirichlet b.c. that spontaneous stochasticity is sufficient for anomalous dissipation of passive scalars.

4.2. Spontaneous Stochasticity Implies Anomalous Dissipation

The argument is very similar to those given earlier. To present it first in the simplest context, we consider a decaying scalar with vanishing source ($S = 0$). We first introduce an analogue of the formula (2.48) for the variance which constitutes the lower bound. There is a natural measure on the set \mathcal{S} which is just the d -dimensional Hausdorff measure H^d on subsets of $(d+1)$ -dimensional spacetime, restricted to \mathcal{S} . This can be described in elementary terms using natural d -dimensional coordinates $\boldsymbol{\sigma}$ on \mathcal{S} , where on \mathcal{S}_b we have $\boldsymbol{\sigma} = (\mathbf{y}, 0)$ for $\mathbf{y} \in \Omega$ and on \mathcal{S}_s we have $\boldsymbol{\sigma} = (\boldsymbol{\chi}, \tau)$ for $\boldsymbol{\chi} \in \partial\Omega$, the presumed smooth bounding wall surface, and $\tau \in [0, t]$. Then for $\boldsymbol{\sigma} \in \mathcal{S}$

$$H^d(d\boldsymbol{\sigma}) = \begin{cases} d^d\mathbf{y} & \boldsymbol{\sigma} = (\mathbf{y}, 0) \in \mathcal{S}_b \\ dS(\boldsymbol{\chi})d\tau & \boldsymbol{\sigma} = (\boldsymbol{\chi}, \tau) \in \mathcal{S}_s \end{cases} \quad (4.12)$$

Here dS is the usual $(d-1)$ -dimensional surface area on the smooth wall surface $\partial\Omega$ (or $(d-1)$ -dimensional Hausdorff measure, in mathematical terms). We can then also define the delta distribution $\delta_{\mathcal{S}}(\boldsymbol{\sigma}', \boldsymbol{\sigma})$ on \mathcal{S} with respect to measure H^d , so that

$$\int_{\mathcal{S}} H^d(d\boldsymbol{\sigma}') f(\boldsymbol{\sigma}') \delta_{\mathcal{S}}(\boldsymbol{\sigma}', \boldsymbol{\sigma}) = f(\boldsymbol{\sigma}) \quad (4.13)$$

for all smooth functions on \mathcal{S} , and we can likewise decompose this delta function as

$$\delta_{\mathcal{S}}(\boldsymbol{\sigma}', \boldsymbol{\sigma}) = \begin{cases} \delta^d(\mathbf{y}' - \mathbf{y}) & \boldsymbol{\sigma}', \boldsymbol{\sigma} \in \mathcal{S}_b \\ \delta_{\partial\Omega}(\boldsymbol{\chi}', \boldsymbol{\chi}) \delta(\tau' - \tau) & \boldsymbol{\sigma}', \boldsymbol{\sigma} \in \mathcal{S}_s \end{cases} \quad (4.14)$$

Denoting by $\tilde{\boldsymbol{\sigma}}(\mathbf{x}, t) = (\tilde{\boldsymbol{\xi}}_{t, \tilde{\tau}(\mathbf{x}, t)}(\mathbf{x}), \tilde{\tau}(\mathbf{x}, t))$ the space-time point where the trajectory first hits \mathcal{S} (going backward in time), we can then introduce 1-time transition probability densities for a particle to go backward in time from points (\mathbf{x}, t) on the “top” surface $\Omega \times \{t\}$ of the space-time cylinder and to arrive first to \mathcal{S} at the point $\boldsymbol{\sigma} \in \mathcal{S}$:

$$\begin{aligned} q^{\nu, \kappa}(\boldsymbol{\sigma} | \mathbf{x}, t) &= \mathbb{E}[\delta_{\mathcal{S}}(\boldsymbol{\sigma}, \tilde{\boldsymbol{\sigma}}(\mathbf{x}, t))] \\ &= \begin{cases} \mathbb{E}[\delta^d(\mathbf{y} - \tilde{\boldsymbol{\xi}}_{t, 0}(\mathbf{x}))] & \boldsymbol{\sigma} = (\mathbf{y}, 0) \in \mathcal{S}_b \\ \mathbb{E}[\delta_{\partial\Omega}(\boldsymbol{\chi} - \tilde{\boldsymbol{\xi}}_{t, \tau}(\mathbf{x})) \delta(\tau - \tilde{\tau}(\mathbf{x}, t))] & \boldsymbol{\sigma} = (\boldsymbol{\chi}, \tau) \in \mathcal{S}_s \end{cases} . \end{aligned} \quad (4.15)$$

This probability density is normalized with respect to H^d on \mathcal{S} so that

$$\int_{\mathcal{S}} H^d(d\boldsymbol{\sigma}) q(\boldsymbol{\sigma} | \mathbf{x}, t) = 1. \quad (4.16)$$

In these terms we obtain a simple formula for the stochastic representation (4.5) in the case of vanishing scalar source:

$$\theta(\mathbf{x}, t) = \mathbb{E}[\Theta(\tilde{\boldsymbol{\sigma}}(\mathbf{x}, t))] = \int_{\mathcal{S}} H^d(d\boldsymbol{\sigma}) \Theta(\boldsymbol{\sigma}) q(\boldsymbol{\sigma} | \mathbf{x}, t). \quad (4.17)$$

We can obtain a similar formula for the variance, if we introduce also the corresponding 2-fold transition probabilities

$$q_2^{\nu, \kappa}(\boldsymbol{\sigma}, \boldsymbol{\sigma}' | \mathbf{x}, t) = \mathbb{E}[\delta_S(\boldsymbol{\sigma}, \tilde{\boldsymbol{\sigma}}(\mathbf{x}, t)) \delta_S(\boldsymbol{\sigma}', \tilde{\boldsymbol{\sigma}}(\mathbf{x}, t))] = \delta_S(\boldsymbol{\sigma}, \boldsymbol{\sigma}') q(\boldsymbol{\sigma} | \mathbf{x}, t), \quad (4.18)$$

so that

$$\begin{aligned} \text{Var}[\Theta(\tilde{\boldsymbol{\sigma}}(\mathbf{x}, t))] &= \int_S H^d(d\boldsymbol{\sigma}) \int_S H^d(d\boldsymbol{\sigma}') \Theta(\boldsymbol{\sigma}) \Theta(\boldsymbol{\sigma}') \\ &\quad \times [q_2(\boldsymbol{\sigma}, \boldsymbol{\sigma}' | \mathbf{x}, t) - q(\boldsymbol{\sigma} | \mathbf{x}, t) q(\boldsymbol{\sigma}' | \mathbf{x}, t)]. \end{aligned} \quad (4.19)$$

These results are formally identical to those for the source-less ($S = 0$) scalar in domains without boundary or with zero-flux Neumann conditions at the wall. Furthermore, \mathcal{S} is a compact subset of space-time. Thus, we can exactly mimic our previous arguments with no change. Limits q^*, q_2^* as $\nu_j, \kappa_j \rightarrow 0$ always exist along suitable subsequences ν_j, κ_j . If the limits were deterministic, then one would have

$$q_2^*(\boldsymbol{\sigma}, \boldsymbol{\sigma}' | \mathbf{x}, t) = q^*(\boldsymbol{\sigma} | \mathbf{x}, t) q^*(\boldsymbol{\sigma}' | \mathbf{x}, t) \quad (4.20)$$

so that q_2^* would factorize in a product of two q^* 's. However, if the limits are non-deterministic so that q_2^* does not factorize for a positive-measure set of \mathbf{x} at time t , then there must be some smooth choice of $\Theta = (\theta_0, \psi)$ that makes the non-negative space-averaged variance in (4.19) in fact non-zero. For such choice of initial condition θ_0 and boundary conditions ψ , the space-average and time-integrated scalar dissipation will then be non-zero taking the limit $\nu_j, \kappa_j \rightarrow 0$. As before, this argument works rigorously only for a passive scalar, not an active one. An additional limitation discussed further in Appendix A.3 is that we cannot use this argument to prove, for a fixed choice of the boundary data ψ , that spontaneous stochasticity implies a smooth initial datum θ_0 to exist for which the scalar dissipation is positive[†].

Minor changes to this argument as before are needed to incorporate the source term. We must introduce a new type of transition probability

$$q^{\nu, \kappa}(\tau, \mathbf{y}, s | \mathbf{x}, t) = \mathbb{E} \left[\delta(\tau - \tilde{\tau}(\mathbf{x}, t)) \delta^d(\mathbf{y} - \tilde{\boldsymbol{\xi}}_{t,s}(\mathbf{x})) \right], \quad \mathbf{y} \in \Omega, \quad 0 \leq \tau < s < t \quad (4.21)$$

which gives the joint probability for the particle released at \mathbf{x} at time t to first hit the space boundary $\partial\Omega$ at time τ (going backward) and also to pass through point \mathbf{y} at time s satisfying $\tau < s < t$. We can then rewrite the stochastic representation (4.5) as

$$\theta(\mathbf{x}, t) = \int_S H^d(d\boldsymbol{\sigma}) \Theta(\boldsymbol{\sigma}) q(\boldsymbol{\sigma} | \mathbf{x}, t) + \int_0^t d\tau \int_{\tau}^t ds \int_{\Omega} d^d \mathbf{y} S(\mathbf{y}, s) q(\tau, \mathbf{y}, s | \mathbf{x}, t). \quad (4.22)$$

To obtain a similar expression for the source variance term, we must introduce corresponding 2-time transition densities

$$\begin{aligned} q_2^{\nu, \kappa}(\tau; \mathbf{y}, s; \tau', \mathbf{y}', s' | \mathbf{x}, t) &= \\ &= \mathbb{E} \left[\delta(\tau - \tilde{\tau}(\mathbf{x}, t)) \delta^d(\mathbf{y} - \tilde{\boldsymbol{\xi}}_{t,s}(\mathbf{x})) \delta(\tau' - \tilde{\tau}(\mathbf{x}, t)) \delta^d(\mathbf{y}' - \tilde{\boldsymbol{\xi}}_{t,s'}(\mathbf{x})) \right], \\ &\quad \mathbf{y}, \mathbf{y}' \in \Omega, \quad \tau < s < t, \tau' < s' < t. \end{aligned} \quad (4.23)$$

[†] These comments have implications for the problem of Rayleigh-Bénard convection with fixed temperatures at top/bottom plates, which is discussed in section 4.4 below. There is some evidence for Richardson dispersion of Lagrangian particles in numerical simulations of turbulent convection (Schumacher 2008). However, even if there were compelling evidence for spontaneous stochasticity associated to this effect, we could not rigorously conclude from our results that there is anomalous thermal dissipation. First, the temperature is an active scalar in that case and, second, our present arguments do not work with fixed boundary data.

and

$$q_2(\tau, \mathbf{y}, s; \tau', \mathbf{y}', s' | \mathbf{x}, t) = \delta(\tau - \tau') q_2(\tau; \mathbf{y}, s; \mathbf{y}', s' | \mathbf{x}, t). \quad (4.24)$$

With this quantity we can write

$$\begin{aligned} \text{Var} \left[\int_{\tilde{\tau}(\mathbf{x}, t)}^t ds S(\tilde{\xi}_{t,s}(\mathbf{x}), s) \right] \\ = \int_0^t d\tau \int_0^t d\tau' \int d^d y \int d^d y' \int_{\tau}^t ds \int_{\tau'}^t ds' S(\mathbf{y}, s) S(\mathbf{y}', s') \times \\ \left[q_2(\tau, \mathbf{y}, s; \tau', \mathbf{y}', s' | \mathbf{x}, t) - q(\tau, \mathbf{y}, s | \mathbf{x}, t) q(\tau', \mathbf{y}', s' | \mathbf{x}, t) \right]. \end{aligned} \quad (4.25)$$

We can also write the initial condition-source covariance in a similar fashion, using the 2-time probability density

$$q_2^{\nu, \kappa}(\boldsymbol{\sigma}; \tau', \mathbf{y}', s' | \mathbf{x}, t) = \mathbb{E} \left[\delta_S(\boldsymbol{\sigma}, \tilde{\boldsymbol{\sigma}}(\mathbf{x}, t)) \delta(\tau' - \tilde{\tau}(\mathbf{x}', t)) \delta^d(\mathbf{y}' - \tilde{\xi}_{t,s'}(\mathbf{x}')) \right], \quad (4.26)$$

which is proportional to $\delta(\tau - \tau')$, if we write $\boldsymbol{\sigma} = (\mathbf{y}, \tau)$. We have

$$\begin{aligned} \text{Cov} \left[\Theta(\tilde{\xi}_{t, \tilde{\tau}(\mathbf{x}, t)}(\mathbf{x}), \tilde{\tau}(\mathbf{x}, t)), \int_{\tilde{\tau}(\mathbf{x}, t)}^t dt' S(\tilde{\xi}_{t,t'}(\mathbf{x}), t') \right] \\ = \int_S H^d(d\boldsymbol{\sigma}) \int_0^t d\tau' \int d^d y' \int_{\tau'}^t ds' \Theta(\mathbf{y}, s) S(\mathbf{y}', s') \times \\ \left[q_2(\boldsymbol{\sigma}; \tau', \mathbf{y}', s' | \mathbf{x}, t) - q(\boldsymbol{\sigma} | \mathbf{x}, t) q(\tau', \mathbf{y}', s' | \mathbf{x}, t) \right], \end{aligned} \quad (4.27)$$

as the corresponding representation. The very close similarity of these formulas to those derived previously for advected scalars in flows without boundaries and for scalars with insulating/adiabatic walls allows us to prove that spontaneous stochasticity is sufficient for anomalous dissipation of passive scalars also for Dirichlet b.c. in the presence of smooth sources. The statement here is that a smooth source S can be chosen for which there is anomalous scalar dissipation, either with zero initial-boundary data or else with a smooth non-zero choice $\Theta = (\theta_0, \psi)$ of such data. For active scalars, it seems likely this remains true but, due to lack of freedom in choosing the initial data, we cannot rigorously draw this conclusion.

4.3. Equality Fluctuation-Dissipation Relation

We now return to the question whether our lower bound (4.9) on the cumulative (time- and space-integrated) scalar dissipation may in fact be an equality. This is certainly not true in the $t \rightarrow \infty$ limit with κ, ν fixed. We note that

$$\lim_{t \rightarrow \infty} \tilde{\Omega}_{t,s} = \Omega, \quad \text{any fixed } s > 0 \quad (4.28)$$

since the boundary hitting times are finite almost surely for $\kappa, \nu > 0$ (see Karlin & Taylor (1981), Ch.15, section 11) and, thus, the particle released in the far distant future t will certainly hit the space boundary $\partial\Omega$ before s (moving backward in time). Thence by dominated convergence

$$\lim_{t \rightarrow \infty} \mathbb{E} \left[\int_{\tilde{\xi}_{t,s}(\tilde{\Omega}_{t,s})} \kappa |\nabla\theta(\mathbf{x}, s)|^2 \right] = \kappa \int_{\Omega} d^d x |\nabla\theta(\mathbf{x}, s)|^2 \quad (4.29)$$

and the contribution of reflected particles coincides at long times with the total dissipation. A strengthened conclusion is that

$$\lim_{t \rightarrow \infty} \tilde{\Omega}_{t,s} = \Omega, \text{ uniformly for all } s \text{ such that } t - \delta(t) \geq s \geq 0, \quad (4.30)$$

for some function $\delta(t) \geq 0$ such that $\lim_{t \rightarrow \infty} \delta(t) = \infty$, $\lim_{t \rightarrow \infty} \frac{\delta(t)}{t} = 0$. This is true because the difference $t - s \geq \delta(t)$ for all such s . In that case, however, we see that

$$\lim_{t \rightarrow \infty} \frac{1}{t} \Delta^{\nu, \kappa}(t) = \lim_{t \rightarrow \infty} \frac{1}{t} \int_0^t ds \frac{1}{|\Omega|} \int_{\Omega} d^d x \kappa |\nabla \theta(\mathbf{x}, s)|^2, \quad (4.31)$$

where $\Delta^{\nu, \kappa}(t)$ is the difference in eq. (4.10). Thus, our lower bound (4.9) on space-time average dissipation becomes vacuous as $t \rightarrow \infty$, with the long-time limit of the lower bound simply tending to zero as reflected particles fill the entire domain.

Now consider the opposite limit with $\nu, \kappa \rightarrow 0$ for fixed t . If we keep ν fixed so that the velocity stays smooth, then no particles will reach the boundary in the finite time interval $[0, t]$ as $\kappa \rightarrow 0$. An increase of hitting times with decreasing κ for fixed ν is clearly observed in Fig. 5. In this limit, the inequality in our lower bound becomes equality. However, as long as \mathbf{u} is smooth, then there will be no dissipative anomaly and the scalar dissipation will vanish! Thus, this limit is of little interest. On the other hand, if we take $\nu, \kappa \rightarrow 0$ together, then it is possible that the particles will hit the boundary and reflect. In fact, this must be the case if there is a scalar dissipative anomaly at finite times t for flux b.c. and vanishing initial data of the scalar and vanishing scalar sources, since then the FDR (3.14) is solely due to the contribution of the boundary local times in (3.12). If particles continue to hit the boundary as $\nu, \kappa \rightarrow 0$ for fixed time t , then our lower bound must be a strict inequality (but possibly non-vanishing for finite t).

It is straightforward, however, to obtain an equality relation for the scalar dissipation by using the same derivation as for flux-b.c, namely, by using the backwards Itô formula (3.9) and integrating from time t down to 0, rather than stopping when hitting the boundary. This argument yields for the scalar itself

$$\theta(\mathbf{x}, t) = \mathbb{E} \left[\theta_0(\tilde{\xi}_{t,0}(\mathbf{x})) + \int_0^t ds S(\tilde{\xi}_{t,s}(\mathbf{x}), s) - \kappa \int_0^t \boldsymbol{\mu} \cdot \nabla \theta(\tilde{\xi}_{t,s}(\mathbf{x}), s) \hat{d}\tilde{\ell}_{t,s}(\mathbf{x}) \right] \quad (4.32)$$

and for the variance

$$\begin{aligned} \frac{1}{2} \left\langle \text{Var} \left[\theta_0(\tilde{\xi}_{t,0}) + \int_0^t ds S(\tilde{\xi}_{t,s}, s) - \kappa \int_0^t \boldsymbol{\mu} \cdot \nabla \theta(\tilde{\xi}_{t,s}(s)) \hat{d}\tilde{\ell}_{t,s} \right] \right\rangle_{\Omega} \\ = \kappa \int_0^t ds \langle |\nabla \theta(s)|^2 \rangle_{\Omega}, \end{aligned} \quad (4.33)$$

which is another version of a fluctuation-dissipation relation for Dirichlet b.c. of the scalar. The total scalar dissipation is now obtained, with the contribution of the reflected particles represented by the boundary local time density term on the left. This result is the physically most natural version of the FDR for scalar Dirichlet b.c., and provides insight into the Lagrangian origin of scalar dissipation. Unfortunately, it is not as convenient for mathematical analysis, because the scalar boundary flux $g(\mathbf{x}, t) = -\boldsymbol{\mu} \cdot \nabla \theta(\mathbf{x}, t)$ is no longer a known input, but is instead a space-time fluctuating quantity which must be determined from the solution of the scalar advection-diffusion equation.

4.4. Mixed Boundary Conditions

The extension of the previous results to scalars with general mixed Dirichlet-Neumann conditions (3.1),(3.2) is straightforward. Again, one considers the backward stochastic

flow with reflection at the boundary. To derive an FDR in the form of an inequality like (4.8), one must stop those particles which hit $\partial\Omega_D$ before time 0 (going backward). The particles which hit $\partial\Omega_N$ are simply reflected. Results like (4.7) and (4.8) are obtained, except that now the stopping time $\tilde{\tau}(\mathbf{x}, t)$ is the first time to hit $\partial\Omega_D$ (or 0, whichever is larger) and the variance on the left includes contributions from the local time density at the piece $\partial\Omega_N$ of the boundary. This FDR inequality omits the contribution to scalar dissipation at locations of particles reflected from $\partial\Omega_D$. It is also easy to obtain an FDR equality like (4.33) by stopping no particles. It has an identical form to (4.33) and the sole difference is that $g(\mathbf{x}, t) = -\boldsymbol{\mu} \cdot \nabla\theta(\mathbf{x}, t)$ is a specified function for points $\mathbf{x} \in \partial\Omega_N$ but must be obtained for $\mathbf{x} \in \partial\Omega_D$ by solving the advection-diffusion equation.

In light of these remarks, we may return to the standard Rayleigh-Bénard problem with the mixed boundary conditions (3.31)-(3.33). We can obtain an FDR equality using the same ideas as in the derivation of (4.33) above. The formula for the temperature field analogous to (3.55) is

$$\begin{aligned} T(\mathbf{x}, t) &= \mathbb{E} \left[T_0(\tilde{\boldsymbol{\xi}}_{t,0}(\mathbf{x})) + \int_0^t J(\tilde{\boldsymbol{\xi}}_{t,s}(\mathbf{x}), s) \hat{d}\tilde{\ell}_{t,s}^{top}(\mathbf{x}) - \int_0^t J(\tilde{\boldsymbol{\xi}}_{t,s}(\mathbf{x}), s) \hat{d}\tilde{\ell}_{t,s}^{bot}(\mathbf{x}) \right] \\ &= \int d^3x_0 T_0(\mathbf{x}_0) p(\mathbf{x}_0, 0|\mathbf{x}, t) \\ &\quad - \sum_{\lambda=\pm 1} \lambda \int_0^t ds \iint_S dx' dy' J(x', y', \lambda \frac{H}{2}, s) p(x', y', \lambda \frac{H}{2}, s|\mathbf{x}, t), \end{aligned} \quad (4.34)$$

where $J(\mathbf{x}, t) = u_z(\mathbf{x}, t)T(\mathbf{x}, t) - \kappa\partial_z T(\mathbf{x}, t)$ is the vertical heat flux (which becomes purely conductive at the top/bottom walls, where $u_z \equiv 0$). This representation has a hybrid Eulerian-Lagrangian character, since it involves both the particle probabilities $p(\mathbf{x}', t'|\mathbf{x}, t)$ and the Eulerian field $J(\mathbf{x}, t)$. The FDR in the steady-state (infinite-time), spatially-local form analogous to (3.66) for the case of flux-b.c. is:

$$\lim_{t \rightarrow \infty} \frac{1}{2t} \text{Var} \left[\int_0^t J(\tilde{\boldsymbol{\xi}}_{t,s}(\mathbf{x}), s) \hat{d}\tilde{\ell}_{t,s}^{top}(\mathbf{x}) - \int_0^t J(\tilde{\boldsymbol{\xi}}_{t,s}(\mathbf{x}), s) \hat{d}\tilde{\ell}_{t,s}^{bot}(\mathbf{x}) \right] = \langle \kappa |\nabla T|^2 \rangle_{V,\infty}, \quad (4.35)$$

As in the case of (3.66), the contributions of the initial data T_0 can be argued to become a spatial constant at long times and the limit becomes independent of \mathbf{x} by the ergodicity of the stochastic Lagrangian flow. Arguments like those in section 3.3.2 and Appendix C allow one to show then that

$$\begin{aligned} \langle \kappa |\nabla T|^2 \rangle_{V,\infty} &= \lim_{t \rightarrow \infty} \frac{1}{Vt} \int_{-t}^0 ds' \int_{-\infty}^0 ds \iint_S dx'' dy'' \iint_S dx' dy' \\ &\times \sum_{\lambda, \lambda' = \pm 1} \lambda \lambda' J(x'', y'', \lambda' \frac{H}{2}, s') J(x', y', \lambda \frac{H}{2}, s) \\ &\times \left[p(x', y', \lambda \frac{H}{2}, s|x'', y'', \lambda' \frac{H}{2}, 0) - \frac{1}{V} \right] \end{aligned} \quad (4.36)$$

analogous to (3.66),(3.67) for the flux-b.c. case. This is consistent with the Eulerian balance relation $\varepsilon_T = J\Delta T/H$ in (3.43) if one notes that for all values of x'', y''

$$\begin{aligned} \Delta T &= \sum_{\lambda, \lambda' = \pm 1} \lambda \lambda' \int_{-\infty}^0 ds \iint_S dx' dy' J(x', y', \lambda \frac{H}{2}, s) \\ &\times \left[p(x', y', \lambda \frac{H}{2}, s|x'', y'', \lambda' \frac{H}{2}, 0) - \frac{1}{V} \right] \end{aligned} \quad (4.37)$$

by taking the limit $t \rightarrow \infty$ in the eq.(4.34) for points \mathbf{x} on the top or bottom wall where the temperature is held fixed[†].

The FDR (4.36) is harder to analyze than (3.66),(3.67) because of the fluctuations of the boundary values of $J(\mathbf{x}, t)$ in space and time, which are unknown until the dynamical equations are solved. However, it is at least plausible that the turbulent Rayleigh-Bénard system with imposed temperature difference ΔT will behave very similarly to the system with imposed flux J_{in} , if the latter is adjusted so that ΔT remains unchanged as $\nu, \kappa \rightarrow 0$. If so, we expect that our results for the flux-b.c. in section 3.3 will carry over to the standard problem with temperature-b.c. at the top and bottom walls. In particular, the FDR (4.36) allows us to write

$$\varepsilon_T = \frac{J^2}{H^2} \tau_{corr} \quad (4.38)$$

where J is the time-average and area- (or volume-)average of $J(\mathbf{x}, t)$ and where τ_{corr} is a J -weighted average mixing time. Thus, while the mathematical analysis is less tractable than before, we expect that most of our conclusions for the flux-b.c. carry over to standard Rayleigh-Bénard with mixed b.c. Needless to say, this is open to question.

5. Summary and Discussion

This paper has derived a Lagrangian fluctuation-dissipation relation for scalars advected by an incompressible fluid. Our relation expresses an exact balance between molecular dissipation of scalar fluctuations and the input of scalar fluctuations from the initial scalar values, boundary fluxes, and internal sources as these are sampled by stochastic Lagrangian trajectories backward in time. We have exploited this relation to give a simple proof for several types of flows (in domains without walls or with no scalar flux through the wall) that spontaneous stochasticity of Lagrangian trajectories is necessary and sufficient for anomalous dissipation of passive scalars, and necessary (but possibly not sufficient) for anomalous dissipation of active scalars. For more general mixed boundary conditions on the scalar, with imposed values at the wall or imposed non-zero fluxes, we can only prove that spontaneous stochasticity is sufficient for anomalous dissipation of passive scalars. As simple examples show, scalar boundary layers for general wall-bounded flows provide another mechanism for non-vanishing scalar dissipation which is distinct from spontaneous stochasticity. Our fluctuation-dissipation relation remains valid in this more general setting, however, and provides there also a novel Lagrangian view of turbulent scalar dissipation. As an example, we have worked out in detail the consequences of our relation for turbulent Rayleigh-Bénard convection. In that case we have shown that the thermal dissipation rate is controlled by a near-wall mixing time of stochastic Lagrangian particles, due to the stirring by thermal plumes and the global convective wind. Nevertheless, we have shown that this mixing time at large Rayleigh numbers must be orders of magnitude longer than the large-eddy circulation time if Kraichnan-Spiegel scaling is invalid. In general, our fluctuation-dissipation relation can be used to provide an exact link between scalar dissipation and Lagrangian fluid mechanisms.

The most important outstanding question is, certainly, the extent to which the results of this paper can be carried over to provide a Lagrangian picture of anomalous energy dissipation in Navier-Stokes turbulence[‡]. We briefly comment upon this issue here. The

[†] Here one uses the asymptotic result $\int_0^t ds \iint_S dx' dy' J(x', y', \lambda \frac{H}{2}, s) \sim Jt$ as $t \rightarrow \infty$ for $\lambda = \pm$ with J the time- and area-average of $J(x, y, z, t)$ (which is independent of z) in order to introduce the term $-1/V$ into the square bracket in (4.37).

[‡] The most direct application of our scalar results to Navier-Stokes might appear to be

formal extension of our fluctuation-dissipation relation to viscous energy dissipation is straightforward. We can exploit the stochastic Lagrangian representation for the incompressible Navier-Stokes equation

$$\partial_t \mathbf{u} + \mathbf{u} \cdot \nabla \mathbf{u} = -\nabla p + \nu \Delta \mathbf{u} \quad (5.1)$$

$$\nabla \cdot \mathbf{u} = 0, \quad (5.2)$$

recently elaborated by Constantin & Iyer (2008, 2011), which is valid both for flows in domains without boundaries and for wall-bounded flows. Their results can be most simply derived using a backward stochastic particle flow $\tilde{\xi}_{t,s}(\mathbf{x})$ and a corresponding “momentum” $\tilde{\pi}_{t,s}(\mathbf{x}) \equiv \mathbf{u}(\tilde{\xi}_{t,s}(\mathbf{x}), s)$ which together satisfy the backward Itô equations

$$\hat{d}\tilde{\xi}_{t,s}(\mathbf{x}) = \tilde{\pi}_{t,s}(\mathbf{x}) ds + \sqrt{2\nu} \hat{d}\tilde{\mathbf{W}}_s, \quad (5.3)$$

$$\hat{d}\tilde{\pi}_{t,s}(\mathbf{x}) = -\nabla p(\tilde{\xi}_{t,s}(\mathbf{x}), s) ds + \sqrt{2\nu} \hat{d}\tilde{\mathbf{W}}_s \cdot \nabla \mathbf{u}(\tilde{\xi}_{t,s}(\mathbf{x}), s). \quad (5.4)$$

These are a stochastic generalization of Hamilton’s particle equations, making contact with traditional methods of Hamiltonian fluid mechanics (Salmon 1988). See more detailed discussion of Eyink (2010); Rezakhanlou (2014). By integrating the second of these Hamilton’s equations from 0 to t and taking expectations over the Brownian motion, one readily obtains

$$\mathbf{u}(\mathbf{x}, t) = \mathbb{E} \left[\mathbf{u}_0(\tilde{\xi}_{t,0}(\mathbf{x})) - \int_0^t \nabla p(\tilde{\xi}_{t,s}(\mathbf{x}), s) ds \right], \quad (5.5)$$

using the fact that the stochastic integral $\sqrt{2\nu} \int_0^t \hat{d}\tilde{\mathbf{W}}_s \cdot \nabla \mathbf{u}^\nu(\tilde{\xi}_{t,s}(\mathbf{x}), s)$ is a backward martingale and so vanishes under expectation. The formula (5.5) was previously derived by Albeverio & Belopolskaya (2010). Moreover, by exploiting the same Itô-isometry argument as applied earlier for scalars, one can derive

$$\nu \int_0^t ds \langle |\nabla \mathbf{u}(s)|^2 \rangle_\Omega = \frac{1}{2} \left\langle \text{Var} \left[\mathbf{u}_0(\tilde{\xi}_{t,0}) - \int_0^t \nabla p(\tilde{\xi}_{t,s}, s) ds \right] \right\rangle_\Omega. \quad (5.6)$$

This can be considered a “fluctuation-dissipation relation” for viscous energy dissipation in a Navier-Stokes solution.

Unfortunately this relation does not appear to be particularly useful for analyzing the high-Reynolds number (or inviscid) limit. It has a mixed Eulerian-Lagrangian character, since it involves both the particle trajectories $\tilde{\xi}_{t,s}(\mathbf{x})$ and the Eulerian pressure-gradient field $\nabla p(\mathbf{x}, t)$. The latter field is furthermore a dissipation-range object, which grows increasingly singular as $\nu \rightarrow 0$. For example, using the classical K41 scaling estimates (Obukhov 1949; Yaglom 1949; Batchelor 1951), one expects an rms value of the pressure-gradient $(\nabla p)_{rms} \sim (\varepsilon^3/\nu)^{1/4}$ and intermittency effects will make this field even more singular. Mathematically speaking, the pressure-gradient cannot be expected to exist as an ordinary function in the limit $\nu \rightarrow 0$ but only as a distribution. Because of these facts, we cannot derive from (5.6) any relation between anomalous energy dissipation and

to analyze the viscous dissipation of enstrophy in freely-decaying 2D turbulence, where the vorticity is an active (pseudo)scalar field. Unfortunately, all of our analysis assumes that the initial scalar field is square-integrable or L^2 , but it has been shown by Eyink (2001) and Tran & Dritschel (2006) that there can be no anomalous enstrophy dissipation for a freely-decaying 2D Navier-Stokes solution with finite initial enstrophy. It may still be the case that there is anomalous enstrophy dissipation for more singular, infinite-enstrophy initial data and that this dissipation is associated to spontaneous stochasticity (see further discussion in Eyink (2001)). However, we cannot investigate this delicate issue using the fluctuation-dissipation relation of the present paper.

spontaneous stochasticity for Navier-Stokes turbulence. In particular, even if there were anomalous energy dissipation, the limiting stochastic particle trajectories might become deterministic as $\nu \rightarrow 0$. In that case, the variance on the righthand side of (5.6) could remain non-vanishing, because the smaller fluctuations due to vanishing stochasticity could be compensated by the diverging magnitude of the pressure-gradient.

More fundamentally, we believe that (5.6) misses essential physics. Note that this relation holds for freely-decaying Navier-Stokes turbulence both in 2D and in 3D, but in the former case there is certainly no anomalous energy dissipation. Furthermore, in forced, steady-state 2D turbulence there is evidence in the inverse-energy cascade range for Richardson dispersion and Lagrangian spontaneous stochasticity (Boffetta & Sokolov (2002); Faber T. (2009)) but this is associated not to small-scale energy dissipation by viscosity but instead to large-scale energy dissipation by Eckman-type damping. A possibly important clue is provided by the fact that Richardson dispersion is faster backward in time for 3D forward energy cascade Sawford *et al.* (2005); Berg *et al.* (2006); Eyink (2011), but faster forward in time for 2D inverse energy cascade Faber T. (2009). By a comparison of these observations for 2D and 3D Navier-Stokes turbulence and by means of exact results for Burgers turbulence, Eyink & Drivas (2015*b*) have argued that anomalous energy dissipation for Navier-Stokes turbulence should be related not simply to presence of spontaneous stochasticity but instead to time-asymmetry of the stochastic Lagrangian trajectories.

Acknowledgements

We would like to thank Charlie Doering, David Goluskin and Sam Punshon-Smith, Cristian C. Lalescu and Jordan Yoder for useful discussions, and Katepalli Sreenivasan for providing us with several important references. We would also like to thank the Institute for Pure and Applied Mathematics (IPAM) at UCLA, where this paper was partially completed during the fall 2014 long program on “Mathematics of Turbulence”. We also acknowledge the Johns Hopkins Turbulence Database for the numerical DNS data employed in this work. G.E. is partially supported by a grant from NSF CBET-1507469 and T.D. was partially supported by the Duncan Fund and a Fink Award from the Department of Applied Mathematics & Statistics at the Johns Hopkins University.

Appendix A. Mathematical Proofs

Here we give the details of the proofs in the main text.

A.1. Proofs for Section 2.3

To make rigorous the arguments in Section 2.3, we note that the transition probabilities $p^{\nu, \kappa}(\mathbf{x}_0, 0 | \mathbf{x}, t)$ discussed there are well-defined for any sequence of continuous (or even just bounded) velocity fields \mathbf{u}^ν . However, we shall generally assume that these fields are even smooth for $\nu > 0$ and their energies are bounded uniformly in ν . Because of the latter assumption we can always extract a subsequence $\nu_j \rightarrow 0$ such that $\mathbf{u}^{\nu_j} \rightarrow \mathbf{u}$, with \mathbf{u} a finite energy or $L^2(\Omega \times [0, T])$ velocity field, where convergence is in the weak sense:

$$\lim_{j \rightarrow \infty} \int_{\Omega} d^d x \int_0^T dt \mathbf{u}^{\nu_j}(\mathbf{x}, t) \cdot \mathbf{w}(\mathbf{x}, t) = \int_{\Omega} d^d x \int_0^T dt \mathbf{u}(\mathbf{x}, t) \cdot \mathbf{w}(\mathbf{x}, t) \quad (\text{A } 1)$$

for all $\mathbf{w} \in L^2(\Omega \times [0, T])$. This is a consequence of the Banach-Alaoglu Theorem (Rudin 2006). Thus, we consider limits in which there is a definite, fixed fluid velocity \mathbf{u} . If the \mathbf{u}^ν are solutions of the incompressible Navier-Stokes equation indexed by viscosity ν ,

then we can furthermore select the subsequence $\nu_k \rightarrow 0$ so that the limiting velocity \mathbf{u} is a “dissipative Euler solution” in the sense of Lions (1996), section 4.4. We must now show that a further subsequence $\nu_k = \nu_{j_k}$ can be selected together with a corresponding subsequence $\kappa_k \rightarrow 0$, so that the transition probabilities $p^{\nu_k, \kappa_k}(\mathbf{x}_0, 0 | \mathbf{x}, t)$ satisfy the following conditions:

(i) There is a transition density $p^*(\mathbf{x}_0, 0 | \mathbf{x}, t)$ which is measurable in \mathbf{x} so that

$$\lim_{k \rightarrow \infty} \int_{\Omega} d^d x_0 \int_{\Omega} d^d x f(\mathbf{x}_0, \mathbf{x}) p^{\nu_k, \kappa_k}(\mathbf{x}_0, 0 | \mathbf{x}, t) = \int_{\Omega} d^d x_0 \int_{\Omega} d^d x f(\mathbf{x}_0, \mathbf{x}) p^*(\mathbf{x}_0, 0 | \mathbf{x}, t),$$

for all continuous functions $f \in C(\Omega \times \Omega)$.

(ii) (normalization) $\int_{\Omega} d^d x_0 p^*(\mathbf{x}_0, 0 | \mathbf{x}, t) = 1$ for a.e. $\mathbf{x} \in \Omega$.

(iii) (volume-conservation) $\int_{\Omega} d^d x_0 \int_{\Omega} d^d x g(\mathbf{x}_0) p^*(\mathbf{x}_0, 0 | \mathbf{x}, t) = \int_{\Omega} d^d x_0 g(\mathbf{x}_0)$ for all continuous $g \in C(\Omega)$.

Assuming for the moment that (i)-(iii) hold, we can complete the proof of section 2.3. Let $\theta_0(\mathbf{x}_0)$ be continuous on Ω and consider

$$\theta^{\nu_k, \kappa_k}(\mathbf{x}, t) = \int_{\Omega} d^d x_0 \theta_0(\mathbf{x}_0) p^{\nu_k, \kappa_k}(\mathbf{x}_0, 0 | \mathbf{x}, t) \quad (\text{A } 2)$$

which is measurable in \mathbf{x} and with scalar energies uniformly bounded as

$$\int_{\Omega} d^d x |\theta^{\nu_k, \kappa_k}(\mathbf{x}, t)|^2 \leq \int_{\Omega} d^d x_0 |\theta_0(\mathbf{x}_0)|^2 \quad (\text{A } 3)$$

by Jensen’s inequality and volume-conservation. From (i) we see that

$$\lim_{k \rightarrow \infty} \int_{\Omega} d^d x f(\mathbf{x}) \theta^{\nu_k, \kappa_k}(\mathbf{x}, t) = \int_{\Omega} d^d x f(\mathbf{x}) \theta^*(\mathbf{x}, t) \quad (\text{A } 4)$$

for all $f \in C(\Omega)$, where we have defined

$$\theta^*(\mathbf{x}, t) \equiv \int_{\Omega} d^d x_0 \theta_0(\mathbf{x}_0) p^*(\mathbf{x}_0, 0 | \mathbf{x}, t) \quad (\text{A } 5)$$

which satisfies

$$\int_{\Omega} d^d x |\theta^*(\mathbf{x}, t)|^2 \leq \int_{\Omega} d^d x_0 |\theta_0(\mathbf{x}_0)|^2 \quad (\text{A } 6)$$

again by Jensen’s inequality using (ii) and the volume conservation property (iii). Because $C(\Omega)$ is dense in $L^2(\Omega)$, the uniform L^2 -bounds (A 3),(A 6) and the convergence (A 4) imply that $\theta^{\nu_k, \kappa_k} \rightarrow \theta^*$ weak in L^2 . Since functionals of the form

$$H[\theta] = \int_{\Omega} d^d x h(\theta(\mathbf{x})) \quad (\text{A } 7)$$

for convex functions h and finite-measure sets Ω are weakly lower-semicontinuous on $L^2(\Omega)$ (e.g. Berkovitz (1974), or Braides (2002), section 2.2), one has

$$\int_{\Omega} d^d x h(\theta^*(\mathbf{x}, t)) \leq \liminf_{k \rightarrow \infty} \int_{\Omega} d^d x h(\theta^{\nu_k, \kappa_k}(\mathbf{x}, t)). \quad (\text{A } 8)$$

Using the inequality (2.44) in the main text, or

$$\int_{\Omega} h(\theta^{\nu, \kappa}(\mathbf{x}, t)) d^d x < \int_{\Omega} h(\theta_0(\mathbf{x}_0)) d^d x_0 - \frac{1}{2} \Delta(t) \quad (\text{A } 9)$$

and the above results, we thus obtain

$$\int_{\Omega} h(\theta^*(\mathbf{x}, t)) d^d x \leq \int_{\Omega} h(\theta_0(\mathbf{x}_0)) d^d x_0 - \frac{1}{2} \Delta(t) < \int_{\Omega} h(\theta_0(\mathbf{x}_0)) d^d x_0, \quad (\text{A } 10)$$

as was claimed. The remainder of the argument is exactly as in the main text.

We therefore need only to establish the properties (i)-(iii) in order to finish the proof. The key fact we shall use is that the transition probability densities for $\nu, \kappa > 0$ can be regarded as *Young measures*

$$\mu_{\mathbf{x}}^{\nu, \kappa, t}(d\mathbf{x}_0) = d^d x_0 p^{\nu, \kappa}(\mathbf{x}_0, 0 | \mathbf{x}, t), \quad (\text{A } 11)$$

that is, as probability measures $\mu_{\mathbf{x}}^{\nu, \kappa, t}$ on Ω which are measurably parameterized by $\mathbf{x} \in \Omega$. Fluid-dynamicists will be familiar with Young measures from theories of long-time statistical equilibria for two-dimensional fluids (Robert 1991; Sommeria *et al.* 1991). A good introduction are the lectures of Valadier (1994) and a comprehensive treatment can be found in the monograph of Florescu & Godet-Thobie (2012).

Here we briefly review the necessary theory. In the context of our problem, Young measures may be defined as families of probability measures μ_x , defined on a compact set $Y \subseteq \mathbb{R}^m$, measurably parametrized by $x \in X \subset \mathbb{R}^n$, with X also compact. This uniquely defines a positive Radon measure μ over $X \times Y$ given on product sets by

$$\mu(A \times B) = \int_A \mu_x(B) dx. \quad (\text{A } 12)$$

By construction, μ satisfies the following identity

$$\langle \mu, f \rangle \equiv \int_{X \times Y} f(x, y) \mu(dx, dy) = \int_X \left(\int_Y f(x, y) \mu_x(dy) \right) dx, \quad (\text{A } 13)$$

for any continuous function $f \in C(X \times Y)$. Moreover, for $f \in C(X)$, one has

$$\langle \mu, f \rangle = \int_X f(x) dx, \quad (\text{A } 14)$$

that is to say, the projection of μ on X is dx , the Lebesgue measure. One may alternatively take these last two properties as the definition of a Young measure. That is, for any positive Radon measure μ on $X \times Y$ whose projection on X is dx there is a mapping $x \mapsto \mu_x$ satisfying (A 13). This is the content of the so-called Disintegration Theorems (Jiřina 1959; Valadier 1973). The mapping $x \mapsto \mu_x$ is unique Lebesgue almost everywhere.

Let us denote by \mathcal{Y} the set of Young measures μ on the product set $X \times Y$. This set has the important property that it is a closed subset of the space $M(X \times Y)$ of Radon measures on $X \times Y$ in the topology of narrow convergence. The *narrow topology* is the coarsest topology on $M(X \times Y)$ for which the maps $\mu \mapsto \langle \mu, f \rangle$ are continuous for all $f \in C_b(X \times Y)$, the space of bounded continuous functions. Since $X \times Y$ is compact, this topology coincides with the so-called *vague topology* which is the coarsest for which the maps $\mu \mapsto \langle \mu, f \rangle$ are continuous for all $f \in C_c(X \times Y)$, the space of compactly-supported continuous functions. Furthermore, it coincides with the topology defined by the maps $\mu \mapsto \langle \mu, f \rangle$ for all $f \in C(X \times Y)$. For a detailed discussion of these different topologies, see Florescu & Godet-Thobie (2012). Here we note only that these make $M(X \times Y)$ into a compact, metrizable topological space for compact X, Y . That \mathcal{Y} is a closed subspace of $M(X \times Y)$ may then easily be seen by noting that for any sequence $\mu^n \in \mathcal{Y}$ with $\mu^n \rightarrow \mu$ narrowly

$$\int_X f(x) dx = \langle \mu^n, f \rangle \rightarrow \langle \mu, f \rangle, \quad \text{for all } f \in C(X) \quad (\text{A } 15)$$

so that the projection of μ onto X is dx and $\mu \in \mathcal{Y}$. A further closed subset $\mathcal{Y}_m \subset \mathcal{Y}$ is the set of *measure-preserving Young measures*, which satisfy the additional condition

that

$$\langle \mu, g \rangle = \int_X \left(\int_Y g(y) \mu_x(dy) \right) dx = \int_Y g(y) dy, \quad \text{for all } g \in C(Y) \quad (\text{A } 16)$$

which may be stated formally as $\int_X dx \mu_x(dy) = dy$. That \mathcal{Y}_m is closed in the narrow topology is shown by an argument exactly like that for \mathcal{Y} above.

From these basic results we can easily derive the consequences (i)-(iii), taking $X = Y = \Omega$, where Ω is the closure of a bounded open set with a smooth boundary. Then with the definition (A 11) one has $\mu^{\nu, \kappa, t} \in \mathcal{Y}_m$ for fixed t and all $\nu, \kappa > 0$. Since \mathcal{Y}_m is a closed subset of the compact, metrizable space $M(X \times Y)$, it is itself (sequentially) compact. Hence, given the subsequence ν_j there is a further subsequence $\nu_k = \nu_{j_k}$ and a corresponding sequence κ_k such that $\mu^{\nu_k, \kappa_k, t} \rightarrow \mu^{*t} \in \mathcal{Y}_m$ in the narrow topology. Note that the limit μ^{*t} need not be unique and may depend upon the selected subsequence. The narrow convergence $\mu^{\nu_k, \kappa_k, t} \rightarrow \mu^{*t}$ is equivalent to (i), with the definition

$$d^d x_0 p^*(\mathbf{x}_0, 0 | \mathbf{x}, t) = \mu_{\mathbf{x}}^{*,t}(d\mathbf{x}_0), \quad (\text{A } 17)$$

where in general $p^*(\mathbf{x}_0, 0 | \mathbf{x}, t)$ is a distribution in the variable \mathbf{x}_0 not an ordinary function. Then (ii) is a restatement that $\mu^{*t} \in \mathcal{Y}$ and (iii) is a restatement that $\mu^{*t} \in \mathcal{Y}_m$. These observations complete the proof in section 2.3.

A.2. Proofs for Section 2.4

As in the main text, we first consider the case without a scalar source ($S = 0$). Our starting point is the FDR (2.12), with formula (2.48) for the variance $\text{Var} \left[\theta_0(\tilde{\xi}_{t,0}^{\nu_k, \kappa_k}(\mathbf{x})) \right]$. It follows from (i)-(ii) of Appendix A.1 that a subsequence $\nu_k = \nu_{j_k}$ can be selected together with a corresponding subsequence $\kappa_k \rightarrow 0$, so that the space-averaged variance will satisfy

$$\begin{aligned} \lim_{k \rightarrow \infty} \left\langle \text{Var} \left[\theta_0(\tilde{\xi}_{t,0}^{\nu_k, \kappa_k}) \right] \right\rangle_{\Omega} &= \int d^d x \int d^d x_0 \int d^d x'_0 \theta_0(\mathbf{x}_0) \theta_0(\mathbf{x}'_0) \\ &\times \left[p_2^*(\mathbf{x}_0, 0; \mathbf{x}'_0, 0 | \mathbf{x}, t) - p^*(\mathbf{x}_0, 0 | \mathbf{x}, t) p^*(\mathbf{x}'_0, 0 | \mathbf{x}, t) \right], \end{aligned} \quad (\text{A } 18)$$

for all $\theta_0 \in C(\Omega)$, where

$$p_2^*(\mathbf{x}_0, 0, \mathbf{x}'_0, 0 | \mathbf{x}, t) \equiv \delta^d(\mathbf{x}_0 - \mathbf{x}'_0) p^*(\mathbf{x}_0, 0 | \mathbf{x}, t). \quad (\text{A } 19)$$

Note that p_2^* is a Young measure on $Y = \Omega \times \Omega$ measurably indexed by elements \mathbf{x} of $X = \Omega$, since it is a narrow limit of the Young measures $p_2^{\nu_k, \kappa_k}$. We shall not use the property (iii) from Appendix A.1 in our argument, although volume-conservation was, of course, used in the derivation of the FDR (2.12). Since that FDR holds for all $\nu, \kappa > 0$, it follows that the limit of the cumulative global scalar dissipation exists and must coincide with the limiting variance:

$$\begin{aligned} \lim_{k \rightarrow \infty} \kappa_k \int_0^t ds \left\langle |\nabla \theta^{\nu_k, \kappa_k}(s)|^2 \right\rangle_{\Omega} &= \int d^d x \int d^d x_0 \int d^d x'_0 \theta_0(\mathbf{x}_0) \theta_0(\mathbf{x}'_0) \\ &\times \left[p_2^*(\mathbf{x}_0, 0; \mathbf{x}'_0, 0 | \mathbf{x}, t) - p^*(\mathbf{x}_0, 0 | \mathbf{x}, t) p^*(\mathbf{x}'_0, 0 | \mathbf{x}, t) \right], \end{aligned} \quad (\text{A } 20)$$

for all $\theta_0 \in C(\Omega)$. It follows immediately that anomalous scalar dissipation requires spontaneous stochasticity since, by the exact formula (A 20), a non-vanishing cumulative dissipation necessitates non-factorization on a finite measure set of \mathbf{x} .

The argument that spontaneous stochasticity implies anomalous dissipation is a bit more involved. We need to show that if non-factorization holds on a finite measure set

of \mathbf{x} , then there exists a smooth choice of θ_0 such that both sides of (A 20) are positive. Thus, assume the opposite, that both sides vanish for all smooth θ_0 . The righthand side then also vanishes for all continuous θ_0 , since $C^\infty(\Omega)$ is dense in $C(\Omega)$ in the uniform norm. For example, this density follows by the Stone-Weierstrass theorem (Rudin 2006), since $C^\infty(\Omega)$ is a subalgebra of $C(\Omega)$ containing the constant 1, closed under complex conjugation, and separating points of Ω . Since the integrand with respect to \mathbf{x} is a variance, it is non-negative, so that the vanishing of the integral over \mathbf{x} implies that there is a subset $\Omega_0 \subset \Omega$ of full measure, such that

$$\int d^d x_0 \int d^d x'_0 \theta_0(\mathbf{x}_0) \theta_0(\mathbf{x}'_0) \left[p_2^*(\mathbf{x}_0, 0; \mathbf{x}'_0, 0 | \mathbf{x}, t) - p^*(\mathbf{x}_0, 0 | \mathbf{x}, t) p^*(\mathbf{x}'_0, 0 | \mathbf{x}, t) \right] = 0, \quad (\text{A 21})$$

for all $\mathbf{x} \in \Omega_0$ and $\theta_0 \in C(\Omega)$. Note furthermore that the quantity in the square brackets “[\cdot]” in the equation above is symmetric in $\mathbf{x}_0, \mathbf{x}'_0$. Thus, for any pair of functions g, h , one can take $\theta_0 = g + h$ to infer that

$$\int d^d x_0 \int d^d x'_0 g(\mathbf{x}_0) h(\mathbf{x}'_0) \left[p_2^*(\mathbf{x}_0, 0; \mathbf{x}'_0, 0 | \mathbf{x}, t) - p^*(\mathbf{x}_0, 0 | \mathbf{x}, t) p^*(\mathbf{x}'_0, 0 | \mathbf{x}, t) \right] = 0 \quad (\text{A 22})$$

for all $\mathbf{x} \in \Omega_0$ and $g, h \in C(\Omega)$. Since the product functions $(g \otimes h)(\mathbf{x}, \mathbf{x}'_0) = g(\mathbf{x}_0) h(\mathbf{x}'_0)$ form a subalgebra of $C(\Omega^2)$ that satisfies all of the conditions of the Stone-Weierstrass theorem, we can use this theorem again to extend the equality to

$$\int d^d x_0 \int d^d x'_0 f(\mathbf{x}_0, \mathbf{x}'_0) \left[p_2^*(\mathbf{x}_0, 0; \mathbf{x}'_0, 0 | \mathbf{x}, t) - p^*(\mathbf{x}_0, 0 | \mathbf{x}, t) p^*(\mathbf{x}'_0, 0 | \mathbf{x}, t) \right] = 0 \quad (\text{A 23})$$

for all $\mathbf{x} \in \Omega_0$ and $f \in C(\Omega^2)$. The parameterized measure $\nu_{\mathbf{x}}$ defined by

$$\nu_{\mathbf{x}}(d\mathbf{x}_0, d\mathbf{x}'_0) = d^d x_0 d^d x'_0 \left[p_2^*(\mathbf{x}_0, 0; \mathbf{x}'_0, 0 | \mathbf{x}, t) - p^*(\mathbf{x}_0, 0 | \mathbf{x}, t) p^*(\mathbf{x}'_0, 0 | \mathbf{x}, t) \right] \quad (\text{A 24})$$

is a difference of two Young measures and, thus, there is a continuous linear functional on $C(\Omega^2)$ for all $\mathbf{x} \in \Omega_0$ also denoted $\nu_{\mathbf{x}}$, defined by $\langle \nu_{\mathbf{x}}, f \rangle = \int_{\Omega^2} f d\nu_{\mathbf{x}}$. Since

$$\langle \nu_{\mathbf{x}}, f \rangle = 0, \text{ for all } f \in C(\Omega^2) \text{ and } \mathbf{x} \in \Omega_0, \quad (\text{A 25})$$

it follows for all $\mathbf{x} \in \Omega_0$ that $\nu_{\mathbf{x}} \equiv 0$, as an element of the dual Banach space $C(\Omega^2)^*$. A direct consequence is that

$$p_2^*(\mathbf{x}_0, 0; \mathbf{x}'_0, 0 | \mathbf{x}, t) = p^*(\mathbf{x}_0, 0 | \mathbf{x}, t) p^*(\mathbf{x}'_0, 0 | \mathbf{x}, t) \quad (\text{A 26})$$

as distributions in $\mathbf{x}_0, \mathbf{x}'_0$, for all $\mathbf{x} \in \Omega_0$. However, this contradicts our starting assumption that factorization fails on a set of full measure. Hence, there must be a smooth choice of θ_0 which makes the righthand side of (A 20) positive, and thus also the lefthand side.

Let us next consider the case with $\theta_0 \equiv 0$, but with the source S non-vanishing. In this circumstance the FDR (2.12) becomes

$$\kappa \int_0^t ds \left\langle |\nabla \theta(s)|^2 \right\rangle_{\Omega} = \frac{1}{2} \left\langle \text{Var} \left[\int_0^t S(\tilde{\xi}_{t,s}^{\nu, \kappa}(s)) ds \right] \right\rangle_{\Omega} \quad (\text{A 27})$$

with expression (2.53) for the variance. We show first that there is a suitable subsequence $\nu_k = \nu_{j_k} \rightarrow 0$ and $\kappa_k \rightarrow 0$ such that

$$\begin{aligned} & \lim_{k \rightarrow \infty} \int_{\Omega} d^d x \text{Var} \left[\int_0^t S(\tilde{\xi}_{t,s}^{\nu_k, \kappa_k}(\mathbf{x}), s) ds \right] \\ &= \int_{\Omega} d^d x \int_0^t ds \int_0^t ds' \int_{\Omega} d^d y \int_{\Omega} d^d y' S(\mathbf{y}, s) S(\mathbf{y}', s') \end{aligned}$$

$$\times \left[p_2^*(\mathbf{y}, s; \mathbf{y}', s' | \mathbf{x}, t) - p^*(\mathbf{y}, s | \mathbf{x}, t) p^*(\mathbf{y}', s' | \mathbf{x}, t) \right]. \quad (\text{A } 28)$$

for any $S \in C(\Omega \times [0, t])$ and for suitable limiting transition probabilities p_2^* and p^* . To show this we note that

$$\mu_{s, s', \mathbf{x}}^{\nu, \kappa}(d\mathbf{y}, d\mathbf{y}') = d^d \mathbf{y} d^d \mathbf{y}' p_2^{\nu, \kappa}(\mathbf{y}, s; \mathbf{y}', s' | \mathbf{x}, t) \quad (\text{A } 29)$$

defines a set of Young measures on $Y = \Omega \times \Omega$ measurably indexed by elements (s, s', \mathbf{x}) of $X = [0, t] \times [0, t] \times \Omega$. Since these spaces X and Y are both compact, we can appeal to the general results on Young measures discussed in Appendix A.1 to infer that a subsequence ν_k, κ_k exists so that, for all $f \in C(X \times Y)$,

$$\begin{aligned} & \lim_{k \rightarrow \infty} \int_0^t ds \int_0^t ds' \int_{\Omega} d^d \mathbf{y} \int_{\Omega} d^d \mathbf{y}' \int_{\Omega} d^d \mathbf{x} f(\mathbf{y}, s; \mathbf{y}', s'; \mathbf{x}) p_2^{\nu_k, \kappa_k}(\mathbf{y}, s; \mathbf{y}', s' | \mathbf{x}, t) \\ &= \int_0^t ds \int_0^t ds' \int_{\Omega} d^d \mathbf{y} \int_{\Omega} d^d \mathbf{y}' \int_{\Omega} d^d \mathbf{x} f(\mathbf{y}, s; \mathbf{y}', s'; \mathbf{x}) p_2^*(\mathbf{y}, s; \mathbf{y}', s' | \mathbf{x}, t) \end{aligned} \quad (\text{A } 30)$$

for some limit Young measure with distributional density p_2^* , which it is easy to show inherits the symmetry of $p_2^{\nu_k, \kappa_k}$ in (\mathbf{y}, s) and (\mathbf{y}', s') . Choosing the function f to be of the form $f(\mathbf{y}, s; \mathbf{y}', s'; \mathbf{x}) = h(s')g(\mathbf{y}, s; \mathbf{x})$ gives also

$$\begin{aligned} & \lim_{k \rightarrow \infty} \int_0^t ds \int_{\Omega} d^d \mathbf{y} \int_{\Omega} d^d \mathbf{x} g(\mathbf{y}, s; \mathbf{x}) p^{\nu_k, \kappa_k}(\mathbf{y}, s | \mathbf{x}, t) \\ &= \int_0^t ds \int_{\Omega} d^d \mathbf{y} \int_{\Omega} d^d \mathbf{x} g(\mathbf{y}, s; \mathbf{x}) p^*(\mathbf{y}, s | \mathbf{x}, t) \end{aligned} \quad (\text{A } 31)$$

for all continuous g with

$$p^*(\mathbf{y}, s | \mathbf{x}, t) = \int_{\Omega} d^d \mathbf{y}' p_2^*(\mathbf{y}, s; \mathbf{y}', s' | \mathbf{x}, t) \quad (\text{A } 32)$$

constant in s' for almost every s, \mathbf{x} and defining a consistent 1-time Young measure. We can also establish volume-preserving properties of these limiting Young measures, although that will not be necessary to our argument. From these results (A 28) follows by taking the limit along the subsequence ν_k, κ_k of the formula (2.53) for the variance.

The proof that spontaneous stochasticity is both necessary and sufficient for anomalous scalar dissipation now follows by arguments almost identical to the situation with $\theta_0 \neq 0$, $S \equiv 0$ that was first considered in this section. Necessity is immediate from (A 27), (A 28). The proof of sufficiency is very similar to that given before, by showing that vanishing of the space-integrated variance (A 28) for all smooth source fields S implies the factorization

$$p_2^*(\mathbf{y}, s; \mathbf{y}', s' | \mathbf{x}, t) = p^*(\mathbf{y}, s | \mathbf{x}, t) p^*(\mathbf{y}', s' | \mathbf{x}, t) \quad (\text{A } 33)$$

for almost every $\mathbf{x} \in \Omega$. The non-negativity of the \mathbf{x} -integrand requires some argument, because it is no longer obviously a variance. However, it is the limit of a variance in the sense that

$$\begin{aligned} & \lim_{k \rightarrow \infty} \int_{\Omega} d^d \mathbf{x} u(\mathbf{x}) \text{Var} \left[\int_0^t S(\tilde{\xi}_{t, s}^{\nu_k, \kappa_k}(\mathbf{x}), s) ds \right] \\ &= \int_{\Omega} d^d \mathbf{x} u(\mathbf{x}) \int_0^t ds \int_0^t ds' \int_{\Omega} d^d \mathbf{y} \int_{\Omega} d^d \mathbf{y}' S(\mathbf{y}, s) S(\mathbf{y}', s') \\ & \quad \times \left[p_2^*(\mathbf{y}, s; \mathbf{y}', s' | \mathbf{x}, t) - p^*(\mathbf{y}, s | \mathbf{x}, t) p^*(\mathbf{y}', s' | \mathbf{x}, t) \right]. \end{aligned} \quad (\text{A } 34)$$

for all $u \in C(\Omega)$ and $S \in C(\Omega \times [0, t])$. If also $u \geq 0$, then the lefthand side is non-negative

and thus so is the righthand side. This is enough to infer that

$$\int_0^t ds \int_0^t ds' \int_{\Omega} d^d y \int_{\Omega} d^d y' S(\mathbf{y}, s) S(\mathbf{y}', s') \\ \times \left[p_2^*(\mathbf{y}, s; \mathbf{y}', s' | \mathbf{x}, t) - p^*(\mathbf{y}, s | \mathbf{x}, t) p^*(\mathbf{y}', s' | \mathbf{x}, t) \right] \geq 0 \quad (\text{A } 35)$$

for all $\mathbf{x} \in \Omega_0$, a set of full measure in Ω . The remainder of the argument uses the same strategy as before, with $\theta_0 \rightarrow S$ and the Banach space $C(\Omega^2) \rightarrow C((\Omega \times [0, t])^2)$.

The argument when both $\theta_0 \neq 0$ and $S \neq 0$ has already been given in the main text. We only add here the technical detail that a single subsequence may be selected so that one has narrow convergence both of the 2-time Young measure

$$\mu_{s, s', \mathbf{x}}^{\nu_k, \kappa_k}(d\mathbf{y}, d\mathbf{y}') = d^d y d^d y' p_2^{\nu_k, \kappa_k}(\mathbf{y}, s; \mathbf{y}', s' | \mathbf{x}, t) \rightarrow d^d y d^d y' p_2^*(\mathbf{y}, s; \mathbf{y}', s' | \mathbf{x}, t) \quad (\text{A } 36)$$

and also of the 1-time Young measure at time $t_0 = 0$

$$\mu_{\mathbf{x}}^{\nu_k, \kappa_k}(d\mathbf{x}_0) = d^d x_0 p^{\nu_k, \kappa_k}(\mathbf{x}_0, 0 | \mathbf{x}, t) \rightarrow d^d x_0 p^*(\mathbf{x}_0, 0 | \mathbf{x}, t). \quad (\text{A } 37)$$

The second statement does *not* follow from the narrow convergence

$$\mu_{s, \mathbf{x}}^{\nu_k, \kappa_k}(d\mathbf{y}) = d^d y p^{\nu_k, \kappa_k}(\mathbf{y}, s | \mathbf{x}, t) \rightarrow d^d y p^*(\mathbf{y}, s | \mathbf{x}, t) \quad (\text{A } 38)$$

because $\{0\}$ is a subset of $[0, t]$ with zero Lebesgue measure. However, after extracting a subsequence for which the 2-time Young measure converges, one can extract a further subsequence so that the 1-time Young measure at time $t_0 = 0$ also converges.

A.3. Proofs for Section 4.2

We can exactly mimic the arguments of Appendix A.2 with no change to show that if there is spontaneous stochasticity, so that non-factorization occurs in (4.20) for a set of \mathbf{x} of positive measure, then there exists a smooth function Θ on \mathcal{S} which makes the variance (4.19) positive. This provides a positive lower bound to the global cumulative dissipation with that choice of Θ for a suitable subsequence $\nu_j, \kappa_j \rightarrow 0$. The existence of a smooth source S on $\Omega \times [0, t]$ which makes the variance (4.25) positive is likewise shown by arguments like those in Appendix A.2. We leave details to the reader.

Unfortunately, it seems to be very difficult to show that, with boundary conditions ψ fixed, spontaneous stochasticity implies anomalous dissipation for a suitable choice of initial data θ_0 . The difficulties are made apparent by the following easily proved identity for the variance (4.19), which separates contributions from θ_0 and ψ :

$$\text{Var} [\Theta(\tilde{\sigma}(\mathbf{x}, t))] = \text{Var} \left[\theta_0(\tilde{\xi}_{t,0}(\mathbf{x})) \Big| \tilde{\tau}(\mathbf{x}, t) = 0 \right] P(\tilde{\tau}(\mathbf{x}, t) = 0) \\ + \text{Var} \left[\psi(\tilde{\xi}_{t, \tilde{\tau}(\mathbf{x}, t)}(\mathbf{x}), \tilde{\tau}(\mathbf{x}, t)) \Big| \tilde{\tau}(\mathbf{x}, t) > 0 \right] P(\tilde{\tau}(\mathbf{x}, t) > 0). \quad (\text{A } 39)$$

Here the variances are conditioned upon the events $\tilde{\tau}(\mathbf{x}, t) = 0$ or $\tilde{\tau}(\mathbf{x}, t) > 0$ and the symbol $P(\dots)$ denotes the probability measure of these same events. By non-negativity of the variance, one gets readily

$$\text{Var} [\Theta(\tilde{\sigma}(\mathbf{x}, t))] \geq \text{Var} \left[\theta_0(\tilde{\xi}_{t,0}(\mathbf{x})) \Big| \tilde{\tau}(\mathbf{x}, t) = 0 \right] P(\tilde{\tau}(\mathbf{x}, t) = 0). \quad (\text{A } 40)$$

If one assumes that there is spontaneous stochasticity for the sub-ensembles specified by $\tilde{\tau}(\mathbf{x}, t) = 0$ for a positive-measure set of $\mathbf{x} \in \Omega$ (which is not an entirely straightforward assumption), then we can again use the arguments of Appendix A.2 to prove that

$$\lim_{j \rightarrow \infty} \text{Var} \left[\theta_0(\tilde{\xi}_{t,0}^{\nu_j, \kappa_j}(\mathbf{x})) \Big| \tilde{\tau}^{\nu_j, \kappa_j}(\mathbf{x}, t) = 0 \right] > 0 \quad (\text{A } 41)$$

for a suitable smooth initial datum θ_0 and for a suitable subsequence $\nu_j, \kappa_j \rightarrow 0$, on a positive measure set of $\mathbf{x} \in \Omega$. However, two difficulties appear. One is that, possibly,

$$\lim_{j \rightarrow \infty} P(\tilde{\tau}^{\nu_j, \kappa_j}(\mathbf{x}, t) = 0) = 0 \quad a.e. \mathbf{x} \in \Omega ! \quad (\text{A } 42)$$

Another technical difficulty is that vague topology of Young measures can be used to establish convergence of the space-average

$$\lim_{j \rightarrow \infty} \left\langle \text{Var} \left[\theta_0(\tilde{\xi}_{t,0}^{\nu_j, \kappa_j}) \Big| \tilde{\tau}^{\nu_j, \kappa_j}(t) = 0 \right] \right\rangle_{\Omega} \quad (\text{A } 43)$$

whenever θ_0 is a continuous function, but to obtain convergence of the needed space-average

$$\lim_{j \rightarrow \infty} \left\langle \text{Var} \left[\theta_0(\tilde{\xi}_{t,0}^{\nu_j, \kappa_j}) \Big| \tilde{\tau}^{\nu_j, \kappa_j}(t) = 0 \right] P(\tilde{\tau}^{\nu_j, \kappa_j}(t) = 0) \right\rangle_{\Omega} \quad (\text{A } 44)$$

by using the same arguments, one must know that the functions

$$g^{\nu, \kappa}(\mathbf{x}, t) \equiv P(\tilde{\tau}^{\nu, \kappa}(\mathbf{x}, t) = 0) \quad (\text{A } 45)$$

converge as $\nu, \kappa \rightarrow 0$ to a continuous (non-zero) function $g(\mathbf{x}, t)$ uniformly in \mathbf{x} . This is a non-trivial statement which cannot be obtained by mere compactness arguments.

Appendix B. Stochastic Representation and Fluctuation-Dissipation Relation for Thermal Conduction

For pure conduction with flux-b.c. we can work out explicit analytical results for the stochastic representation and fluctuation-dissipation relation in two relevant limits: $\kappa \rightarrow 0$ at fixed t and $t \rightarrow \infty$ at fixed κ . This example is interesting both as an illustration of the general formalism and as a ‘‘control experiment’’ to assess the effects of fluid advection. Heat conduction in a right cylindrical cell with arbitrary cross-section and no-flux conditions on the sidewalls reduces to a 1D problem. Therefore, without loss of generality, we consider the Neumann problem for the heat equation on the interval of length H . In order to simplify the analysis (so that cosine series suffice), we consider not the symmetric interval $[-H/2, H/2]$ but instead $[0, H]$. The problem then becomes:

$$\begin{aligned} \partial_t T &= \kappa \partial_x^2 T & \text{for } x &\in [0, H] \\ \kappa \partial_x T &= -J & \text{at } x &= 0, H \\ T &= 0 & \text{at } t &= 0. \end{aligned} \quad (\text{B } 1)$$

The scalar flux J at the boundaries is a space-time constant and also independent of κ . The solution can be represented via mean boundary local times at $x = 0$ and $x = H$ as:

$$T(x, t) = -J \left(\mathbb{E} \tilde{\ell}_{t,0}^0(x) - \mathbb{E} \tilde{\ell}_{t,0}^H(x) \right) = J \int_0^t ds \left(p(0, s|x, t) - p(H, s|x, t) \right), \quad (\text{B } 2)$$

which is a special case of the general stochastic representation formula (3.11). The transition density of the reflected process appearing in (B 2) (or Green’s function for the problem (B 1)) satisfies, for all $t > 0$ and $x \in [0, H]$, the backward evolution equation:

$$\begin{aligned} \partial_s p(a, s|x, t) &= -\kappa \partial_a^2 p(a, s|x, t) & \text{for } (a, s) &\in [0, H] \times [0, t] \\ \partial_a p(a, s|x, t) &= 0 & \text{at } a &= 0, H \\ p(a, t|x, t) &= \delta(a - x). \end{aligned} \quad (\text{B } 3)$$

The solution to the problem in (B 3) can be represented using Fourier cosine series:

$$p(a, s|x, t) = \frac{1}{H} + \frac{2}{H} \sum_{n=1}^{\infty} \cos\left(\frac{n\pi}{H}x\right) \cos\left(\frac{n\pi}{H}a\right) e^{-\kappa\left(\frac{n\pi}{H}\right)^2(t-s)}. \quad (\text{B } 4)$$

We will investigate “dissipative anomalies” for the solution of (B 1) as $\kappa \rightarrow 0$ through our fluctuation-dissipation relations at both finite and infinite time. As discussed in Section 3.3.1, these are not anomalies in the true sense, but are simply an artifact of keeping J fixed as $\kappa \rightarrow 0$. This constraint forces there to be large (unbounded) gradients of temperature. As a matter of fact, the role of a true turbulent anomaly for Rayleigh-Bénard convection (if it exists) is to prevent such divergences, so that the temperature difference ΔT across the domain remains finite as $\nu, \kappa \rightarrow 0$.

B.1. Zero diffusion limit at finite time

We first study the limiting temperature profile $T(x, t)$ as $\kappa \rightarrow 0$ via the stochastic representation (B 2). In the coarsest sense, this limit can be obtained from the convergence of the mean local times to delta-distributions at the boundary. Indeed, integrating against an arbitrary smooth test function $\varphi \in C^\infty[0, H]$ satisfying $\varphi'(0) = \varphi'(H) = 0$, we have, using the representation (B 4):

$$-\int_0^H dx \varphi(x) \mathbb{E} \tilde{\ell}_{t,0}^{\sigma H}(x) = a_0 t + \frac{H^2}{\kappa \pi^2} \sum_{n=1}^{\infty} \frac{(-1)^{n\sigma}}{n^2} \left(1 - e^{-\kappa\left(\frac{n\pi}{H}\right)^2 t}\right) a_n, \quad (\text{B } 5)$$

where $\sigma = 0, 1$ and

$$a_0 = \frac{1}{H} \int_0^H \varphi(x) dx, \quad a_n = \frac{2}{H} \int_0^H \varphi(x) \cos\left(\frac{n\pi}{H}x\right) dx. \quad (\text{B } 6)$$

Because the Fourier coefficients a_n are rapidly decaying in n for smooth φ , the series is absolutely convergent and the $\kappa \rightarrow 0$ limit yields:

$$\lim_{\kappa \rightarrow 0} \int_0^H dx \varphi(x) \left(-\mathbb{E} \tilde{\ell}_{t,0}^{\sigma H}(x)\right) = t \left[a_0 + \sum_{n=1}^{\infty} (-1)^{n\sigma} a_n \right] = t\varphi(\sigma H) \quad (\text{B } 7)$$

where we have used $\varphi(x) = a_0 + \sum_{n=1}^{\infty} a_n \cos\left(\frac{n\pi}{H}x\right)$. Therefore we find:

$$-\lim_{\kappa \rightarrow 0} \mathbb{E} \left[\tilde{\ell}_{t,0}^0(x) \right] = t\delta(x), \quad -\lim_{\kappa \rightarrow 0} \mathbb{E} \left[\tilde{\ell}_{t,0}^H(x) \right] = t\delta(x - H), \quad (\text{B } 8)$$

in the sense of distributions and thus

$$\lim_{\kappa \rightarrow 0} T(x, t) = Jt \left(\delta(x) - \delta(x - H) \right) \quad (\text{B } 9)$$

in the sense of distributions.

These delta-functions represent thin thermal boundary layers for small values of $\kappa > 0$. The small- κ asymptotics can be inferred by rewriting the transition density (B 4) as:

$$\begin{aligned} p(a, s|x, t) &= \frac{1}{H} \sum_{n=-\infty}^{\infty} \cos\left(\frac{n\pi}{H}x\right) \cos\left(\frac{n\pi}{H}a\right) e^{-\kappa\left(\frac{n\pi}{H}\right)^2(t-s)} \\ &= \frac{1}{\sqrt{4\kappa\pi(t-s)}} \sum_{n=-\infty}^{\infty} \left(e^{-\frac{(x-a+2nH)^2}{4\kappa(t-s)}} + e^{-\frac{(x+a+2nH)^2}{4\kappa(t-s)}} \right). \end{aligned} \quad (\text{B } 10)$$

where we have employed the Poisson summation formula (e.g. see Katznelson (2004)) in passing to the second equality. This is a useful reformulation since series (B 10) is rapidly

convergent for $\kappa(t-s)/H^2 \ll 1$ whereas (B 4) converges rapidly for $\kappa(t-s)/H^2 \gg 1$. Thus, at fixed t and H we can study the zero-diffusion limit $\kappa \rightarrow 0$ directly from this formula. In particular, since $x, a \in [0, H]$, the asymptotic transition probability is:

$$p(a, s|x, t) \sim \frac{1}{\sqrt{4\kappa\pi(t-s)}} \left(e^{-\frac{(x-a)^2}{4\kappa(t-s)}} + e^{-\frac{(x+a)^2}{4\kappa(t-s)}} + e^{-\frac{(x+a-2H)^2}{4\kappa(t-s)}} \right) \quad \text{as } \kappa \rightarrow 0. \quad (\text{B 11})$$

All other terms in the sum (B 10) vanish transcendentally. In fact, for $0 \leq a, x \ll H$ only two terms remain,

$$p(a, s|x, t) \sim \frac{1}{\sqrt{4\kappa\pi(t-s)}} \left(e^{-\frac{(x-a)^2}{4\kappa(t-s)}} + e^{-\frac{(x+a)^2}{4\kappa(t-s)}} \right) \quad \text{as } \kappa \rightarrow 0, \quad (\text{B 12})$$

which may be recognized as the transition probability for the diffusion process $\tilde{X}(s) = |x + \sqrt{2\kappa}W(t-s)|$ on the half-line $[0, \infty)$, which is a (scaled) Brownian process starting at x at time t moving backward in time s and reflected at the origin. This result is intuitively clear, since the right boundary of the interval at H should play no role for $a, x \ll H$ in the limit $\kappa \rightarrow 0$ at fixed times. By the exact symmetry $p(H-a, s|H-x, t) = p(a, s|x, t)$, there is a similar asymptotics with only two terms surviving in (B 11) for a, x near H .

We shall thus restrict our asymptotic analysis of the thermal boundary-layer to that near $x = 0$, and infer the result near $x = H$ by symmetry. We introduce a scaled coordinate $\xi = x/\sqrt{\kappa t}$ which is held fixed as $\kappa \rightarrow 0$. From $-\mathbb{E}\tilde{\ell}_{t,0}^0(x) = \int_0^t ds p(0, s|x, t)$ and (B 12) one easily obtains that

$$-\mathbb{E}\tilde{\ell}_{t,0}^0(\sqrt{\kappa t}\xi) \sim \left(\frac{t}{\kappa}\right)^{1/2} f(\xi), \quad \text{as } \kappa \rightarrow 0, \quad \text{with } f(\xi) = \frac{1}{\sqrt{\pi}} \int_0^1 \frac{du}{\sqrt{u}} \exp\left(-\frac{\xi^2}{4u}\right).$$

The scaling function $f(\xi)$ satisfies $f(0) = 2/\sqrt{\pi}$, $\int_0^\infty d\xi f(\xi) = 1$, and vanishes rapidly for $\xi \gg 1$. The mean of the boundary local time $\tilde{\ell}_{t,0}^0(x)$ vanishes transcendentally for x in the interior $(0, H)$ of the domain, but the convergence is highly non-uniform. In particular, at points within a distance $\sqrt{\kappa t}$ of the walls, the mean local times are of order $\sqrt{t/\kappa}$. We immediately conclude for the temperature field that

$$T(x, t) \sim J \left(\frac{t}{\kappa}\right)^{1/2} \left[f\left(\frac{x}{\sqrt{\kappa t}}\right) - f\left(\frac{H-x}{\sqrt{\kappa t}}\right) \right] \quad (\text{B 13})$$

when $\kappa \ll H^2/t$. This asymptotics refines the earlier result (B 9). Without the aid of the diffusivity to spread it, the temperature rises unboundedly at the walls as $\kappa \rightarrow 0$.

We can use the above asymptotics to study also the temperature gradient and the scalar dissipation. Indeed, by differentiating the formula (B 13) and using $f'(\xi) = -\text{erfc}(\xi/2)$ in terms of the complementary error function, we obtain

$$\partial_x T(x, t) = -\frac{J}{\kappa} \left[\text{erfc}\left(\frac{x}{\sqrt{4\kappa t}}\right) + \text{erfc}\left(\frac{H-x}{\sqrt{4\kappa t}}\right) \right] \quad (\text{B 14})$$

for $\kappa \ll H^2/t$. This clearly satisfies the flux b.c. in (B 1). We can exploit this formula to evaluate the space-time average of the thermal dissipation field $\varepsilon_T(x, t) = \kappa |\partial_x T(x, t)|^2$ in the limit $\kappa \rightarrow 0$. Using the improper integral $\int_0^\infty \text{erfc}^2(z) dz = \frac{1}{\sqrt{\pi}}(2 - \sqrt{2})$ (Ng & Geller 1969), it is straightforward to show that

$$\langle \varepsilon_T \rangle_{V,t} \equiv \frac{1}{t} \int_0^t ds \frac{1}{H} \int_0^H dx \kappa |\partial_x T(x, s)|^2 \sim \frac{8}{3\sqrt{\pi}} (2 - \sqrt{2}) \frac{J^2}{H} \sqrt{\frac{t}{\kappa}}. \quad (\text{B 15})$$

Apart from the precise numerical prefactor, this is the scaling that one would expect for temperature gradients of magnitude $\partial_x T \sim J/\kappa$ in a boundary layer of thickness $\sim \sqrt{\kappa t}$.

We now evaluate the mean scalar variance (3.63) in our FDR:

$$\begin{aligned} \langle \varepsilon_T^{fluc} \rangle_{V,t} &= \frac{J^2}{2t} \left\langle \text{Var} \left[\left(\tilde{\ell}_{t,0}^L - \tilde{\ell}_{t,0}^R \right) \right] \right\rangle_V = \frac{2J^2}{H} \int_0^H dx \frac{1}{t} \int_0^t ds \int_s^t ds' \\ &\times \left(\left[p(0, s|0, s') - p(0, s|x, t) \right] - \left[p(H, s|0, s') - p(H, s|x, t) \right] \right) p(0, s'|x, t). \end{aligned} \quad (\text{B 16})$$

Here we have used the symmetry of the integral in s, s' and the backward Markov property of the transition probabilities (e.g. see (C 3) in the following appendix). We have also made use of the $0 \leftrightarrow H$ symmetry after integrating over $[0, H]$. Using the asymptotics (B 11), we have for any $x \in [0, H]$, keeping only the leading terms:

$$\begin{aligned} [p(H, s|0, s') - p(H, s|x, s')] p(0, s'|x, t) &\sim \left[\frac{e^{-\frac{H^2}{4\kappa(t-s)}}}{\sqrt{4\kappa\pi(s'-s)}} - \frac{e^{-\frac{(x-H)^2}{4\kappa(t-s)}}}{\sqrt{4\kappa\pi(t-s)}} \right] \left[\frac{e^{-\frac{x^2}{4\kappa(t-s')}}}{\sqrt{4\kappa\pi(t-s')}} \right] \\ &\rightarrow 0 \text{ transcendentally, as } \kappa \rightarrow 0. \end{aligned} \quad (\text{B 17})$$

Thus, all heterohedral terms vanish as $\kappa \rightarrow 0$ and only homohedral terms contribute to the scalar variance. Because of our use of the $0 \leftrightarrow H$ symmetry, only the contributions from $\langle \varepsilon_T^{fluc}(x) \rangle_t$ for $0 \leq x \ll H$ survive (multiplied by 2), where as $\kappa \rightarrow 0$

$$\begin{aligned} \langle \varepsilon_T^{fluc}((\kappa t)^{1/2} \xi) \rangle_t &\sim \frac{J^2}{t} \int_0^t ds \int_s^t ds' \left[p(0, s|0, s') - p(0, s|\sqrt{\kappa t} \xi, t) \right] p(0, s'|\sqrt{\kappa t} \xi, t) \\ &\sim \frac{J^2}{\kappa\pi t} \int_0^t ds \int_s^t ds' \left[\frac{\exp\left(-\frac{\xi^2 t}{4(t-s')}\right)}{\sqrt{(s'-s)(t-s')}} - \frac{\exp\left(-\frac{\xi^2 t(2t-s-s')}{4(t-s)(t-s')}\right)}{\sqrt{(t-s)(t-s')}} \right] \end{aligned}$$

Integrating over ξ from 0 to ∞ and multiplying by $2/H$ gives, after a change of variables to $u = s/t, u' = s'/t$,

$$\langle \varepsilon_T^{fluc} \rangle_{V,t} \sim \frac{2}{\sqrt{\pi}} \frac{J^2}{H} \left(\frac{t}{\kappa} \right)^{1/2} \int_0^1 du \int_u^1 du' \left[\frac{1}{\sqrt{u'-u}} - \frac{1}{\sqrt{2-(u+u')}} \right]. \quad (\text{B 18})$$

The double integral is easily reduced to elementary integrals, with the value $\frac{4}{3}(2 - \sqrt{2})$. Thus, we obtain finally

$$\langle \varepsilon_T^{fluc} \rangle_{V,t} \sim \frac{8}{3\sqrt{\pi}} (2 - \sqrt{2}) \frac{J^2}{H} \sqrt{\frac{t}{\kappa}}, \quad \kappa \rightarrow 0, \quad (\text{B 19})$$

in exact agreement with (B 15).

The local dissipation measures $\langle \varepsilon_T^{fluc}(x) \rangle_t$ and $\langle \varepsilon_T(x) \rangle_t$ need not be the same pointwise, but, as argued in Section 3.3.2, they should be closely correlated. To test this idea for pure heat conduction, we have numerically evaluated our local formula for the fluctuation variance (3.63), using the analytical representation (B 10) of the transition probabilities, truncated to a finite number of terms. The double time-integral in (B 16) was evaluated using the Matlab function `integral2`, setting absolute tolerance `abstol=1e-10` and relative tolerance `reltol=1e-8`. In Fig. 6 we plot the resulting local scalar variance $\langle \varepsilon_T^{fluc}(x) \rangle_t$ using the three-term expansion (B 11), but we have verified that adding further terms from the full expansion (B 10) made no observable change. We also plot for comparison the local dissipation $\langle \varepsilon_T(x) \rangle_t$ obtained from the asymptotic temperature gradient (B 14). Though not identical, we see a close qualitative correspondence of the spatial behavior of these two dissipation measures, particularly for small dimensionless time $\tau \equiv \kappa t/H^2$ when the dissipation accumulates at the walls.

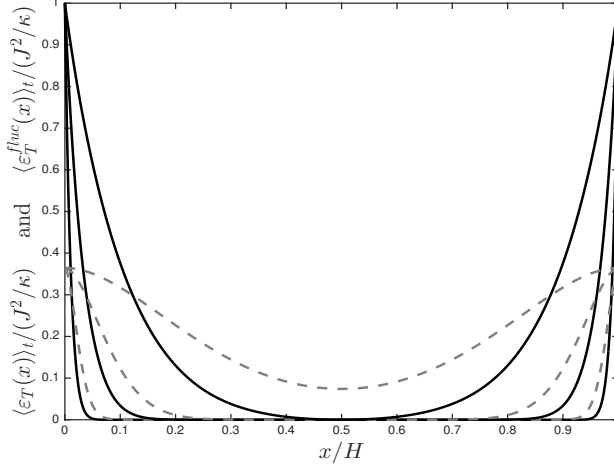


Figure 6: Local thermal dissipation (solid) and scalar variance (dashed) for pure heat conduction on a 1D interval, non-dimensionalized by J^2/κ , plotted for three dimensionless times $\tau \equiv \kappa t/H^2 = 5 \times 10^{-2}$, 5×10^{-3} , 5×10^{-4} . The dissipation and variance both localize near the walls as τ decreases.

B.2. Infinite-time limit for fixed diffusivity

We now consider the opposite limit of $t \rightarrow \infty$ with κ fixed, appropriate to steady-state conduction. The large- t asymptotics of the mean local times are

$$\begin{aligned} -\mathbb{E} \left[\tilde{\ell}_{t,0}^{\sigma H}(x) \right] &= \frac{t}{H} + \frac{2H}{\kappa\pi^2} \sum_{n=1}^{\infty} (-1)^{\sigma H} \frac{\cos\left(\frac{n\pi}{H}x\right)}{n^2} \left(1 - e^{-\kappa\left(\frac{n\pi}{H}\right)^2 t}\right) \\ &\sim \frac{t}{H} + \frac{2H}{\kappa\pi^2} \sum_{n=1}^{\infty} (-1)^{\sigma H} \frac{\cos\left(\frac{n\pi}{H}x\right)}{n^2}, \quad t \gg H^2/\kappa \end{aligned} \quad (\text{B 20})$$

The above cosine series can be computed by standard methods as:

$$-\mathbb{E} \left[\tilde{\ell}_{t,0}^0(x) \right] = \frac{t}{H} + \frac{H}{6\kappa} \left[3 \left(\frac{x}{H}\right)^2 - 6 \left(\frac{x}{H}\right) + 2 \right], \quad -\mathbb{E} \left[\tilde{\ell}_{t,0}^H(x) \right] = \frac{t}{H} + \frac{H}{6\kappa} \left[3 \left(\frac{x}{H}\right)^2 - 1 \right].$$

With these, one obtains using the representation (B 2) of the temperature field:

$$T(x, t) = -\frac{J}{\kappa} \left(x - \frac{H}{2} \right) \quad \text{as } t \rightarrow \infty. \quad (\text{B 21})$$

This is indeed the exact steady-state solution of (B 1) (unique up to an arbitrary constant). From this one gets the thermal dissipation field

$$\langle \varepsilon_T(x) \rangle_{\infty} \equiv \langle \kappa |\partial_x T|^2 \rangle_{\infty} = \frac{J^2}{\kappa}, \quad (\text{B 22})$$

pointwise in x and averaged over a time-interval $[0, t]$ with $t \gg H^2/\kappa$.

We next evaluate the mean scalar fluctuation variance in the limit $t \rightarrow \infty$. For this purpose, we could use the general infinite-time limit formula (3.67) that is derived in Appendix C. Here we shall instead proceed directly from eq.(B 16) above. After minor

manipulation, this formula becomes here:

$$\begin{aligned} \frac{J^2}{2t} \text{Var} \left[J \left(\tilde{\ell}_{t,0}^L(x) - \tilde{\ell}_{t,0}^R(x) \right) \right] &= \frac{J^2}{t} \int_0^t ds \int_s^t ds' \left\{ \left(\frac{2}{H} \right) \left[\delta p(0, s|0, s') - \delta p(0, s|H, s') \right] \right. \\ &+ \left[\delta p(H, s|H, s') - \delta p(H, s|x, t) \right] \delta p(H, s'|x, t) + \left[\delta p(0, s|0, s') - \delta p(0, s|x, t) \right] \delta p(0, s'|x, t) \\ &\left. - \left[\delta p(H, s|0, s') - \delta p(H, s|x, t) \right] \delta p(0, s'|x, t) - \left[\delta p(0, s|H, s') - \delta p(0, s|x, t) \right] \delta p(H, s'|x, t) \right\} \end{aligned}$$

where $\delta p(a, s|x, t) = p(a, s|x, t) - 1/H$ was introduced to eliminate the common contributions arising from the $1/H$ term in the transition densities. All terms in the above formula which are x -dependent vanish in the infinite-time limit. To see this explicitly, for times $t \gg H^2/\kappa$ we obtain by substituting the cosine series (B 4) that

$$\begin{aligned} &\int_0^t ds \int_s^t ds' \delta p(\sigma H, s|\sigma' H, s') \delta p(\sigma' H, s'|x, t) \\ &\rightarrow \left(\frac{2}{\pi} \right)^4 \frac{H^2}{(2\kappa)^2} \sum_{n,m=1}^{\infty} (-1)^{(\sigma+\sigma')m+\sigma'n} \frac{\cos\left(\frac{n\pi}{H}x\right)}{n^2 m^2} \end{aligned} \quad (\text{B 23})$$

$$\begin{aligned} &\int_0^t ds \int_s^t ds' \delta p(\sigma H, s|x, s') \delta p(\sigma' H, s'|x, t) \\ &\rightarrow \left(\frac{2}{\pi} \right)^4 \frac{H^2}{(2\kappa)^2} \sum_{n,m=1}^{\infty} (-1)^{\sigma m+\sigma'n} \frac{\cos\left(\frac{n\pi}{H}x\right) \cos\left(\frac{m\pi}{H}x\right)}{n^2 m^2}. \end{aligned} \quad (\text{B 24})$$

For all combinations of $\sigma, \sigma' = 0, 1$, these sums are absolutely convergent and can be calculated by the same means as the average local times. However, the important point is that they are independent of time and therefore their contribution to the total variance vanishes like $1/t$. The only non-vanishing contribution to $\langle \varepsilon_T^{fluc}(x) \rangle_{\infty}$ arises from the first x -independent term, which is identical to the general infinite-time result (3.67). There are both homohedral and heterohedral contributions, which may be calculated again by substituting the cosine series (B 4) and performing the time-integrals to obtain for $t \gg H^2/\kappa$

$$(-1)^{\sigma} \frac{2}{H} \int_0^t ds \int_s^t ds' \delta p(0, s|\sigma H, s') \sim \frac{t}{\kappa} \left(\frac{2}{\pi} \right)^2 \sum_{n=1}^{\infty} \frac{(-1)^{\sigma(n+1)}}{n^2} = \frac{t}{3\kappa} \times \begin{cases} 2 & \sigma = 0 \\ 1 & \sigma = 1 \end{cases}$$

In terms of the homohedral and heterohedral correlation times as defined by (3.81), our result states:

$$\tau_{corr}^{hom} = \frac{2}{3} \frac{H^2}{\kappa}, \quad \tau_{corr}^{het} = \frac{1}{3} \frac{H^2}{\kappa} \quad (\text{B 25})$$

in agreement with the general inequality (3.84) discussed in Section 3.3.3 of the main text. Finally, the scalar variance is calculated as

$$\langle \varepsilon_T^{fluc}(x) \rangle_{\infty} = \frac{J^2}{H^2} (\tau_{corr}^{hom} + \tau_{corr}^{het}) = \frac{J^2}{\kappa}, \quad (\text{B 26})$$

As dictated by the general result (3.15), the infinite-time fluctuational dissipation (B 26) for all points $x \in [0, H]$ equals the space-average thermal dissipation calculated from the exact steady-state solution (B 22).

B.3. Boundary Local Time Density of Reflected Brownian on the Half-Line

The formula (3.23) invoked in section 3.2 is a standard result for Brownian motion, at least forward in time. Since the Wiener process is time-reversible, it holds also backward

in time. However, even forward in time we could find no reference which gave the result (3.23) for general values of diffusivity $\kappa > 0$. Thus, we here very succinctly review the standard arguments which lead to (3.23), with references to more detailed discussions.

If $\tilde{B}(t)$ is a standard Brownian motion (Wiener process), then the Brownian motion with diffusivity κ started at $x \geq 0$ and reflected at 0 is given by the simple formula

$$\tilde{X}(t) = |\sqrt{2\kappa}\tilde{B}(t) - x|. \quad (\text{B } 27)$$

Note that $\tilde{B}(t)$ has units of $(\text{time})^{1/2}$ whereas $\tilde{X}(t)$ has units of (length). The evolution of $\tilde{X}(t)$ can be obtained from the Tanaka equation for $a \geq 0$:

$$\begin{aligned} |\tilde{B}(t) - a| &= a + \int_0^t \text{sign}(\tilde{B}(t) - a) d\tilde{B}(t) + \int_0^t ds \delta(\tilde{B}(s) - a) \\ &= a + \tilde{W}(t) + \tilde{L}_t(a), \end{aligned} \quad (\text{B } 28)$$

where $\tilde{W}(t) = \int_0^t \text{sign}(\tilde{B}(t) - a) d\tilde{B}(t)$ is another standard Brownian motion and $\tilde{L}_t(a)$ is the local time of $\tilde{B}(t)$ at point a . For these well-known results, see Karatzas & Shreve (1991), section 3.6 and Rogers & Williams (2000), sections IV.6.43-44. (Possibly confusingly, there are different normalizations of local time in the literature, as discussed by Karatzas & Shreve (1991), Remark 3.6.4 and Rogers & Williams (2000), Remark IV.6.43.12. We follow the conventions of the latter.) Setting $a = x/\sqrt{2\kappa}$ in the Tanaka equation and multiplying through by $\sqrt{2\kappa}$ gives

$$\begin{aligned} \tilde{X}(t) &= x + \sqrt{2\kappa}\tilde{W}(t) + \kappa \int_0^t ds \delta(\tilde{X}(s)) \\ &= x + \sqrt{2\kappa}\tilde{W}(t) + \kappa \tilde{\ell}_{0,t}(x). \end{aligned} \quad (\text{B } 29)$$

We used here that $\delta(\tilde{X}(t) - \epsilon) = \delta(\sqrt{2\kappa}\tilde{B}(t) - x - \epsilon) + \delta(\sqrt{2\kappa}\tilde{B}(t) - x + \epsilon)$ for any $\epsilon > 0$, in order to relate the local times of $\tilde{B}(t)$ and $\tilde{X}(t)$. See Rogers & Williams (2000), p.101 and Karatzas & Shreve (1991), Remark 3.7.4. We have also used our normalization convention for the boundary local time density $\tilde{\ell}_{0,t}(x)$, which does not incorporate the factor of κ into the definition of the local time density.

We next note the expression for the boundary local time density given by the Skorohod equation

$$\kappa \tilde{\ell}_{0,t}(x) = \max\{0, \sup_{0 \leq s \leq t} (-x - \sqrt{2\kappa}\tilde{W}(s))\}. \quad (\text{B } 30)$$

See Karatzas & Shreve (1991), Lemma 3.6.14. Define $\tilde{W}_-(t) = -\tilde{W}(t)$, which is another standard Brownian motion, and denote its maximum up to time t by $\tilde{M}(t) = \sup_{0 \leq s \leq t} \tilde{W}_-(s)$, so that

$$\kappa \tilde{\ell}_{0,t}(x) = \max\{0, -x + \sqrt{2\kappa}\tilde{M}(t)\}. \quad (\text{B } 31)$$

It is well-known (and easy to see) that if $\tilde{\tau}(z)$ is the time for $\tilde{W}_-(t)$ to first hit z , then

$$P(\tilde{M}(t) > z) = P(\tilde{\tau}(z) < t). \quad (\text{B } 32)$$

The latter probability can be evaluated by the reflection principle:

$$P(\tilde{\tau}(z) < t) = 2P(\tilde{W}_-(t) > z). \quad (\text{B } 33)$$

See Karatzas & Shreve (1991), section 2.6. Thus, for $z > 0$,

$$P(\tilde{M}(t) < z) = 2P(\tilde{W}_-(t) < z) - 1 = 2\Phi_t(z) - 1 \quad (\text{B } 34)$$

with

$$\Phi_t(z) = \frac{1}{\sqrt{2\pi t}} \int_{-\infty}^z dy \exp(-y^2/2t). \quad (\text{B } 35)$$

Using this result and eq.(B 31) gives

$$P(\tilde{\ell}_{0,t}(x) < \ell) = \begin{cases} 2\Phi_t\left(\frac{x+\kappa\ell}{\sqrt{2\kappa}}\right) - 1 & \text{for } \ell > 0 \\ 0 & \text{for } \ell < 0 \end{cases} \quad (\text{B } 36)$$

Finally, differentiating with respect to ℓ gives (3.23) in the main text.

Appendix C. Derivation of Steady-State Fluctuation-Dissipation Relation for Rayleigh-Bénard Convection

We here derive (3.67) in the main text. In contrast to the complete proofs presented in the other appendices, our arguments here are exact but not fully rigorous. By this we mean that various assumptions in the argument (e.g. about ergodicity) are carefully stated, but not proved. We also give only brief explanations for error estimates on contributions vanishing in the limit $t \rightarrow \infty$. However, if the stated assumptions are indeed correct, then rigorous proofs along the lines indicated should be straightforward.

The starting point of our argument is

$$\begin{aligned} & \lim_{t \rightarrow \infty} \frac{1}{2t} \text{Cov} \left[\tilde{\ell}_{t,0}^\lambda(\mathbf{x}), \tilde{\ell}_{t,0}^{\lambda'}(\mathbf{x}) \right] \\ &= \lim_{t \rightarrow \infty} \frac{1}{t} \int_0^t ds \int_0^t ds' \\ & \quad \times \left[p_{2z}(\lambda H/2, s; \lambda' H/2, s' | \mathbf{x}, t) - p_z(\lambda H/2, s | \mathbf{x}, t) p_z(\lambda' H/2, s' | \mathbf{x}, t) \right], \end{aligned} \quad (\text{C } 1)$$

which is a restatement of (3.63). First, we use symmetry of the integrand in s, s' to restrict the time-integration range to $s < s' < t$ and then use the Markov property of the backward stochastic flow to write

$$p_{2z}(\lambda H/2, s; \lambda' H/2, s' | \mathbf{x}, t) = \iint_S dx' dy' p_z(\lambda H/2, s | x', y', z', s') p(x', y', z', s' | \mathbf{x}, t), \quad (\text{C } 2)$$

giving

$$\begin{aligned} & \lim_{t \rightarrow \infty} \frac{1}{2t} \text{Cov} \left[\tilde{\ell}_{t,0}^\lambda(\mathbf{x}), \tilde{\ell}_{t,0}^{\lambda'}(\mathbf{x}) \right] = \lim_{t \rightarrow \infty} \frac{1}{t} \int_0^t ds \int_s^t ds' \iint_S dx' dy' \\ & \quad \times \left[p_z(\lambda H/2, s | x', y', \lambda' H/2, s') - p_z(\lambda H/2, s | \mathbf{x}, t) \right] p(x', y', \lambda' H/2, s' | \mathbf{x}, t) \end{aligned} \quad (\text{C } 3)$$

Next, we divide the triangular region $R = \{(s, s') : 0 < s < s' < t\}$ into three subregions:

$$\begin{aligned} R_I &= \{(s, s') : 0 < s < s' < t - n\tau\} \\ R_{II} &= \{(s, s') : 0 < s < t - 2n\tau, t - n\tau < s' < t\} \\ R_{III} &= R \setminus (R_I \cup R_{II}) \end{aligned} \quad (\text{C } 4)$$

where τ is the scalar mixing time used in deriving (3.15) and n is a positive integer. Region R_{III} gives a contribution which is $O(n^2\tau^2/t)$ and can be neglected in the limit $t \rightarrow \infty$. In Region R_{II} one has both $t - s > n\tau$ and $s' - s > n\tau$, so that as $n \rightarrow \infty$ one may use the ergodicity of the Lagrangian flow in physical space to obtain

$$p_z(\lambda H/2, s | x', y', \lambda' H/2, s') \rightarrow \frac{1}{H}, \quad p_z(\lambda H/2, s | \mathbf{x}, t) \rightarrow \frac{1}{H}, \quad (\text{C } 5)$$

for $\lambda, \lambda' = \pm 1$, which give canceling contributions in (C3). Thus, this region makes an arbitrarily small contribution for sufficiently large n . Finally, in region R_I one has $t - s > t - s' > n\tau$, so that again by ergodicity of the Lagrangian flow as $n \rightarrow \infty$

$$p_z(\lambda H/2, s|\mathbf{x}, t) \rightarrow \frac{1}{H}, \quad p(x', y', \lambda' H/2, s'|\mathbf{x}, t) \rightarrow \frac{1}{AH}. \quad (\text{C6})$$

Taking the limit $t \rightarrow \infty$ and using the independence of the limit value upon n one obtains

$$\lim_{t \rightarrow \infty} \frac{1}{2t} \text{Cov} \left[\tilde{\ell}_{t,0}^\lambda(\mathbf{x}), \tilde{\ell}_{t,0}^{\lambda'}(\mathbf{x}) \right] = \frac{1}{H} \lim_{t \rightarrow \infty} \frac{1}{t} \int_0^t ds \int_s^t ds' \left[p_z(\lambda H/2, s|\lambda' H/2, s') - \frac{1}{H} \right] \quad (\text{C7})$$

Finally, to simplify still further, change the order of the integrals over s, s' and then set $s \rightarrow s - s'$ to obtain

$$\begin{aligned} \lim_{t \rightarrow \infty} \frac{1}{2t} \text{Cov} \left[\tilde{\ell}_{t,0}^\lambda(\mathbf{x}), \tilde{\ell}_{t,0}^{\lambda'}(\mathbf{x}) \right] &= \frac{1}{H} \lim_{t \rightarrow \infty} \frac{1}{t} \int_0^t ds' \int_0^{s'} ds \left[p_z(\lambda H/2, s|\lambda' H/2, s') - \frac{1}{H} \right] \\ &= \frac{1}{H} \lim_{t \rightarrow \infty} \frac{1}{t} \int_0^t ds' \int_{-s'}^0 ds \left[p_z(\lambda H/2, s' + s|\lambda' H/2, s') - \frac{1}{H} \right] \\ &= \frac{1}{H} \lim_{s' \rightarrow \infty} \int_{-s'}^0 ds \left[p_z(\lambda H/2, s' + s|\lambda' H/2, s') - \frac{1}{H} \right] \\ &= \frac{1}{H} \lim_{s' \rightarrow \infty} \int_{-s'}^0 ds \left[p_z(\lambda H/2, s'' + s|\lambda' H/2, s'') - \frac{1}{H} \right] \end{aligned} \quad (\text{C8})$$

for any s'' , since the integral should be the same for any pair of times $s'' + s, s''$ replacing $s' + s, s'$ in the transition probability. The underlying assumption here is that this integral over an infinitely long time interval (in the past) should be independent of the state at the present time. This is an assumption about the ergodicity of the Eulerian dynamics defined by the Boussinesq equation, i.e. the existence of a unique statistical steady-state obtained by an infinite time-average. Under this hypothesis, one can take in particular $s'' = 0$ to obtain that

$$\lim_{t \rightarrow \infty} \frac{1}{2t} \text{Cov} \left[\tilde{\ell}_{t,0}^\lambda(\mathbf{x}), \tilde{\ell}_{t,0}^{\lambda'}(\mathbf{x}) \right] = \frac{1}{H} \int_{-\infty}^0 ds \left[p_z(\lambda H/2, s|\lambda' H/2, 0) - \frac{1}{H} \right], \quad (\text{C9})$$

as was claimed in (3.67).

Appendix D. Averages of the Fluctuation-Dissipation Relation over Random Sources and Initial Data

Here we shall derive the specific consequences of our FDR mentioned in section 2.1. We begin with the balance equation (2.14) for the mean scalar dissipation in a statistical steady-state maintained by a random scalar source, delta-correlated in time. We shall consider any compact space domain Ω either without boundary (e.g. a torus) or with zero scalar flux through the wall. In addition to the delta-in-time covariance (2.13), the source is assumed to satisfy the condition that the ensemble-average is zero and also that the space-integral is zero in every realization:

$$\int_{\Omega} d^d x \tilde{S}(\mathbf{x}, t) = 0 \quad a.s. \quad (\text{D1})$$

This latter condition means that there is no net input of scalar by the source. The starting point of the derivation is the formula (2.53) for the source variance. Averaging this over the random source using the zero ensemble-average and the covariance (2.13) yields

$$\begin{aligned} \left\langle \text{Var} \left[\int_0^t \tilde{S}(\tilde{\boldsymbol{\xi}}_{t,s}(\mathbf{x}), s) \, ds \right] \right\rangle_S &= 2 \int_0^t ds \int_{\Omega} d^d y \, C_S(\mathbf{y}, \mathbf{y}) p(\mathbf{y}, s | \mathbf{x}, t) \\ &\quad - 2 \int_0^t ds \int_{\Omega} d^d y \int_{\Omega} d^d y' \, C_S(\mathbf{y}, \mathbf{y}') p(\mathbf{y}, s | \mathbf{x}, t) p(\mathbf{y}', s | \mathbf{x}, t) \end{aligned} \quad (\text{D } 2)$$

Because of the space-ergodicity of the stochastic Lagrangian flow for $\kappa, \nu > 0$, one has $p(\mathbf{y}, s | \mathbf{x}, t) \rightarrow 1/V$ for $t - s \gg \tau$ and one may use the arguments of section 3.3.2 and Appendix C to show that

$$\begin{aligned} \lim_{t \rightarrow \infty} \frac{1}{2t} \left\langle \text{Var} \left[\int_0^t \tilde{S}(\tilde{\boldsymbol{\xi}}_{t,s}(\mathbf{x}), s) \, ds \right] \right\rangle_S \\ = \frac{1}{V} \int_{\Omega} d^d y \, C_S(\mathbf{y}, \mathbf{y}) - \frac{1}{V^2} \int_{\Omega} d^d y \int_{\Omega} d^d y' \, C_S(\mathbf{y}, \mathbf{y}') = \frac{1}{V} \int_{\Omega} d^d y \, C_S(\mathbf{y}, \mathbf{y}), \end{aligned} \quad (\text{D } 3)$$

where the condition (D 1) was used for the last equality. Consistent with (2.19) and (3.15), this limit is independent of the space point \mathbf{x} . Finally, in the FDR's (2.12) and (3.18) one has $\lim_{t \rightarrow \infty} \frac{1}{2t} \text{Var} \left[\theta_0(\tilde{\boldsymbol{\xi}}_{t,0}(\mathbf{x})) \right] = 0$ for bounded initial data θ_0 , and thus the average over volume, infinite time-interval and random source yields

$$\kappa \left\langle |\nabla \theta|^2 \right\rangle_{\Omega, \infty, S} = \frac{1}{V} \int_{\Omega} d^d x \, C_S(\mathbf{x}, \mathbf{x}), \quad (\text{D } 4)$$

which is the standard scalar balance equation (2.14).

Next we derive from our general FDR the relation (2.16) of Sawford *et al.* (2005); Buaria *et al.* (2016) for a decaying passive scalar with a random initial linear profile satisfying the statistical isotropy condition (2.15). To obtain this result, note that for any random variable \tilde{X} , $\text{Var}(\tilde{X}) = \frac{1}{2} \mathbb{E} |\tilde{X}^{(1)} - \tilde{X}^{(2)}|^2$ where $\tilde{X}^{(1)}, \tilde{X}^{(2)}$ are two independent random variables identically distributed as \tilde{X} . Therefore, our FDR's (2.12) and (3.18) in the case of vanishing scalar sources and random scalar initial-values can be re-expressed as:

$$\kappa \int_0^t ds \left\langle |\nabla \tilde{\theta}(s)|^2 \right\rangle_{\Omega} = \frac{1}{4} \left\langle \mathbb{E} \left| \tilde{\theta}_0(\tilde{\boldsymbol{\xi}}_{t,0}^{(1)}) - \tilde{\theta}_0(\tilde{\boldsymbol{\xi}}_{t,0}^{(2)}) \right|^2 \right\rangle_{\Omega}. \quad (\text{D } 5)$$

Assuming that $\tilde{\theta}_0(\mathbf{x}) = \tilde{\mathbf{G}} \cdot \mathbf{x}$ and averaging over random initial data using (2.15) gives

$$\kappa \int_0^t ds \left\langle |\nabla \tilde{\theta}(s)|^2 \right\rangle_{\Omega, \theta_0} = \frac{1}{4} G^2 \left\langle \mathbb{E}^{1,2} \left| \tilde{\boldsymbol{\xi}}_{t,0}^{(1)} - \tilde{\boldsymbol{\xi}}_{t,0}^{(2)} \right|^2 \right\rangle_{\Omega}, \quad (\text{D } 6)$$

which is (2.16).

The interest of this relation is that it directly connects the temporal evolution of the mean scalar dissipation to two-particle dispersion of stochastic Lagrangian trajectories. For example, it relates dissipative anomalies of scalar fluctuations and kinetic energy if the Prandtl number is fixed and if the dispersion on the right of (D 6) exhibits a Richardson scaling $\sim \varepsilon t^3$ with ε independent of ν . This relation can be used to establish equivalence of spontaneous stochasticity and anomalous scalar dissipation for situations that satisfy the specific assumptions under which it is derived. One can obtain such a relation for more general initial data than linear profiles by instead assuming only that the initial scalar field is smooth and that its 2nd-order structure function satisfies the

pair of inequalities for all $\mathbf{x}, \mathbf{x}' \in \Omega$ that

$$c_{\theta_0} |\mathbf{x} - \mathbf{x}'|^2 \leq \langle |\tilde{\theta}_0(\mathbf{x}) - \tilde{\theta}_0(\mathbf{x}')|^2 \rangle_{\theta_0} \leq C_{\theta_0} |\mathbf{x} - \mathbf{x}'|^2, \quad (\text{D } 7)$$

for some constants $0 < c_{\theta_0} < C_{\theta_0} < \infty$. Averaging (D 5) over such initial data then yields

$$\frac{1}{4} c_{\theta_0} \left\langle \mathbb{E} \left| \tilde{\boldsymbol{\xi}}_{t,0}^{(1)} - \tilde{\boldsymbol{\xi}}_{t,0}^{(2)} \right|^2 \right\rangle_{\Omega} \leq \kappa \int_0^t ds \left\langle |\nabla \tilde{\theta}(s)|^2 \right\rangle_{\Omega, \theta_0} \leq \frac{1}{4} C_{\theta_0} \left\langle \mathbb{E} \left| \tilde{\boldsymbol{\xi}}_{t,0}^{(1)} - \tilde{\boldsymbol{\xi}}_{t,0}^{(2)} \right|^2 \right\rangle_{\Omega}. \quad (\text{D } 8)$$

This gives upper and lower bounds for the cumulative scalar dissipation directly in terms of two-particle dispersion, which again relate anomalous scalar dissipation to spontaneous stochasticity. If there is a smooth, random scalar source whose structure-function satisfies bounds similar to (D 7), then one can obtain analogous bounds relating cumulative scalar dissipation to the time-integrated 2-particle dispersion.

Appendix E. Numerical Methods

E.1. Methods for Section 2.2

In order to integrate backward Itô SDE's (2.3) of the form

$$\hat{d}\tilde{\boldsymbol{\xi}}(s) = \mathbf{u}(\tilde{\boldsymbol{\xi}}(s), s) ds + \sqrt{2\kappa} \hat{d}\tilde{\mathbf{W}}(s) \quad (\text{E } 1)$$

we use a reflected time $\hat{s} = t_f - s$ which converts them into forward Itô SDE's. The latter are integrated with the standard Euler-Maruyama scheme (Kloeden & Platen 1992). We must only very briefly explain our methods to estimate the particle dispersions and the transition probability densities $p_y(y', 0 | \mathbf{x}, t_f)$ using N -sample ensembles of stochastic trajectories $\tilde{\boldsymbol{\xi}}_n(s)$, $n = 1, \dots, N$ solving the above SDE. The particle dispersions were calculated by the unbiased estimators

$$\begin{aligned} \mathbb{E}^{1,2} \left[|\tilde{\boldsymbol{\xi}}^{(1)}(s) - \tilde{\boldsymbol{\xi}}^{(2)}(s)|^2 \right] &\doteq \frac{2}{N(N-1)} \sum_{n < m} |\tilde{\boldsymbol{\xi}}_n(s) - \tilde{\boldsymbol{\xi}}_m(s)|^2 \\ &= \frac{2}{N-1} \sum_{n=1}^N |\tilde{\boldsymbol{\xi}}_n(s) - \bar{\boldsymbol{\xi}}_N(s)|^2 \end{aligned} \quad (\text{E } 2)$$

with $\bar{\boldsymbol{\xi}}_N(s) = \frac{1}{N} \sum_{n=1}^N \tilde{\boldsymbol{\xi}}_n(s)$ the sample mean. For large N these are nearly the same as

$$\mathbb{E}^{1,2} \left[|\tilde{\boldsymbol{\xi}}^{(1)}(s) - \tilde{\boldsymbol{\xi}}^{(2)}(s)|^2 \right] \doteq \frac{2}{N} \sum_{n=1}^N |\tilde{\boldsymbol{\xi}}_n(s) - \mathbb{E}[\tilde{\boldsymbol{\xi}}(s)]|^2 \quad (\text{E } 3)$$

which is twice the sample average over N independent random variables each with the same distribution as $|\tilde{\boldsymbol{\xi}}(s) - \mathbb{E}[\tilde{\boldsymbol{\xi}}(s)]|^2$. Our error bars for the particle dispersion are thus taken to be twice the standard error of the mean (s.e.m.) for this N -sample average.

To estimate the position PDF's, we use kernel density estimator (KDE) methods (Silverman 1986). For the y -coordinate at time 0 of the particle $\tilde{\boldsymbol{\xi}}(0) = (\tilde{\xi}(0), \tilde{\eta}(0), \tilde{\zeta}(0))$ started at \mathbf{x} at time t_f , one has for a grid y'_i of possible y -values

$$\tilde{p}_h(y'_i, 0 | \mathbf{x}, t_f) \doteq \frac{1}{N} \sum_{n=1}^N K_h(\tilde{\eta}_n(0) - y'_i) \quad (\text{E } 4)$$

where $K_h(y) = (1/h)K(y/h)$ is a filter kernel with bandwidth h . We take K to be a Gaussian with unit variance and we choose the bandwidth h by the ‘‘principle of minimal sensitivity’’ from renormalization-group theory (Stevenson 1981). The latter procedure is based upon the observation that, when the number N of samples is sufficiently large

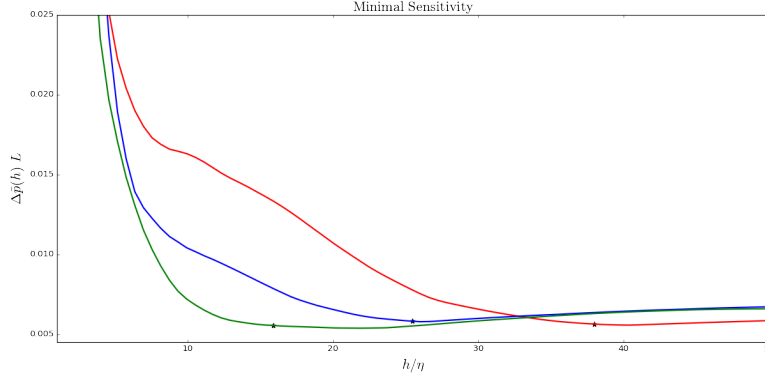


Figure 7: L^1 -differences of PDF estimates for successive bandwidths h_j are plotted for $Pr = 0.1$ (green), 1.0 (blue) and 10 (red). The optimum bandwidths correspond to the local minima at smallest h_j -values, marked with a filled star (\star) on the plots.

for the average in (E4) to be converged to the convolution $(K_h * p)(y'_i, 0 | \mathbf{x}, t_f)$, then the result will be independent of h for any value less than the scale of variation of the limit PDF. Since this is an exact invariance property of the limiting result, the “principle of minimal sensitivity” selects the optimal bandwidth h_* for finite N so that varying the bandwidth has minimal effect on the PDF-estimate. Precisely, one picks h_* by considering a decreasing sequence of candidate values h_j , computing the L_1 -difference $\Delta\tilde{p}(h_j) := \|\tilde{p}_{h_j} - \tilde{p}_{h_{j-1}}\|_{L^1}$ for successive bandwidths, and picking h_* where $\Delta\tilde{p}(h_j)$ is most nearly flat. This procedure is illustrated in Figure 7 for the particle position PDF’s that were presented in Fig. 1(f) but using $N = 1024$ samples. The L^1 -differences are plotted versus h_j in Figure 7 for the three choices of Prandtl number. The bandwidths chosen correspond to the local minima for each curve at the smallest h_j -value indicated by the star (\star) on the graph, i.e. $h_*/\eta \approx 16$ for $Pr = 0.1$, $h_*/\eta \approx 26$ for $Pr = 1$, $h_*/\eta \approx 39$ for $Pr = 10$. In some cases we did not observe local minima as in Fig. 7 and in those instances our procedure was to select as “optimal” bandwidth h_* the smallest h_j in an interval where the plot of $\Delta\tilde{p}(h_j)$ vs. h_j had a slope of magnitude less than 0.01.

Finally, after selecting the optimal bandwidth h_* , we obtained the sample-size error for the PDF estimate as the standard error of the mean for the sample average (E4) over N independent random variables identically distributed as $K_{h_*}(\tilde{\eta}(0) - y'_i)$, with bandwidth h_* fixed. In addition to this statistical error, an additional source of error arises from the choice of h_* . To assess this, we recalculated the kernel density estimator with a 10% increase in bandwidth, or $1.1h_*$, and took the absolute difference in the two PDF estimates as a measure of the error associated to small variations in bandwidth. The two types of errors were found to have more or less comparable magnitudes and the error bars in Fig. 1(e),(f) represent the total error obtained from their sum.

E.2. Methods for Section 3.1

To solve the backward Itô SDE’s with reflection at the channel walls, Eqs. (3.5), (3.6), we again use a reflected time $\hat{s} = t - s$ which transforms them into forward Itô SDE’s with boundary reflection. To solve the latter, we employ the Lépingle (1995) algorithm which (dropping hats on the reflected time) takes at the k th time-step

$$\tilde{\xi}(s_{k+1}) = \tilde{\xi}(s_k) + \Delta\tilde{\xi}(s_{k+1}; s_k) + \kappa\mathbf{n}^+ \Delta\tilde{\ell}^+(s_k) + \kappa\mathbf{n}^- \Delta\tilde{\ell}^-(s_k) \quad (\text{E5})$$

where $\Delta\tilde{\xi}(s; s_k)$ is given by the Euler-Maruyama discretization

$$\Delta\tilde{\xi}(s; s_k) = \mathbf{u}(\tilde{\xi}(s_k), s_k)(s - s_k) + \sqrt{2\kappa}(\tilde{\mathbf{W}}(s) - \tilde{\mathbf{W}}(s_k)) \quad (\text{E } 6)$$

and where $\Delta\tilde{\ell}^\pm(s_k) = \tilde{\ell}^\pm(s_{k+1}) - \tilde{\ell}^\pm(s_k)$ is given by the Skorohod equation (see Karatzas & Shreve (1991), Lemma 3.6.14 and Eq. (B 30)):

$$\kappa\Delta\tilde{\ell}^\pm(s_k) = \max \left\{ 0, \max_{s_k \leq s \leq s_{k+1}} \left\{ -\mathbf{n}^\pm \cdot [\tilde{\xi}(s_k) + \Delta\tilde{\xi}(s; s_k)] \right\} - h \right\}. \quad (\text{E } 7)$$

At the top wall $y = +h$, $\mathbf{n}^+ = -\hat{\mathbf{y}}$ and at the bottom wall $y = -h$, $\mathbf{n}^- = +\hat{\mathbf{y}}$. The stochastic solution of the Skorohod equation is exactly realized by a closed formula that involves an independent exponential random variable. See Lépingle (1995), Theorem 1. To minimize the additional computational cost of solving the Skorohod equation Eq. (E 7), the algorithm of Lépingle (1995) adds the local time density terms into Eq. (E 5) only when the particle is within a distance ϵ of the walls, fixed independent of $\Delta s = s_{k+1} - s_k$ †. We chose $\epsilon = 10\delta_\nu$ in our channel-flow simulations.

To study strong convergence of the approximate solutions of Eqs. (E 5),(E 7) for the results presented in Fig. 2, we first generated a realization of a Brownian motion $\tilde{\mathbf{W}}(s_i)$ sampled on an extremely fine grid of times s_i with a very small time-step δs . We then applied the above algorithm of Lépingle (1995) for a larger time-step $\Delta s = m \delta s$ which is a multiple of δs by a big integer m , using the same previously sampled Brownian motion $\tilde{\mathbf{W}}(s_i)$ for all $\Delta s = m\delta s$. We reduced the size of m until the numerical results for the joint process $(\tilde{\xi}(s), \tilde{\ell}(s))$ were converged to within 0.1%, which required a time-step $\Delta s = 6.5 \times 10^{-6}$, as reported in the text. To check for weak convergence of ensemble averages of the approximate solutions of Eqs. (E 5),(E 7) with $\Delta s = 2.16 \times 10^{-3}$ we numerically integrated the equations with double this time-step and found a relative change in the ensemble averages of less than 0.1%.

The N -sample averages used for particle dispersions and PDF's were the same as those for isotropic turbulence discussed in Appendix E.1. In particular, local time PDFs were estimated with kernel density techniques. One key difference is that the absolute local times $|\tilde{\ell}_{t,0}|$ are positive quantities, so that their PDF's have a support boundary at 0 and naive application of kernel density estimators leads to “seepage” of mass to negative values. Since the exact PDF is expected to have a maximum at 0 (highest probability for particles never to hit the wall), we employ the “reflection method” (Karunamuni & Alberts 2005). This procedure involves performing the kernel density estimation on a symmetric dataset constructed by augmenting the original data by its negation. The optimal bandwidth was again chosen by the “principle of minimal sensitivity”. Using these procedures and the same number of samples ($N = 1024$) as for channel-flow, we were able to recover the analytical results in Appendix B.3 for the PDF of local times of a Brownian motion on the half-axis reflected at the origin.

E.3. Methods for Section 4.1

To obtain the hitting times for channel-flow from the numerical solution of the SDE (3.5) with the Euler-Maruyama scheme, we simply monitored the solution until the first time-

† In principle, the boundary local time densities for channel-flow that appear in Figs. 2,4 are thus a sum of contributions from both top and bottom walls. However, in practice, no particles released at the bottom wall were ever observed to be incident upon the top wall within the entire time available in the database and thus $\tilde{\ell}(s) = \tilde{\ell}^-(s)$. This is to be expected, since wall-normal velocities in turbulent channel-flow generally have maximum magnitudes of order u_τ and, in the archived flow, advection at this maximum speed would require about double the archived time interval for a particle to transit from the bottom wall to the top wall.

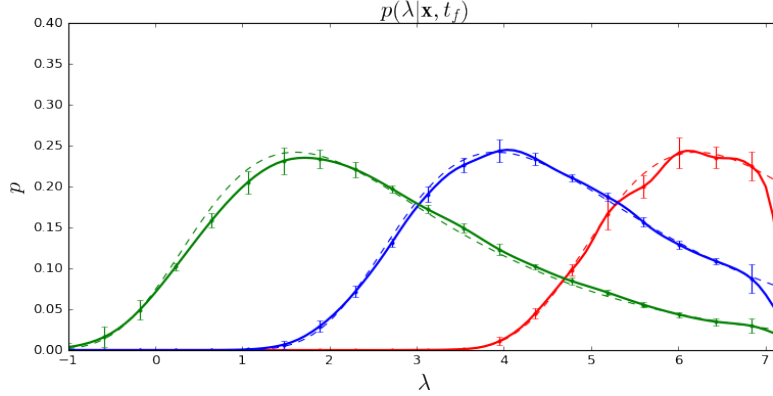


Figure 8: Hitting-time PDF's of Brownian motion for $Pr = 0.1$ (green), 1.0 (blue) and 10 (red). Analytical results represented by dashed lines, numerical results by solid lines.

step where the y -component satisfied $\tilde{\eta}(s_k) > -h$ but $\tilde{\eta}(s_{k+1}) < -h$. We then stopped the integration and set $\tilde{\tau} = (s_k + s_{k+1})/2$. With a time-step of $\Delta s = 2.1\bar{6} \times 10^{-3}$, this gives the hitting-time accurately to within $1.08\bar{3} \times 10^{-3}$, or 5.41% of the viscous time t_ν . To obtain PDF's of $\lambda = \ln((t_f - \tau)/t_\nu)$ from the channel flow data, we applied the same kernel density techniques as in Appendix E.1. Note for Brownian motion (see Eq. (E8) below) the mean hitting is infinite and with fluid-advection the hitting times are expected to be even larger. Thus, many solutions do not ever hit the wall over the total time available in the channel-flow database and this necessitates a very large number of samples. The results presented in the text were for $N=14,336$ samples. The PDF's were verified to be converged with $\Delta s = 2.1\bar{6} \times 10^{-3}$ to within 0.1% and the plotted error bars represent both s.e.m. and the change due to 10% increase in h_* , as described in Appendix E.2.

We applied identical numerical procedures to calculate the PDF's of $\lambda = \ln((t_f - \tau)/t_\nu)$ for a Brownian motion with diffusivity κ started at position $y > -h$ at time $t = t_f$ and going backward in time to $t = 0$. These PDF's are obtained analytically by differentiating $P(\tilde{\tau}(z) < \tau)$ in Eq.(B33) with respect to τ (see also Karatzas & Shreve (1991), section 2.6) and then replacing $z \rightarrow \Delta y = y + h$ and $\tau \rightarrow t_f - \tau$. This yields for $\Delta y > 0$:

$$p^\kappa(\tau|y, t_f) = \begin{cases} \frac{\Delta y}{\sqrt{4\pi\kappa(t_f - \tau)^3}} \exp\left(-\frac{(\Delta y)^2}{4\kappa(t_f - \tau)}\right) & \tau < t_f \\ 0 & \tau > t_f \end{cases}. \quad (\text{E8})$$

Numerical and analytical results for Brownian motion are plotted together in Figure 8. For $\lambda < 1.6$ one can see that the error from time-discretization leads to a $\sim 5\%$ shift of the PDF to the right, toward larger hitting times. To correct this would require either a smaller time-step or a more sophisticated stochastic interpolation scheme. For $\lambda > 6.5$, the lack of samples for $\lambda = \ln(t_f/t_\nu) \doteq 7.17$ leads the kernel density estimators to clearly under-predict the PDF's. Similar errors must exist in the channel-flow results.

REFERENCES

- AHLERS, G., GROSSMANN, S. & LOHSE, D. 2009 Heat transfer and large scale dynamics in turbulent Rayleigh-Bénard convection. *Rev. Mod. Phys.* **81** (2), 503.
- ALBEVERIO, S. & BELOPOLSKAYA, YA. 2010 Generalized solutions of the Cauchy problem for the Navier-Stokes system and diffusion processes. *Cubo (Temuco)* **12** (2), 77–96.
- BATCHELOR, G. K. 1951 Pressure fluctuations in isotropic turbulence. *Proc. Phil. Soc.* **47**.

- BERG, J., LÜTHI, B., MANN, J. & OTT, S. 2006 Backwards and forwards relative dispersion in turbulent flow: An experimental investigation. *Phys. Rev. E* **74**, 016304.
- BERGÉ, P. & DUBOIS, M. 1984 Rayleigh-Bénard convection. *Contemp Phys.* **25** (6), 535–582.
- BERKOVITZ, L. D. 1974 Lower semicontinuity of integral functionals. *Trans. Am. Math. Soc.* **192**, 51–57.
- BERNARD, D., GAWĘDZKI, K. & KUPIAINEN, A. 1998 Slow modes in passive advection. *J. Stat. Phys.* **90**, 519–569.
- BITANE, R., HOMANN, H. & BEC, J. 2013 Geometry and violent events in turbulent pair dispersion. *J. Turb.* **14** (2), 23–45.
- BOFFETTA, G. & SOKOLOV, I. M. 2002 Relative dispersion in fully developed turbulence: The Richardson’s law and intermittency corrections. *Phys. Rev. Lett.* **88**, 094501.
- BRAIDES, A. 2002 *Gamma-convergence for Beginners*. Oxford University Press.
- BUARIA, D., YEUNG, P.K. & SAWFORD, B. 2016 A Lagrangian study of turbulent mixing: forward and backward dispersion of molecular trajectories in isotropic turbulence. Accepted to *J. Fluid Mech.*
- BURDZY, K. 2009 Differentiability of stochastic flow of reflected Brownian motions. *Electron. J. Probab.* **14**, 2182–2240.
- BURDZY, K., CHEN, Z-Q. & SYLVESTER, J. 2004 The heat equation and reflected Brownian motion in time-dependent domains. *Ann. Prob.* **32** (1B), 775–804.
- CASTAING, B., GUNARATNE, G., KADANOFF, L. P., LIBCHABER, A. & HESLOT, F. 1989 Scaling of hard thermal turbulence in Rayleigh-Bénard convection. *J. Fluid Mech.* **204** (1), 1–30.
- CHAVES, M., GAWĘDZKI, K., HORVAI, P., KUPIAINEN, A. & VERGASSOLA, M. 2003 Lagrangian dispersion in Gaussian self-similar velocity ensembles. *J. Stat. Phys.* **113** (5-6), 643–692.
- CHILLÀ, F. & SCHUMACHER, J. 2012 New perspectives in turbulent Rayleigh-Bénard convection. *Eur. Phys. J. E* **35** (7), 1–25.
- CONSTANTIN, P. & IYER, G. 2008 A stochastic Lagrangian representation of the three-dimensional incompressible Navier-Stokes equations. *Commun. Pure Appl. Math.* **61**, 330–345.
- CONSTANTIN, P. & IYER, G. 2011 A stochastic-Lagrangian approach to the Navier-Stokes equations in domains with boundary. *Ann. Appl. Probab.* **21**, 1466–1492.
- CORRSIN, S. 1951 On the spectrum of isotropic temperature fluctuations in an isotropic turbulence. *J. Appl. Phys.* **22** (4), 469–473.
- CORRSIN, S. 1953 Remarks on turbulent heat transfer. In *Proceeding of the Thermodynamics Symposium*, pp. 5–30. University of Iowa, Iowa City, Iowa.
- DONZIS, D. A., SREENIVASAN, K. R. & YEUNG, P. K. 2005 Scalar dissipation rate and dissipative anomaly in isotropic turbulence. *J. Fluid Mech.* **532**, 199–216.
- E, W. & VANDEN-EIJNDEN, E. 2000 Generalized flows, intrinsic stochasticity and turbulent transport. *Proc. Natl. Acad. Sci.* **97**, 8200–8205.
- E, W. & VANDEN-EIJNDEN, E. 2001 Turbulent Prandtl number effect on passive scalar advection. *Physica D* **152-153**, 636–645.
- EMRAN, M. S. & SCHUMACHER, J. 2008 Fine-scale statistics of temperature and its derivatives in convective turbulence. *J. Fluid Mech.* **611**, 13–34.
- EMRAN, M. S. & SCHUMACHER, J. 2012 Conditional statistics of thermal dissipation rate in turbulent Rayleigh-Bénard convection. *Eur. Phys. J. E* **35** (10), 1–8.
- EYINK, G. L. 2001 Dissipation in turbulent solutions of 2D Euler equations. *Nonlinearity* **14** (4), 787.
- EYINK, G. L. 2010 Stochastic least-action principle for the incompressible Navier-Stokes equation. *Physica D* **239**, 1236–1240.
- EYINK, G. L. 2011 Stochastic flux freezing and magnetic dynamo. *Phys. Rev. E* **83** (5), 056405.
- EYINK, G. L. & DRIVAS, T. D. 2015a Quantum spontaneous stochasticity. *arXiv preprint arXiv:1509.04941*.
- EYINK, G. L. & DRIVAS, T. D. 2015b Spontaneous stochasticity and anomalous dissipation for Burgers equation. *J. Stat. Phys.* **158** (2), 386–432.
- FABER T., VASSILICOS, J. C. 2009 Turbulent pair separation due to multiscale stagnation point structure and its time asymmetry in two-dimensional turbulence. *Phys. Fluids* **21**.
- FALKOVICH, G., GAWĘDZKI, K. & VERGASSOLA, M. 2001 Particles and fields in fluid turbulence. *Rev. Mod. Phys.* **73**, 913–975.

- FLORESCU, L.C. & GODET-THOBIE, C. 2012 *Young Measures and Compactness in Measure Spaces*. De Gruyter.
- FREĀDLIN, M. I. 1985 *Functional Integration and Partial Differential Equations*. Princeton University Press.
- FRIEDMAN, A. 2006 *Stochastic Differential Equations and Applications*. Mineola, NY: Dover.
- FRISCH, U. 1995 *Turbulence: The Legacy of A. N. Kolmogorov*. Cambridge: Cambridge University Press.
- GAWĘDZKI, K. 2008 Soluble models of turbulent transport. In *Non-equilibrium statistical mechanics and turbulence* (ed. John Cardy, Gregory Falkovich & Krzysztof Gawędzki), *London Mathematical Society Lecture Note Series*, vol. 355, pp. 44–107. Cambridge University Press.
- GAWĘDZKI, K. & VERGASSOLA, M. 2000 Phase transition in the passive scalar advection. *Physica D* **138**, 63–90.
- GOLUSKIN, D. 2015 *Internally Heated Convection and Rayleigh-Bénard Convection*. Springer International Publishing.
- GRAHAM, J., KANOV, K., YANG, X. I. A., LEE, M., MALAYA, N., LALESCU, C. C., BURNS, R., EYINK, G., SZALAY, A. & MOSER, R. D. 2016 A Web services accessible database of turbulent channel flow and its use for testing a new integral wall model for LES. *J. Turb.* **17** (2), 181–215.
- GROSSMANN, S. & LOHSE, D. 2000 Scaling in thermal convection: a unifying theory. *J. Fluid Mech.* **407**, 27–56.
- HARTMAN, P. 2002 *Ordinary Differential Equations*, 2nd edn. SIAM.
- HE, X., FUNFSCHILLING, D., NOBACH, H., BODENSCHATZ, E. & AHLERS, G. 2012 Transition to the ultimate state of turbulent Rayleigh-Bénard convection. *Phys. Rev. Lett.* **108** (2), 024502.
- HE, X. & TONG, P. 2009 Measurements of the thermal dissipation field in turbulent Rayleigh-Bénard convection. *Phys. Rev. E* **79** (2), 026306.
- HE, X., TONG, P. & XIA, K-Q. 2007 Measured thermal dissipation field in turbulent Rayleigh-Bénard convection. *Phys. Rev. Lett.* **98** (14), 144501.
- IKEDA, N. & WATANABE, S. 1989 *Stochastic differential equations and diffusion processes*. North-Holland.
- ITÔ, K. 1984 *An Introduction to Probability Theory*. Cambridge University Press.
- JIRINA, M. 1959 On regular conditional probabilities. *Czech. Math. J.* **9** (3), 445–451.
- JOHNSTON, H. & DOERING, C. R. 2009 Comparison of turbulent thermal convection between conditions of constant temperature and constant flux. *Phys. Rev. Lett.* **102** (6), 064501.
- KANEDA, Y., ISHIHARA, T., YOKOKAWA, M., ITAKURA, K. & UNO, A. 2003 Energy dissipation rate and energy spectrum in high resolution direct numerical simulations of turbulence in a periodic box. *Phys. Fluids* **15**, L21–L24.
- KARATZAS, I. & SHREVE, S.E. 1991 *Brownian Motion and Stochastic Calculus*. Springer New York.
- KARLIN, S. & TAYLOR, H. E. 1981 *A Second Course in Stochastic Processes*. Elsevier Science.
- KARUNAMUNI, R. J & ALBERTS, T. 2005 On boundary correction in kernel density estimation. *Stat. Meth.* **2** (3), 191–212.
- KATZNELSON, Y. 2004 *An Introduction to Harmonic Analysis*. Cambridge University Press.
- KEANINI, R. G. 2007 Random walk methods for scalar transport problems subject to Dirichlet, Neumann and mixed boundary conditions. *Proc. Roy. Soc. Lond. A* **463**, 435–460.
- KLINE, S. J., REYNOLDS, W. C., SCHRAUB, F. A. & RUNDSTADLER, P. W. 1967 The structure of turbulent boundary layers. *J. Fluid Mech.* **30**, 741–773.
- KLOEDEN, P.E. & PLATEN, E. 1992 *Numerical Solutions of Stochastic Differential Equations*. Springer-Verlag.
- KOLMOGOROV, A. N. 1941a Dissipation of energy in locally isotropic turbulence. *Dokl. Akad. Nauk SSSR* **32** (1), 16–18.
- KOLMOGOROV, A. N. 1941b Equations of turbulent motion in an incompressible fluid. *Dokl. Akad. Nauk SSSR* **30**, 299–303.
- KOLMOGOROV, A. N. 1941c The local structure of turbulence in incompressible viscous fluid for very large Reynolds numbers. *Dokl. Akad. Nauk SSSR* **30** (4), 299–303.

- KRAICHNAN, R. H. 1962 Turbulent thermal convection at arbitrary Prandtl number. *Phys. Fluids* **5** (11), 1374–1389.
- KRAICHNAN, R. H. 1968 Small-scale structure of a scalar field convected by turbulence. *Phys. Fluids* **11**, 945–953.
- KUNITA, H. 1997 *Stochastic Flows and Stochastic Differential Equations*, Cambridge Studies in Advanced Mathematics, vol. 24. Cambridge, UK: Cambridge Univ. Press.
- KUPIAINEN, A. 2003 Nondeterministic dynamics and turbulent transport. *Ann. Henri Poincaré* **4** (Suppl. 2), S713–S726.
- LE JAN, Y. & RAIMOND, O. 2002 Integration of Brownian vector fields. *Ann. Prob.* **30**, 826–873.
- LE JAN, Y. & RAIMOND, O. 2004 Flows, coalescence and noise. *Ann. Prob.* **32**, 1247–1315.
- LÉPINGLE, D. 1995 Euler scheme for reflected stochastic differential equations. *Math. Comput. Simulat.* **38** (1), 119–126.
- LI, Y., PERLMAN, E., WAN, M., YANG, Y., BURNS, R. & MENEVEAU, C., CHEN, S., SZALAY, A. & EYINK, G. L. 2008 A public turbulence database cluster and applications to study Lagrangian evolution of velocity increments in turbulence. *J. Turb.* **9** (31).
- LIONS, P. L. 1996 *Mathematical Topics in Fluid Mechanics: Volume 1: Incompressible Models*. Oxford University Press, Incorporated.
- LIONS, P.-L. & SZNITMAN, A. S. 1984 Stochastic differential equations with reflecting boundary conditions. *Comm. Pure Appl. Math.* **37** (4), 511–537.
- MALKUS, W. V. R. 1954 The heat transport and spectrum of thermal turbulence. *Proc. Roy. Soc. Lond. A* **225** (1161), 196–212.
- MIL'SHTEIN, G. N. 1996 Application of the numerical integration of stochastic equations to solving boundary-value problems with Neumann's boundary conditions. *Teoriya Veroyatnostei i ee Primeneniya* **41** (1), 210–218.
- NG, E. W. & GELLER, M. 1969 A table of integrals of the error functions. *J. Res. NBS - B Math. Sci.* **73** (1), 1–20.
- NIEMELA, J. J. & SREENIVASAN, K. R. 2003 Confined turbulent convection. *J. Fluid Mech.* **481**, 355–384.
- NIEMELA, J. J. & SREENIVASAN, K. R. 2006 Turbulent convection at high Rayleigh numbers and aspect ratio 4. *J. Fluid Mech.* **557**, 411–422.
- NOVIKOV, E. A. 1965 Functionals and the random-force method in turbulence theory. *Sov. Phys. JETP* **20** (5), 1290–1294.
- OBUKHOV, A. M. 1949 Structure of the temperature field in turbulent flow. *Izv. Akad. Nauk. SSSR, Ser. Geogr. i Geofiz.* **13**, 58–69.
- OKSENDAL, B. 2013 *Stochastic differential equations: an introduction with applications*. Springer Science & Business Media.
- ONSAGER, L. 1945 The distribution of energy in turbulence. *Phys. Rev.* **68**, 286–286.
- ONSAGER, L. 1949 Statistical hydrodynamics. *Nuovo Cim. Suppl.* **VI**, 279–287.
- OTERO, J., WITTENBERG, R. W., WORTHING, R. A. & DOERING, C. R. 2002 Bounds on Rayleigh–Bénard convection with an imposed heat flux. *J. Fluid Mech.* **473**, 191–199.
- PEARSON, B. R., KROGSTAD, P.-A. & VAN DE WATER, W. 2002 Measurements of the turbulent energy dissipation rate. *Phys. Fluids* **14**, 1288–1290.
- PILIPENKO, A. 2014 *An Introduction to Stochastic Differential Equations with Reflection*. Potsdam University Press.
- PILIPENKO, A. YU. 2005 Properties of the flows generated by stochastic equations with reflection. *Ukr. Math. J.* **57** (8), 1262–1274.
- PRIESTLEY, C.H.B. 1959 *Turbulent transfer in the lower atmosphere*. University of Chicago Press.
- PROCACCIA, I., CHING, E. S. C., CONSTANTIN, P., KADANOFF, L. P., LIBCHABER, A. & WU, X. 1991 Transitions in convective turbulence: The role of thermal plumes. *Phys. Rev. A* **44** (12), 8091.
- QIU, X.-L. & TONG, P. 2002 Temperature oscillations in turbulent Rayleigh–Bénard convection. *Phys. Rev. E* **66** (2), 026308.
- REZAKHANLOU, F. 2014 Regular flows for diffusions with rough drifts. *arXiv preprint arXiv:1405.5856*.
- RICHARDSON, L. F. 1926 Atmospheric diffusion shown on a distance-neighbor graph. *Proc. R. Soc. Lond. Ser. A* **110**, 709–737.

- ROBERT, R. 1991 A maximum-entropy principle for two-dimensional perfect fluid dynamics. *J. Stat. Phys.* **65** (3-4), 531–553.
- ROBERT, R. & SOMMERIA, J. 1991 Statistical equilibrium states for two-dimensional flows. *J. Fluid Mech.* **229**, 291–310.
- ROCHE, P.-E., GAUTHIER, F., KAISER, R. & SALORT, J. 2010 On the triggering of the ultimate regime of convection. *New J. Phys.* **12** (8), 085014.
- ROGERS, L.C.G. & WILLIAMS, D. 2000 *Diffusions, Markov Processes and Martingales: Volume 2, Itô Calculus*. Cambridge University Press.
- RUDIN, W. 2006 *Functional Analysis*. McGraw-Hill.
- SALMON, R. 1988 Hamiltonian fluid mechanics. *Annu. Rev. Fluid Mech.* **20** (1), 225–256.
- SAWFORD, B. 2001 Turbulent relative dispersion. *Annu. Rev. Fluid Mech.* **33** (1), 289–317.
- SAWFORD, B. L., YEUNG, P. K. & BORGAS, M. S. 2005 Comparison of backwards and forwards relative dispersion in turbulence. *Phys. Fluids* **17**, 095109.
- SCHEEL, J. D. & SCHUMACHER, J. 2014 Local boundary layer scales in turbulent Rayleigh–Bénard convection. *J. Fluid Mech.* **758**, 344–373.
- SCHUMACHER, J. 2008 Lagrangian dispersion and heat transport in convective turbulence. *Phys. Rev. Lett.* **100** (13), 134502.
- SHRAIMAN, B. I. & SIGGIA, E. D. 1990 Heat transport in high-Rayleigh-number convection. *Phys. Rev. A* **42.6**, 3650.
- SILVERMAN, B. W. 1986 *Density estimation for statistics and data analysis*. CRC press.
- SŁOMIŃSKI, L. 2013 Weak and strong approximations of reflected diffusions via penalization methods. *Stoch. Proc. Appl.* **123** (3), 752–763.
- SOMMERIA, J., STAQUET, C. & ROBERT, R. 1991 Final equilibrium state of a two-dimensional shear layer. *J. Fluid Mech.* **233**, 661–689.
- SONER, H. M. 2007 Stochastic representations for nonlinear parabolic PDEs. *Handbook of Differential Equations: Evolutionary Equations* **3**, 477–526.
- SPIEGEL, E. A. 1971 Convection in stars: I. Basic Boussinesq convection. *Annu. Rev. Astron.* **9**, 323.
- SREENIVASAN, K. R. 1998 An update on the energy dissipation rate in isotropic turbulence. *Phys. Fluids* **10** (2), 528–529.
- SREENIVASAN, K. R. & SCHUMACHER, J. 2010 Lagrangian views on turbulent mixing of passive scalars. *Phil. Trans. R. Soc. A* **368** (1916), 1561–1577.
- STEVENS, R. J. A. M., LOHSE, D. & VERZICCO, R. 2011 Prandtl and Rayleigh number dependence of heat transport in high Rayleigh number thermal convection. *J. Fluid Mech.* **688**, 31–43.
- STEVENSON, R. M. 1981 Optimized perturbation theory. *Phys. Rev. D* **23** (12), 2916.
- STROOCK, D. W. & VARADHAN, SR S. 1971 Diffusion processes with boundary conditions. *Comm. Pure Appl. Math.* **24** (2), 147–225.
- TAYLOR, G. I. 1917 Observations and speculations on the nature of turbulent motion. *Reports and Memoranda of the Advisory Committee for Aeronautics, no.345*. Reprinted in *The Scientific Papers of Sir Geoffrey Ingram Taylor: Volume 2, Meteorology, Oceanography and Turbulent Flow*, G. K. Batchelor, Ed. (Cambridge University Press, 1960).
- TAYLOR, G. I. 1922 Diffusion by continuous movements. *Proc. Lond. Math. Soc.* **20** (1), 196–212.
- TRAN, CHUONG V & DRITSCHEL, DAVID G 2006 Vanishing enstrophy dissipation in two-dimensional Navier–Stokes turbulence in the inviscid limit. *J. Fluid Mech.* **559**, 107–116.
- TSINOBER, A. 2009 *An Informal Conceptual Introduction to Turbulence*. Springer.
- VALADIER, M. 1973 Désintégration d'une mesure sur un produit. *C. R. Acad. Sci. A* **276**, 33–35.
- VALADIER, M. 1994 A course on Young measures. *Rend. Istit. Mat. Univ. Trieste, Supplemento* **XXVI**, 349–394.
- YAGLOM, A. M. 1949 On the local structure of the temperature field in a turbulent flow. *Doklady Acad. Sci. U.S.S.R.* **69** (6).
- YEUNG, P. K., DONZIS, D. A. & SREENIVASAN, K. R. 2005 High-Reynolds-number simulation of turbulent mixing. *Phys. Fluids* **17** (8), 081703.
- YU, H., KANOV, K., PERLMAN, E., GRAHAM, J., FREDERIX, E., BURNS, R., SZALAY, A., EYINK, G. L. & MENEVEAU, C. 2012 Studying Lagrangian dynamics of turbulence using on-demand fluid particle tracking in a public turbulence database. *J. Turb.* **12** (13).